National Technical University of Athens
School of Naval Architecture and Marine Engineering
Division of Ship Design and Maritime Transport

PARAMETRIC DESIGN AND OPTIMIZATION OF LARGE RO-PAX FERRY

Fotios Papadopoulos

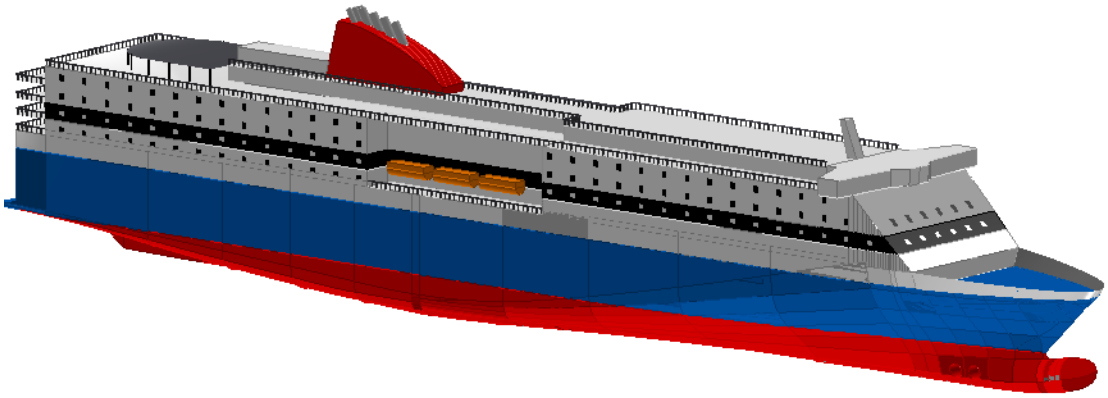

Diploma thesis

Supervisor: Professor George Zaraphonitis

October 2019

NATIONAL TECHNICAL UNIVERSITY OF ATHENS

SCHOOL OF NAVAL ARCHITECTURE AND MARINE ENGINEERING

DIVISION OF SHIP DESIGN AND MARITIME TRANSPORT

DIPLOMA THESIS

PARAMETRIC DESIGN AND OPTIMIZATION OF LARGE RO-PAX FERRY

Fotios Papadopoulos

Supervisor:

George Zaraphonitis, Professor

Examination committee:

Eleftheria Eliopoulou, Dr.-Eng., EDIP

Alexandros Ginnis, Associate Professor

George Zaraphonitis, Professor

October 2019

Summary

Parametric methods in ship design have been used for decades, enabling naval architects to explore the design space efficiently and effectively. Current developments in computer hardware and software have provided designers with modeling and analysis tools of increased accuracy and acceptable computational demands, enabling more aspects to be taken into account early into the ship design process. Meanwhile, the ship design optimization problem is constantly becoming more complex due to the addition of new regulatory constraints, further favoring parametric optimization methods against the use of heuristic methodologies for design space exploration.

In this diploma thesis, a parametric procedure is implemented for the preliminary design of large ro-pax ferries. A parametric model is developed which can generate ship designs within a range of sizes, as well as properties of the hull form (C_B, LCB) and of the general arrangement. The generated designs are automatically assessed in terms of various technical and techno-economic aspects of interest. Subsequently, the developed model is utilized in combination with design space exploration and optimization algorithms so as to design a techno-economically optimal ship, adhering to a series of owner's requirements while considering relevant physical and regulatory (safety and environmental) constraints. The entire parametric model is set up in the well-known naval architectural software NAPA, by developing macros using the programming language NAPA Basic. For the optimization case study, the NAPA project is linked with CAD/CAE system CAESES.

More specifically, this thesis is structured into three parts, each comprising of two chapters.

Part I provides relevant background information. Chapter 1 describes ro-pax ships and their design characteristics, while Chapter 2 is an overview of parametric design and optimization methods as applied in ship design.

Part II is the core of the thesis, providing a detailed presentation of the developed parametric design procedure. Chapter 3 describes the geometric design of the ship, with emphasis on the parametrization of the general arrangement and its adaption to the surrounding hull form. Chapter 4 presents the calculation methods which have been employed for the assessment of each design alternative, namely for the ship's powering, lightship weight and payload, loading conditions, intact and damage stability, energy efficiency and profitability.

Part III presents two applications. The first (Chapter 5) is an example design, where reasonable values are given to the various parameters, the series of macros is executed and indicative results are presented. Finally, Chapter 6 presents an optimization case study, where consistent owner's requirements are assumed and the parametric model is utilized for the design of a feasible and techno-economically optimal ship.

Περίληψη

Η χρήση παραμετρικών μεθόδων στη μελέτη και σχεδίαση πλοίου δεν αποτελεί καινοτομία. Σήμερα ωστόσο, οι σημαντικές εξελίξεις στους ηλεκτρονικούς υπολογιστές και στα λογισμικά σχεδίασης και ανάλυσης δίνουν στο ναυπηγό τη δυνατότητα να λαμβάνει υπόψη πλήθος παραγόντων και να χρησιμοποιεί ακριβέστερες μεθόδους με αποδεκτό υπολογιστικό κόστος, ήδη από τα αρχικά στάδια της μελέτης. Παράλληλα, το πρόβλημα της βελτιστοποίησης του πλοίου καθίσταται ολοένα και πιο πολύπλοκο λόγω της εισαγωγής νέων κανονισμών που δρουν ως περιορισμοί του προβλήματος. Οι δύο αυτοί παράγοντες ευνοούν περαιτέρω τη χρήση παραμετρικών μεθόδων έναντι των παραδοσιακών μεθοδολογιών σχεδίασης.

Στην παρούσα διπλωματική εργασία αναπτύσσεται ένα παραμετρικό μοντέλο για την προκαταρκτική μελέτη και σχεδίαση μεγάλων επιβατηγών – οχηματαγωγών (Ε/Γ – Ο/Γ) πλοίων. Μέσω του παραμετρικού μοντέλου μπορούν να παραχθούν μοντέλα Ε/Γ – Ο/Γ πλοίων σε ένα εύρος κυρίων διαστάσεων καθώς και χαρακτηριστικών μορφής γάστρας και γενικής διάταξης. Οι παραγόμενες σχεδιάσεις αξιολογούνται αυτόματα όσον αφορά διάφορα τεχνικά και τεχνικοοικονομικά μεγέθη. Στη συνέχεια, το μοντέλο χρησιμοποιείται σε συνδυασμό με αλγορίθμους αναζήτησης και βελτιστοποίησης για το σχεδιασμό ενός τεχνικοοικονομικά βέλτιστου πλοίου, το οποίο πληροί συγκεκριμένες απαιτήσεις πλοιοκτήτη, υπακούει σε φυσικούς περιορισμούς και ικανοποιεί κανονισμούς ασφαλείας και προστασίας του περιβάλλοντος. Το μοντέλο αναπτύσσεται εντός του γνωστού ναυπηγικού λογισμικού NAPA χρησιμοποιώντας τη γλώσσα προγραμματισμού NAPA Basic. Για την εφαρμογή βελτιστοποίησης, το μοντέλο διασυνδέεται με το CAD / CAE σύστημα CAESES.

Πιο συγκεκριμένα, η εργασία δομείται από τρεις ενότητες, καθεμία από τις οποίες αποτελείται από δύο κεφάλαια.

Η Ενότητα Ι είναι εισαγωγική. Το Κεφάλαιο 1 αφορά τα σύγχρονα Ε/Γ – Ο/Γ πλοία και τα σχεδιαστικά χαρακτηριστικά τους, ενώ το Κεφάλαιο 2 ασχολείται με τις εφαρμογές της παραμετρικής σχεδίασης και βελτιστοποίησης στη μελέτη και σχεδίαση πλοίου.

Η Ενότητα ΙΙ αποτελεί τον πυρήνα της εργασίας, όπου περιγράφεται λεπτομερώς η διαδικασία παραμετρικού σχεδιασμού που ακολουθείται. Το Κεφάλαιο 3 παρουσιάζει το γεωμετρικό παραμετρικό μοντέλο του πλοίου, με έμφαση στην παραμετροποίηση της γενικής διάταξης και στη συμβατότητα εσωτερικής και εξωτερικής γεωμετρίας για ένα εύρος τιμών των παραμέτρων σχεδίασης. Στο Κεφάλαιο 4 αναλύονται οι χρησιμοποιούμενες μέθοδοι υπολογισμού όσον αφορά την αντίσταση και πρόωση του πλοίου, το ωφέλιμο φορτίο, το βάρος κενού σκάφους, τις καταστάσεις φόρτωσης, την ευστάθεια σε άθικτη και βεβλαμμένη κατάσταση, την ενεργειακή αποδοτικότητα και την οικονομική αξιολόγηση.

Η Ενότητα ΙΙΙ αποτελείται από δύο εφαρμογές. Στο Κεφάλαιο 5 παρουσιάζεται αναλυτικά ένα παράδειγμα παραγόμενης σχεδίασης, όπου δίνονται συγκεκριμένες τιμές στις διάφορες παραμέτρους, εκτελείται η σειρά κωδίκων και παρατίθενται ενδιαφέροντα αποτελέσματα. Τέλος, το Κεφάλαιο 6 αποτελεί την εφαρμογή βελτιστοποίησης, όπου υποτίθενται ρεαλιστικές απαιτήσεις πλοιοκτήτη και το μοντέλο χρησιμοποιείται για την εύρεση ενός τεχνικοοικονομικά βέλτιστου πλοίου που ικανοποιεί τις απαιτήσεις αυτές καθώς και τους προαναφερθέντες περιορισμούς.

Acknowledgements

At this point, I would like to express my gratitude towards my supervisor Professor George Zaraphonitis, who gave me the opportunity to work on the most interesting topic I could imagine and closely supervised my work during the past months. Without exaggeration, his profound knowledge in ship design, his constant willingness to help, the much time he devoted to my project and our excellent cooperation in general have largely shaped this end result. I would also like to thank him, along with Professors Gerasimos Politis, Emmanuel Samuelides and Christos Papadopoulos, for standing out and inspiring me with their teaching during the past five years.

Furthermore, I would like to thank the members of NTUA-SDL who contributed to this work. Particular thanks to PhD candidate Aphrodite Kanellopoulou for the CFD runs and the linking of NAPA and CAESES, PhD candidate George Dafermos for the help with damage stability and his comments on the text, as well as Dr.-Eng. Eleftheria Eliopoulou for her comments on the text.

I would also like to acknowledge the Panagiotis Triantafyllidis Foundation, the American Bureau of Shipping and the National Technical University of Athens for financially supporting my studies through awards and scholarships.

Last but not least, I am thankful to my family and friends, inside and outside NTUA, for their love and support during these years.

Table of Contents

PART III
APPLICATIONS

Nomenclature

Latin symbol	Description
A	Attained subdivision index
A_{ACC}	Accommodation area
A_c	Partial attained subdivision index at loading condition c, $c = d, p, l$
B	Beam (moulded)
b_{LH}	Distance of longitudinal bulkheads from the ship's shell at T_d
b_{LSA}	Required breadth on each side of the ship for life-saving appliances
C_{ACC}	Accommodation weight coefficient
C_B	Block coefficient at design draft
$C_{B,0.8h_6}$	Block coefficient at 80% of h_6
C_{FAE}	Carbon factor for auxiliary engines
C_{FME}	Carbon factor for main engines
C_{fuel}	Fuel cost per unit
C_{GEAR}	Reduction gear weight coefficient
C_{K-M}	Machinery cost per ton, excluding scrubber
$C_{K-OT\&ACC}$	Outfitting and accommodation cost per ton
C_{K-rest}	Non-weight cost factor
C_{K-ST}	Steel cost per ton
$C_{KG-hull}$	Coefficient for vertical center of hull steel weight
C_{KG-M}	Coefficient for vertical center of machinery weight
$C_{KG-OT\&ACC}$	Coefficient for vertical center of outfitting and accommodation weight
$C_{KG-supst}$	Coefficient for vertical center of superstructure steel weight
C_{LCG}	Coefficient for longitudinal center of lightship weight
C_{OT}	Outfitting weight coefficient
D	Depth to bulkhead deck (same as h_3)
d_l	Light service draft
d_p	Partial service draft
d_s	Subdivision draft (same as $T_{\max}$)
DHP	Delivered horsepower
DWT	Deadweight
E_N	Equipment number according to Watson
$EEDI$	Attained energy efficiency design index
$EEDI_{req}$	Required energy efficiency design index
EHP	Effective horsepower
$\vec{F}$	Vector of objective functions
f_c	EEDI cubic capacity correction factor
f_i	Objective function i, $i = 1, \dots, n$
f_j	EEDI ship design correlation factor for ro-pax ships
fra	Number of frames to be added / removed aft of the engine rooms (in comparison with the baseline design) for the aft engine room bulkhead to reach the minimum acceptable position
frf	Number of frames to be added forward of the engine rooms (in comparison with the baseline design) for the collision bulkhead to reach the minimum acceptable position
$frperweb$	Frames per web frame
Fn_L	Froude number based on the rule length L and EEDI condition speed V_{ref}
FS	Transverse frame spacing
FSM	Free surface moment

GM	Metacentric height
GM_c	Metacentric height at loading condition c, $c = d, p, l$
GT	Gross tonnage
GZ	Righting lever
$h_{DB,aft}$	Double bottom height aft of engine rooms
$h_{DB,E/R}$	Double bottom height at engine rooms
$h_{DB,fore}$	Double bottom height forward of engine rooms
h_i	Height of deck i, $i = 1, \dots, ndecks$
H_{ME}	Height of main engine, including required height for the removal of a piston
I	Number of inequality constraints
IN_t	Yearly inflows
J	Number of equality constraints
K	Steel weight coefficient for Watson's method
K_{build}	Building cost
K_{final}	Resale price at end of lifetime
K_{fuel}	Fuel cost per trip
K_M	Machinery cost
$K_{OT\&ACC}$	Outfitting & accommodation cost
K_{scrub}	Scrubber cost
K_{ST}	Steel cost
KG_i	Vertical center of gravity at loading condition i, $i = 1, \dots . n_{LC}$
KG_{LS}	Vertical center of lightship weight
KG_M	Vertical center of machinery weight
$KG_{max,i}$	Maximum permissible vertical center of gravity for compliance with intact stability regulations at loading condition i, $i = 1, \dots . n_{LC}$
$KG_{max.ij}$	Maximum permissible vertical center of gravity at loading condition i to comply with intact stability criterion j, $i = 1, \dots . n_{LC}$, $j = 1, \dots, n_{CR}$
$KG_{OT\&ACC}$	Vertical center of outfitting and accommodation weight
KG_{ST}	Vertical center of steel weight
$KG_{ST-hull}$	Vertical center of hull steel weight
$KG_{ST-supst}$	Vertical center of superstructure steel weight
l	Number of parameters
L	Rule length according to International Load Line Convention
L_{aft}	Distance of the aftmost main engine room bulkhead from aft perpendicular
$L_{aft,min}$	Minimum allowable distance of the aftmost main engine room bulkhead from aft perpendicular
l_i	Length of deck i, $i = 6, \dots, ndecks$
L_{ME}	Length of main engine
L_{PP}	Length between perpendiculars
LCB	Longitudinal center of buoyancy, measured from the aft perpendicular unless otherwise stated
LCG	Longitudinal center of gravity
LCG_{LS}	Longitudinal center of lightship weight
$lifetime$	Lifetime of the ship
LS	Lightship weight
m	Number of design variables
MCR	Installed power of main engines
MCR_i	Maximum continuous rating of engine i, $i = 1, \dots, 4$
MVZ	Number of main vertical zones of the ship
n	Number of objective functions
n_{CR}	Number of relevant intact stability criteria
n_{decks}	Number of decks
n_{LC}	Number of examined loading conditions

N_{PAX}	Passenger capacity of the ship
N_{PAXeff}	Effective passenger capacity of the ship
$N_{PAXinit}$	Reference number of passengers / owner's requirement
NPV	Net present value
OUT_t	Yearly outflows
$\vec{p}$	Vector of parameters
p_i	Parameter i, $i = 1, \dots, l$
P_{AE}	Mean consumed power of shaft generator and/or auxiliary engines
$P_{AE,EEDI}$	Auxiliary power for EEDI calculation
$P_{shaftgen}$	Consumed power of shaft generator
$P_{shaftgen,EEDI}$	Power of shaft generator for EEDI calculation
PC	Propulsive coefficient
PM	Power margin
R	Bare hull towing resistance
r	Interest rate
$resaft$	Remaining number of frames to be added / removed aft of the engine rooms for the aft engine room bulkhead to reach the minimum acceptable position, after new compartments have been added / existing ones removed
$resfore$	Remaining number of frames to be added / removed forward of the engine rooms for the collision bulkhead to reach the minimum acceptable position, after new compartments have been added / existing ones removed
RFR	Required freight rate
r_{REST}	Coefficient for machinery weight calculation (minus main engine and reduction gear)
s_i	Survival probability after damage of compartment or group of compartments i, according to damage stability regulations
$SFOC$	Specific fuel oil consumption of main engines (ISO conditions)
$SFOC_{AE}$	Specific fuel oil consumption of auxiliary engines (ISO conditions)
$SFOC_{AE,eff}$	Specific fuel oil consumption of auxiliary engines during operation
$SFOC_{eff}$	Specific fuel oil consumption of main engines during operation
$shiftbhdaft$	Number of transverse bulkheads aft of the engine rooms to be moved forward / aftward for the aft engine room bulkhead to reach the desired position
$shiftbhdfore$	Number of transverse bulkheads forward of the engine rooms to be moved forward / aftward for the collision bulkhead to reach the desired position
SHP	Calculated propulsion power (service speed, design draft, calm sea, clean hull), corrected with data from existing ships
SHP_0	Propulsion power as calculated with empirical and/or computational methods
SHP_{eff}	Mean required propulsion power during operation
SHP_{max}	Maximum power for propulsion with shaft generators in operation
t	Thrust deduction factor
T	Draft (moulded)
T_d	Design draft
$T_{\max}$	Maximum draft (same as d_s)
t_{trip}	Trip duration
t'_{trip}	Trip duration, including time at port
u_i	Inequality constraint i, $i = 1, \dots, I$
V	Design speed of the ship
v_j	Equality constraint j, $j = 1, \dots, J$
V_{net}	Net volumetric capacity of tank (with steel reduction)
V_{ref}	Attained speed at "EEDI condition"
V_{return}	Night trip design speed of the ship
w	Wake fraction
W_{ACC}	Accommodation weight

w_c	Weight coefficient of loading condition c, $c = d, p, l$
W_{GEAR}	Weight of reduction gear
W_{HULL}	Hull steel weight
W_M	Machinery weight
W_{ME}	Weight of main engines
W_{OT}	Outfitting weight
$W_{OT-rest}$	Outfitting weight excluding ro-ro ramps
W_{RAMPS}	Weight of ro-ro ramps
W_{ST}	Steel weight
W_{SUPST}	Superstructure steel weight
$webspercompt$	Length of inserted compartment in web frames
X	EEDI reduction rate
$\vec{x}$	Vector of design variables
x_i	Design variable i, $i = 1, \dots, m$

Greek symbol	**Description**
α_i	Polynomial coefficient i of resistance response surface, $i = 1, \dots, 6$
ΔA	Attained subdivision index margin
ΔA_c	Partial attained subdivision index margin at loading condition c, $c = d, p, l$
$\Delta comptsaft$	Change in number of watertight compartments aft of the engine rooms in comparison with the baseline design
$\Delta comptsfore$	Change in number of watertight compartments forward of the engine rooms in comparison with the baseline design
$\Delta EEDI$	EEDI margin for compliance with phase 2
ΔKG_{intact}	Intact stability VCG margin
$\Delta KG_{R8.1}$	SOLAS Ch. II-1 – regulation 8.1 VCG margin
$\Delta KG_{R8.2-3}$	SOLAS Ch. II-1 – regulations 8.2-8.3 VCG margin
ΔKG_{WOD}	Stockholm agreement VCG margin
ΔN_{BHD}	Change in number of transverse bulkheads in comparison with the baseline design
η_0	Propeller open water efficiency
η_R	Relative rotative efficiency
η_s	Efficiency of shafting system
λ_{SHP}	Correction factor for shaft horsepower
ρ	Density of liquid load

List of Abbreviations

Abbreviation	Meaning
A/E	Auxiliary Engine(s)
CAD	Computer – Aided Design
CAE	Computer – Aided Engineering
CFD	Computational Fluid Dynamics
CPP	Controllable-Pitch Propeller
DoE	Design of Experiment
DWT	Deadweight
EU	European Union
E/R	Engine Room
EEDI	Energy Efficiency Design Index
FSM	Free Surface Moment
HFO	Heavy Fuel Oil
HSB	Hochschule Bremen
ILLC	International Load Line Convention
IMO	International Maritime Organisation
LCB	Longitudinal Center of Buoyancy
LCG	Longitudinal Center of Gravity
LSFO	Low Sulfur Fuel Oil
M/E	Main Engine(s)
MARPOL	Marine Pollution
MCR	Maximum Continuous Rating
NPV	Net Present Value
NTUA	National Technical University of Athens
NTUA-SDL	National Technical University of Athens – Ship Design Laboratory
PCC	Pure Car Carrier
PTI	Power Take-In
RANS	Reynolds-Averaged Navier-Stokes
RFR	Required Freight Rate
Ro-Pax	Roll on – roll off / Passenger
Ro-Ro	Roll on – Roll off
SOLAS	Safety Of Life At Sea
US	United States
VAT	Value Added Tax
VCG	Vertical Center of Gravity
WOD	Water On Deck

List of Figures

List of Tables

Chapter 1. Design Characteristics of Ro-Pax Ferries

This chapter provides an overview of the design of modern ro-pax ships, particularly of conventional (monohull, displacement), closed-type ferries. Chapter 1.1 presents some general information. Chapters 1.2 to 1.5 aim to explain their various design characteristics, which stem from a compromise of multiple and sometimes contradicting objectives and constraints. Chapter 1.6 briefly presents the most important safety issues of ro-pax ships, while Chapter 1.7 summarizes the basic rules and regulations that affect their preliminary design.

1.1. Introduction

The ro-pax (roll on - roll off / passenger) ship is a hybrid of the pure passenger ship and the ro-ro (roll on - roll off) cargo ship, used to transfer passengers and vehicles in short-sea liner shipping. The term "roll on – roll off" refers to the loading and unloading of vehicles (private cars and / or trucks) by their own means, through ramps at the stern and sometimes at the bow or – mostly in older designs – at the sides of the ship. This implies the existence of at least one large deck which practically extends through the entire length and breadth of the ship, allowing the unobstructed movement of vehicles. Another distinguishing characteristic is the large extent of superstructures, both in terms of deck area as well as number of decks, enabling the accommodation of a large number of passengers.

It is a relatively new ship type, the development of which can be attributed to the large growth of road transport [1]. Ro-pax ships have displaced large pure passenger ships as a means of transport, which today exist only as cruise ships, while, for longer routes, passenger ships have been replaced altogether by air transportation. This is not the case with pure ro-ro carriers, which continue to operate both in short and medium routes along with ro-pax ships, but also in longer ones (pure car carriers – PCC).

The size of a ferry is usually measured in terms of overall length, passenger / vehicle capacity or gross tonnage (GT). In comparison with cargo ships, their average size is smaller – in 2015, passenger ships constituted 7.7% of ships in the world, but only 3.1% of the fleet in terms of GT [2]. Typical sizes range from around 30 m to over 200 m in overall length and from 150 to over 70,000 GT [3]. The lower limits correspond to ships with very limited vehicle capacity, while the largest ones can carry up to over 3,000 passengers and be fitted with multiple ro-ro decks with thousands of lane meters. Today, the longest ro-pax ships in the world are the sister vessels *Cruise Roma* and *Cruise Barcelona*, with an overall length of 254 m, following conversions (addition of parallel midbody) in 2019.

Figure 1-1. The Cruise Roma during her conversion in Fincantieri shipyards. Source: Fincantieri.

According to [4], the world's busiest seaways are in Europe, including the Mediterranean, the Baltic and the North Sea. About half of the world's ro-ro fleet operates in Europe [3]. Significant numbers of ferries also operate in Japan and North America.

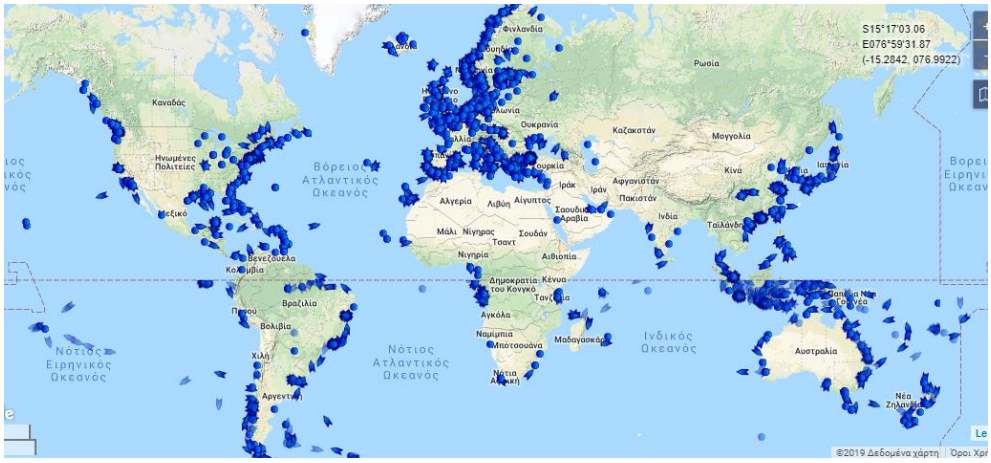

Figure 1-2. Snapshot of worldwide passenger ship positions. Note that pure passenger ships (small ferries and large cruise ships) are also included. Source: Marinetraffic.

In comparison with other conventional ship types, passenger ferries are among the most demanding in terms of design. The two major challenges the naval architect faces both stem from the presence of passengers on board:

1. A high service speed is essential in order to be competitive as a means of passenger transport. Ro-pax ships typically operate at speeds of over 20 knots, while fast displacement ferries can exceed 30 knots, corresponding to Froude numbers over 0.3 and even close to 0.4.[*] Meanwhile, the achievement of a reasonable operating cost is of course crucial. This calls for improved hydrodynamic design of the hull and efficiency of the propulsion system (propellers – engines).

[*] The upper limit is rarely encountered today, due to a trend towards lower operational speeds in recent years, for both financial and regulatory reasons (EEDI).

2. The required level of safety is very high, as large numbers of passengers are carried, without any special training in case of an emergency. Regulations regarding intact / damage stability, fire protection and other safety issues are much more stringent than those of a cargo vessel. In ro-pax ferries, the situation is further worsened by the existence of large car decks at a small distance above the waterline, which are the root of various safety issues to be dealt with.

As usually happens in ship design, these challenges are also partially conflicting. For example, compliance with strict stability requirements may be achieved by increasing the ship's beam – this, however, is disadvantageous for its resistance and therefore operating cost.

Figure 1-3. Fast displacement ferry Nissos Mykonos operates at a service speed of 26 knots, corresponding to a Froude number of 0.38. Source: Attica Group.

Another important characteristic is the low specific weight of the cargo (passengers and vehicles), meaning that the ship's maximum capacity in terms of volume is reached before exceeding the maximum allowable draft. Therefore, passenger ships are classified as *volume carriers*, in contrast with *displacement carriers* such as tankers and bulk carriers [5]. Thus, one of the basic goals of the naval architect is to maximize, for given main dimensions, the total area of vehicle and passenger accommodation decks [1].

Keeping in mind the above, in combination with other factors that must be taken into account irrespective of the ship type, the presentation of the basic characteristics of a typical ro-pax ferry follows.

1.2. Main dimensions

Ro-pax ships are generally slender, meaning their length is large compared to the displacement volume (slenderness coefficient $L/\nabla^{\frac{1}{3}}$ in the order of 6.5 [5]). For constant displacement, increased slenderness leads to reduced wave resistance, but at the same time increased wetted surface and thus frictional resistance. At relatively high Froude numbers, where wavemaking is dominant, increased length generally reduces the overall resistance. Furthermore, superposition phenomena of the bow and

stern transverse wave systems, which result in favorable and unfavorable Froude numbers, are to be taken into account during the selection of the length [6].

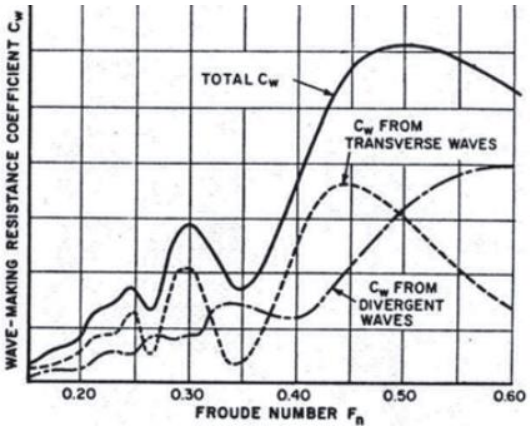

Figure 1-4. Wavemaking resistance coefficient as a function of the Froude number. The effect of the wave superposition phenomena is evident. Source: [6]

Of course, an increase of the length for constant displacement leads to increased lightship weight and building cost. These issues, along with possible navigational constraints, set limits to the slenderness of the ship. However, further increases are likely in the near future, as a means of satisfying new energy efficiency regulations (EEDI).

Compliance with demanding stability requirements is mainly achieved by increasing the ship's breadth (and, for damage stability, by a dense watertight subdivision). This results in length to beam ratios comparable to those of cargo ships, despite the large differences in terms of slenderness coefficient [5]. Furthermore, ro-ro ships are "*linear dimension"* ships in the sense that their beam varies discontinuously, with a step approximately equal to the width of a lane[*] [5].

The draft is generally small, resulting in values of B/T around 4, significantly higher than those considered "optimal" [5]. This is due to the low weight of the transported cargo, in combination with the requirement for a large beam. Limitations to the maximum draft are also set by the depth of the approached ports, shallow straits or canals.

Finally, the large number of accommodation decks increases the total depth of the ship, which, in combination with the low draft, translates to increased air draft. On the other hand, the position of the bulkhead deck must be relatively low to enable fast and convenient loading and unloading of vehicles, but high enough to protect the main ro-ro deck from flooding in case of damage resulting to a hull breach.

Due to the constantly increasing damage stability requirements, L/B, T/B and T/D ratios have decreased over the years [3].

[*] Of course, deviations are possible, for example by increasing the side margins to improve stability.

1.3. Hull form

In general, the hull form of a ferry is very different from that of a low-speed cargo vessel. Some complexities are introduced due to the demand for a high speed with a reasonable operating cost. The associated hydrodynamic improvement outweighs possible disadvantages, such as the increase of the building cost or the lightship weight.

The block coefficient (C_B) takes low values, around 0.52 – 0.62 [3] [5]. A decrease of the block coefficient increases the wetted surface, to which the frictional resistance is proportional, but at the same time decreases the wavemaking resistance, which is dominant at high speeds. Decreasing the C_B also contributes to a smooth flow towards the propellers. The low C_B is achieved by reducing the volume concentration in the forward and aft parts, but also with a small or completely eliminated parallel midbody.

The longitudinal center of buoyancy (LCB) is placed aft of the midship section in order to minimize the transverse bow wave, which contributes the most to the wavemaking resistance. Typical positions are around 2% to 5% of L_{PP} aft of midship, with the percentage increasing the higher the design Froude number [5].

Moving towards the bow, the most prominent hull characteristic is the bulb. Ro-pax ships are usually equipped with long, “goose-neck” type bulbs which pierce the design waterline. At relatively high Froude numbers, the major advantage of a bulbous bow is the generation of an independent wave system, which starts with a crest and, if designed correctly, interferes destructively with the bow wave, reducing its height [6]. A bulbous bow modifies the flow in other ways as well, such as by increasing the “effective” hydrodynamic length of the ship, with a positive impact of wavemaking, but also by increasing the wetted surface of the ship for given displacement, with a negative effect on frictional resistance.

Above the waterline, the bow is usually flared and raked forward to increase the total available deck area.

Figure 1-5. Bulbous bow of modern ro-pax ferry. Source: www.shipfriends.gr.

Regarding the stern, “buttock-flow” forms with a central skeg are typical. Above the waterline, maximum beam is usually maintained throughout the entire stern area up to the transom. This maximizes the deck areas, allows for the installation of the loading / unloading ramps and improves stability. Aft of the transom, an extension of the hull called “duck tail” is often found. The duck tail increases the waterline length (decreasing the effective Froude number) and also provides buoyancy which reduces the dynamic trim towards stern which is developed at high speeds.

Figure 1-6. Stern of modern ro-pax ferry. Source: www.gcaptain.com.

1.4. General arrangement

Figure 1-7 and Figure 1-8 present the general arrangement of a typical large ro-pax ferry. As seen in the figures, the decks of a ro-pax ship can be divided in three distinct groups: the lower decks, which are mainly occupied by machinery spaces, the ro-ro decks where vehicles are loaded, and the passenger accommodation decks on the superstructure.

Regarding the lower region (below deck 3), the aft part of the ship contains the engine room(s) as well as other auxiliary rooms (engine control room, auxiliary machinery spaces, provisions) and tanks (fuels and lubricants, fresh water, ballast water etc). The engine room(s) and the propulsion system will be discussed further in Chapter 1.5. Forward of the engine rooms, one or more relatively small car decks (lower holds) may be arranged in larger ships, which are protected in case of side damage by longitudinal bulkheads.

Moving upwards, the first extensive car deck is the main ro-ro deck, on which the vehicles are loaded. The main deck is connected to the other ro-ro decks by fixed or movable internal ramps. Since the main ro-ro deck must allow the unobstructed movement of vehicles, the transverse watertight bulkheads cannot extend above it. In the particular design, as in many large ro-pax ships, an additional ro-ro deck for trucks lies above the main deck. In order to adjust the payload to seasonal demand variations, hoistable car decks are also frequently used. A hoistable deck can be lowered when the demand for private car transportation is high, converting one ro-ro deck for trucks into two decks for private cars [1].

The main and the upper ro-ro decks are penetrated by the engine casing, a long and narrow structure which provides connection between the upper and lower decks as well as ventilation of the lower decks. Some ships are equipped with one central casing, while others with two casings at the sides. Each choice has its advantages and its disadvantages. For example, a central casing supports the upper decks, constituting an important strength element of the ship and reducing vibrations and eventually the steel weight, while side casings can improve survivability after side damage and at the same time provide a large unobstructed area for easier movement and maneuvering of large vehicles [1]. In order to maximize truck capacity, a central casing is placed symmetrically around the center plane if the number of lanes is odd, or on one side of the center plane if the number of lanes is even.

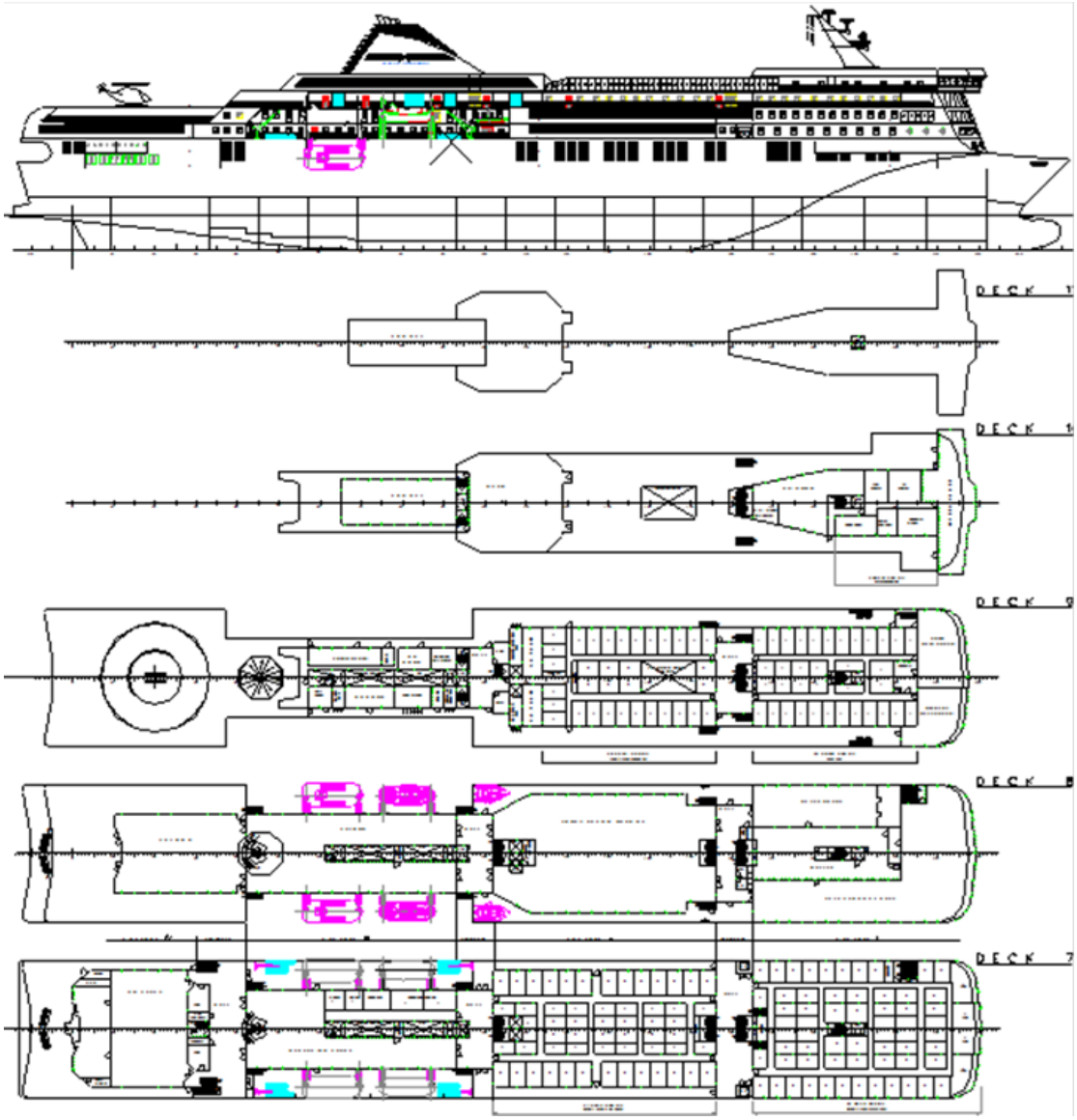

Figure 1-7. Profile and upper decks.

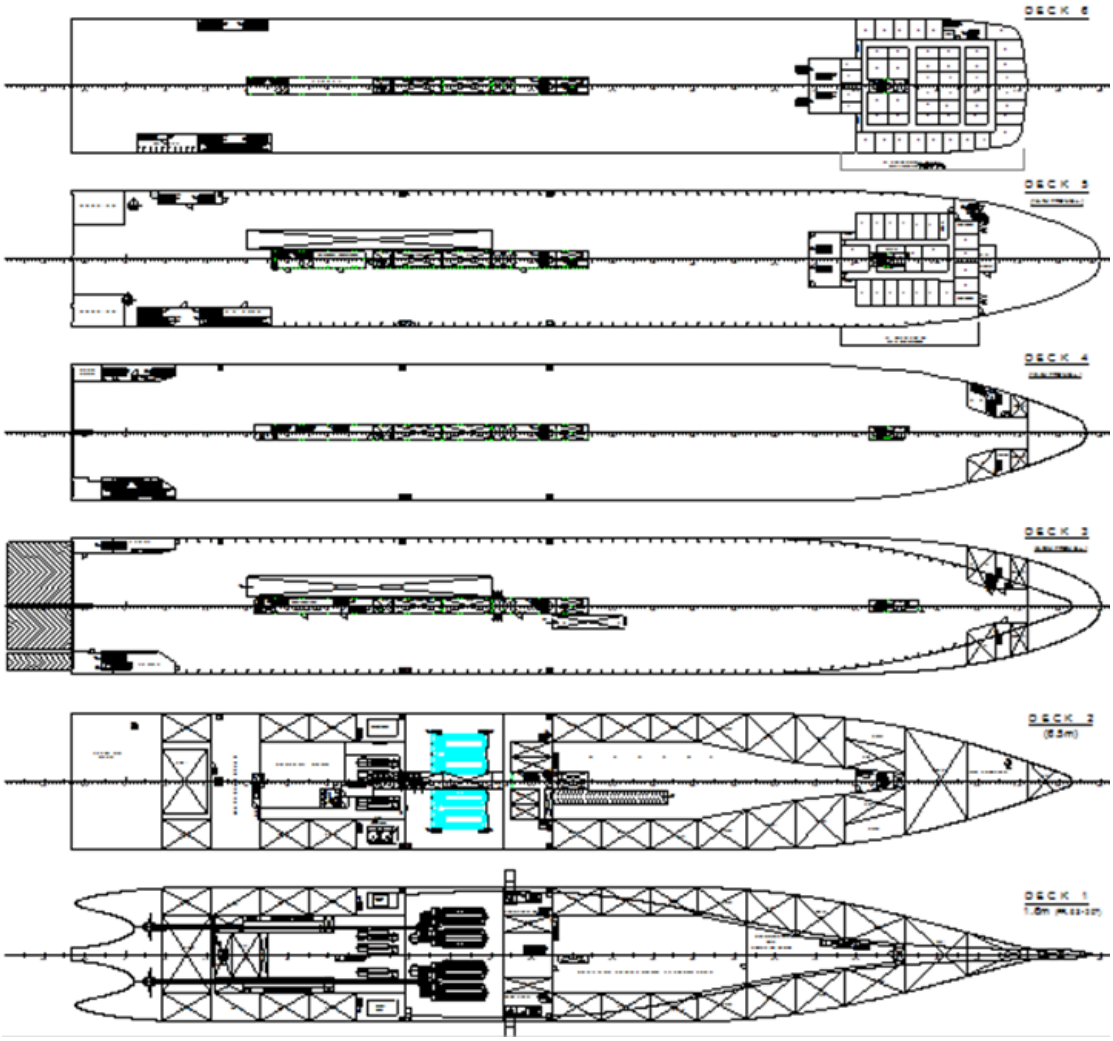

Figure 1-8. Ro-ro decks and lower decks.

Finally, the upper decks are occupied by cabins for passengers, officers and lower crew, airseats for passengers as well as various internal and external public spaces. Depending on ship size, trip duration and accommodation standards, these can include restaurants and galleys, bars, shops etc. The upper decks also house the wheelhouse, lifesaving equipment (lifeboats and/or liferafts), the funnel, the emergency generator room and other service spaces.

The most important safety concern regarding the accommodation decks is fire protection. In terms of the general arrangement, each deck is subdivided into "main vertical zones" by "A-class" divisions, designed to delay the spreading of fire. In general, the maximum allowable length of a main vertical zone is 48 m, as long as its total area on any deck does not exceed 1,600 m^2. Increased fire protection is also required for spaces with large ignition probability (eg. galleys), as well as for spaces which are vital for the safe operation and evacuation of the ship (eg. wheelhouse and staircases). Other spaces are also transversely and horizontally subdivided by thermal barriers.

The minimization of such barriers within the limits prescribed by the rules is desired by the naval architect, in order to facilitate the design of large public spaces and to maintain the ship's building cost at a reasonable level. For example, it is noted that the addition of a fire zone comes not only with an extra fire-resistant steel bulkhead, but also a staircase, an air conditioning station, active fire protection equipment etc.

1.5. Propulsion system

The fact that the main ro-ro deck must be continuous sets a limitation to the maximum vertical extent of the engine room(s), and therefore to the height of the main engines. This is one of the reasons why four-stroke, medium-speed Diesel engines are used in ro-pax ferries rather than two-stroke engines. These are coupled to the propellers with gearboxes, as the operating speeds of these engines are significantly above a propeller's optimal point. Furthermore, due to the "buttock-flow" stern the engine rooms are shifted forward from the transom, which unavoidably increases the length of the shafting system and reduces useful cargo space in the lower hold(s).

Passenger ships are usually equipped with two or four main engines, firstly for redundancy reasons and secondly because of their increased power requirements. This also increases the flexibility of the system, for example by allowing the operator to shut down half of the engines and operate the rest at a relatively high load when the ship is slow steaming. Until recently, all engines were usually placed in a single main engine room. Since 2010 however, large passenger ships must be able to survive the flooding of any one watertight compartment and be able to return to a port using their own means and at a minimum speed. One way to fulfill this requirement is to divide the engines between two engine rooms. The useful cargo space which is lost may be in part retrieved by eliminating the auxiliary engine room and installing the auxiliary engines in the two main engine rooms. This solution also increases the cost of the ship and means that there are two adjacent large compartments in the aft part of the ship, jeopardizing its safety in case of a side damage resulting in the flooding of both. Another solution is to maintain the "traditional" engine room arrangement, but enable the shafts to take in power from the auxiliary engines (PTI) in case of an emergency [1]. Overall, the "safe return to port" regulation is estimated to have increased the building cost of a ro-pax between 2% and 5% [4].

Ro-pax ships are equipped with two propellers, powered by one or two main engines each. Once again, one reason for this is redundancy. Moreover, the small draft imposes a limitation to the maximum propeller diameter. In combination with the large delivered horsepower, the use of two propellers is required in order to achieve higher efficiency and avoid cavitation issues. Controllable pitch propellers (CPP) are a popular choice for ro-pax ships, enabling the master to optimize the pitch for speeds lower than the design speed, as well as enabling easier astern propulsion and maneuvering in ports. It should be noted that, although the nominal pitch of the propellers can change, its distribution is optimized only for one operation point [5]. Finally, the efficiency of a CPP at the design point is generally lower than that of an equivalent fixed pitch propeller, due to the increased hub diameter.

The use of Azipods as propulsors has also been examined. Unlike cruise ships however, this system has – so far – not prevailed in ro-pax ships, possibly due to its increased cost.

In the last few years, newly-adopted environmental regulations have set the spotlight on alternative power and propulsion systems. Possible power alternatives include the use of gas engines, hybrid electric or purely electric propulsion (for short routes) etc. Various systems that utilize "green" energy to assist the main propulsion system are also under examination, with characteristic examples being sails, flapping foils and Flettner rotors [7].

1.6. Safety issues

The characteristics of ro-pax ships come with certain inherent problems which can jeopardize their safety and have in fact led to tragic accidents in the past. Some of the most important issues according to the International Maritime Organization (IMO) [8] are presented below.

- **The lack of internal bulkheads / low freeboard.** As mentioned already, transverse bulkheads cannot extend above the main ro-ro deck, which is located close to the waterline. In case of damage that breaches that deck, not only is a large volume flooded but also a very large free surface is generated, the effect of which to the ship's stability can be detrimental. Furthermore, the lack of bulkheads means that fire can spread very easily.
- **The loading ramps.** These are weak spots of the structure and cannot be considered completely watertight, especially due to possible damages over the years.
- **The transported cargo.** This applies to both cargo transported inside a trailer, but also to the vehicles themselves. Potential results of cargo breaking loose are increased list, spillage of dangerous substances or even damage to the ship's structure. Meanwhile, refrigerated trucks can be a source of ignition.
- **Life-saving equipment**. As lifeboats are located high on the superstructures, at large heeling angles half of them are impossible to launch. This problem is not as important today due to the partial replacement of lifeboats by liferafts.

Other potential problems can also be traced:

- **Local strength of the ro-ro decks.** The cargo transported on ro-ro ships in trucks might be relatively light, but the loads are received by the structure through the small areas of the trucks' wheels. This means that the plates of the ro-ro decks are locally subject to high pressures, which must be taken into account during the structural design [1].
- **Dynamic instabilities.** The combination of a flared bow and a flat stern can potentially lead to dynamic instabilities, such as parametric rolling [9].

Of course, accidents are usually caused by an unfortunate combination of more than one factors. An example is one of the deadliest maritime disasters of the 20th century, the sinking of the Estonia in 1994. The under-designed lockings and hinges of the bow visor failed due to rough weather [10]. Subsequently, the large inflow of water on the car deck quickly created a very large free surface which resulted in the ship capsizing within minutes and 852 lives being lost.

Figure 1-9. The tragic MS Estonia with her bow visor opened.

1.7. Regulatory framework

The entire life of a ship, including its design, construction, operation, maintenance and recycling, is governed by a set of rules and regulations, which impose constraints to the ship design optimization problem. Most of them aim to protect human life and the environment. Very important are those set by the International Maritime Organization (IMO), mainly through international conventions: Safety of Life at Sea (SOLAS), Marine Pollution (MARPOL), International Load Line Convention (ILLC), International Code on Intact Stability (Res. MSC.267(85)) etc. The same goes for class rules, which are set by classification societies and have to do with the ship's construction (materials, global and local strength), machinery, electrical installations etc. Regional and national regulations often also apply, for example the EU Stockholm agreement and regulations by the US Coast Guard respectively.

Table 1-1 lists examples of such constraints which considerably affect a ship's preliminary design. A very brief presentation of some of the most important rules and regulations regarding safety of human life and environmental protection follows.

Table 1-1. Examples of rules and regulations affecting the basic design of a ro-pax [11], [12], [13]. The list is in no way exhaustive.

Constraint	**Description**	**Imposing Authority – Convention**
Intact stability criteria	General stability criteria based on the righting lever (GZ) curve and special criteria for passenger ships.	IMO – Intact Stability Code
Damage stability criteria	Damage stability assessment based on a probabilistic method. Supplementary deterministic requirements apply for passenger ships.	IMO – SOLAS
Water on deck	Additional damage stability criteria regarding survivability after flooding of ro-ro deck.	European Union – Stockholm agreement
Collision bulkhead and double bottom positions	Sets forward and aft limits of collision bulkhead and lower limit of inner bottom height.	IMO – SOLAS
Maximum allowable draft	Limits the ship's draft as a function of its main characteristics. Not critical for passenger ships and volume carriers in general.	IMO – ILLC
Structural member scantlings	Determines minimum allowable dimensions and/or thickness of each structural member of the ship according to its expected loading, including empirical, semi-empirical as well as first-principle calculations.	Class rules
Fire protection	Defines thermal subdivision requirements, tank arrangement constraints, required firefighting equipment etc.	IMO – SOLAS
Safe return to port	Requires large passenger ships to be able to return to port by their own means after one-compartment damage.	IMO – SOLAS
Evacuation	Affects arrangement of accommodation spaces by setting a maximum allowable time for evacuation of the vessel.	IMO – SOLAS
Life-saving appliances	Governs the required capacity of lifeboats and liferafts on board.	IMO – SOLAS
SO_X, NO_X emissions reduction	Requires use of low-sulfur fuel (eg. low sulfur fuel oil, LNG) or installation of scrubber for SO_X emission reduction, and selection of compliant engines for NO_X emission reduction.	IMO – MARPOL
CO_2 emissions reduction	Requires ships to be energy efficient by imposing a maximum "energy efficiency design index" (EEDI), possibly limiting the maximum speed.	IMO – MARPOL

Arguably, the basic pillars of safety for a passenger ship are stability and fire protection.

Stability can be subdivided into intact and damage stability. The relevant regulations are critical and must be examined from early stages of the design, as they affect the main dimensions and the watertight subdivision of the ship. Intact stability is covered by IMO's intact stability code, specifying various criteria to be satisfied for a loading condition to be deemed acceptable. These include inequality constraints regarding properties of the righting lever curve, the severe wind and rolling criterion (weather criterion), as well as additional requirements for passenger ships specifying maximum heeling angles due to crowding of passengers and due to turning.

Regulations governing damage stability are more complicated. They include the probabilistic assessment method of IMO, requiring investigation of multiple damage scenarios in order to determine the probability of survival after damage ("attained subdivision index", A), which must be at least equal to a minimum value ("required subdivision index", R). For large passenger ships, SOLAS incorporates also some deterministic elements in order to ensure survival after minor side damages and bow damages. The above are defined in Chapter II-1 of SOLAS. Finally, the EU Stockholm Agreement imposes deterministic requirements for ro-pax ships sailing in the European Union, aiming to provide protection against capsizing after accumulation of water on ro-ro decks.

Regarding fire protection, various prescriptive requirements are defined in Chapter II-2 of SOLAS, the most important of which have already been mentioned in Chapter 1.4.

Environmental protection is the second major concern after the safety of human life. This has become increasingly important in recent years, with the introduction of regulations in MARPOL Chapter VI [12] regarding the reduction of pollutants (NO_X, SO_X) and CO_2 emissions from ships. An important implication of these regulations in ship design is the drastic reduction of SO_X emissions starting in 2020. This will require either the use of an alternative fuel instead of heavy fuel oil or the installation of a scrubber, a system of high complexity and initial cost.

The other important addition of MARPOL Chapter VI is the adoption of the Energy Efficiency Design Index (EEDI), aiming to reduce CO_2 emissions from ships. The regulation "forces" new ships to be more energy efficient, and thus more environmentally friendly. It is to be implemented in three phases, gradually requiring more efficient ships in comparison with the reference EEDI line (phase 0) which was determined from a regression analysis of operating ships, representing the state of the industry at that time.

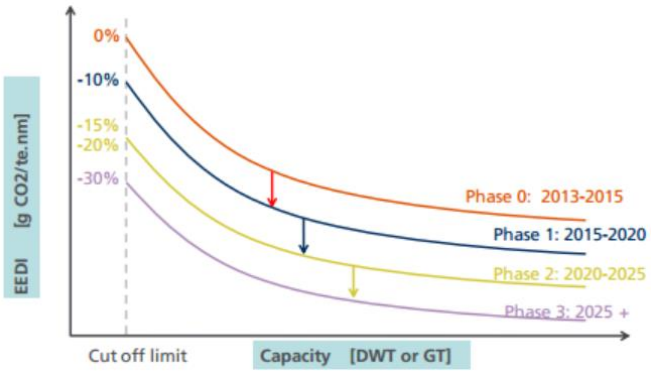

Figure 1-10. Required EEDI curves [14].

The goal is to improve the efficiency of the hull – propeller – engine system, or adopt innovative efficiency technologies that make use of "green" energy. If, however, this is not achieved, ships might be required to reduce speed, especially as the requirement gets stricter with time (approximately: $EEDI = \frac{emissions}{transport\ work} \propto \frac{V^k}{V} = V^{k-1}, k \geq 3$).

Chapter 2. Parametric Ship Design and Optimization

This chapter deals with parametric ship design and optimization. Chapter 2.1 presents the phases the design of a ship is traditionally divided into. Chapter 2.2 defines ship design as a parametric optimization problem. Chapter 2.3 elaborates on the use of parametric methods for basic ship design. Finally, Chapter 2.4 briefly presents genetic algorithms as a method for solving the optimization problem.

2.1. Ship design phases

During the design of a new ship, the naval architect faces the challenge of translating a set of owner's requirements into a functional vessel, which adheres to a number of physical and regulatory constraints and is techno-economically optimal (or near-optimal). The complexity of the problem prohibits addressing it fully at once. In general, ship design is divided in four basic phases [5]:

A. Concept Design – Feasibility Study. The goals of this stage are a rough estimation of the mail technical characteristics of the ship (main dimensions, block coefficient, propulsion power) and a sketch of the general arrangement, according to the owner's requirements.
B. Preliminary Design. In this stage, calculations are performed in more detail in order for the main dimensions and basic characteristics, the hull form and the general arrangement of the ship to be determined with good accuracy. After the preliminary design, all important technical characteristics of the ship, as well as the building and operational cost, can be reliably estimated. The feasibility study and the preliminary design are often jointly referred to as the "basic design".
C. Contract Design, where detailed calculations are performed and drawings are elaborated with the required accuracy for the shipbuilding contract between the yard and the owner to be drawn up.
D. Detailed Design, which includes the design of each element of the ship's structure, equipment and machinery, in order to provide the necessary drawings to the manufacturer or the supplier of each element.

Each phase contains various design steps, including some or all of the following: main dimensions, hull form, lightship weight, general arrangement, loading conditions, intact and damage stability, resistance and powering, structure, seakeeping and maneuverability analysis etc.

As the design progresses, more advanced methods are employed for the realization of the aforementioned studies. For instance, in the concept design stage the required power is roughly estimated using empirical formulas and data from similar ships (eg. the British Admiralty formula). During preliminary design, estimations can be improved using more detailed empirical methods or computational methods (potential

flow or RANS calculations). In the contract design, when the hull form is finalized, the previous predictions can be verified by constructing a model and performing tank tests.

The above traditional methodology is illustrated in the well-known design spiral, introduced by Evans in 1959 [15]. According to Papanikolaou [5], the first loop corresponds to the concept design, loops 2-4 to the preliminary design while loop 5 to the contract design. The design spiral emphasizes the sequential and iterative nature of the process required to converge to an "optimal" ship.

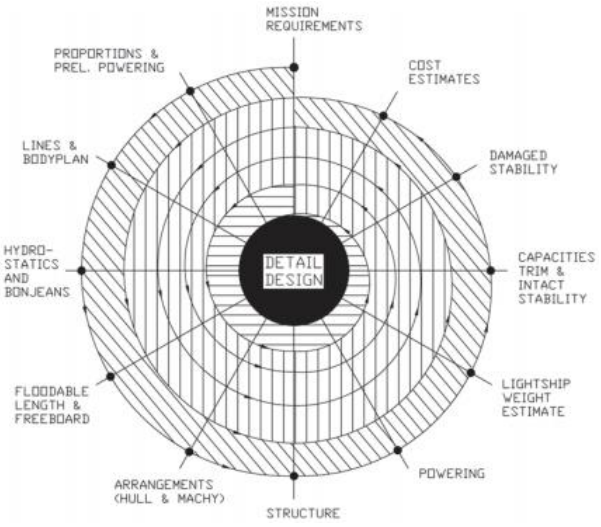

Figure 2-1. The ship design spiral [5].

2.2. The ship design optimization problem

The design of a ship can be mathematically expressed as a generic optimization problem in the following form:

$$\min_{\vec{x}} \vec{F}(\vec{x},\vec{p}) = \min_{\vec{x}} \begin{Bmatrix} f_1(\vec{x},\vec{p}) \\ f_2(\vec{x},\vec{p}) \\ \vdots \\ f_n(\vec{x},\vec{p}) \end{Bmatrix}, \quad \begin{matrix} \vec{x} = (x_1 \quad x_2 \quad \dots \quad x_m) \in \Omega \subseteq \mathbb{R}^m \\ \vec{p} = (p_1 \quad p_2 \quad \dots \quad p_l) \in \Omega' \subseteq \mathbb{R}^l \end{matrix}$$

$$subject\ to: u_i(\vec{x},\vec{p}) \geq 0,\ \ i = 1,\dots,I\ ,\ \ v_j(\vec{x},\vec{p}) = 0,\ \ j = 1,\dots,J$$

The terms and symbols that appear in the above definition are explained below.

- $\vec{x}$ is the vector of **design variables**, the characteristics of the vessel which are to be optimized. For example, design variables of a ship design optimization problem could be the main dimensions, the block coefficient, the LCB, the shape of the bulbous bow or the transom, the number and positions of transverse bulkheads etc.
- $\vec{p}$ is the vector of **parameters**, the factors which affect the design but are either out of the designer's control or the designer chooses to keep them constant during the optimization procedure. Some examples are the clear height of a ro-ro deck, the dimensions of a standardized container and the cost per ton of steel weight.

- $\vec{F}(\vec{x},\vec{p})$ is the vector of the **evaluation criteria (objective functions)**, the criteria according to which a design is assessed. Examples of objective functions to be minimized are: resistance or propulsion power, lightship weight, building cost, required freight rate (RFR) etc. It is obvious that maximization problems are also addressed by the above definition by replacing $f_i(\vec{x},\vec{p})$ for example with $-f_i(\vec{x},\vec{p})$, with relevant examples being the maximization of payload or DWT and the maximization of the net present value (NPV) of the investment.
- $u_i(\vec{x},\vec{p})$ and $v_j(\vec{x},\vec{p})$ represent **constraints**, the inequalities or equalities to be satisfied in order for the design to be acceptable. In ship design, constraints can arise from physical laws (eg. Archimedes' principle), owner's requirements (eg. deadweight, speed, navigational constraints) and relevant rules and regulations (eg. SOLAS, MARPOL, ILLC, Class rules).

As can be deduced from the above, the design of a ship is in general a multi-objective, multi-parametric and multi-constrained problem. Moreover, it is highly non-linear, with the influence of each design variable on the objective functions being complex and sometimes not even qualitatively predictable.

A special case of the above general formulation is the existence of only one objective function, in which case $\vec{F}(\vec{x},\vec{p})$ is replaced by a scalar quantity (single-objective optimization). This is a relatively simple case, as the optimum can be uniquely determined. However, practical applications usually involve more than one evaluation criteria (multi-objective optimization), which are frequently inherently conflicting. In such cases, the optimum is to be selected from a set of possible solutions.

An example is the two-criteria optimization of a ship in terms of building cost and operating cost. Minimization of the building cost usually results in short and full designs (small length, high block coefficient) in order to minimize the weight of the required steel. On the other hand, minimization of the operating cost is typically attained by long and slender designs, due to their reduced resistance and thus fuel consumption [5]. From a shipowner's perspective, the final decision is a compromise between the two. Of course, it can be argued that the two criteria can be merged in a more comprehensive criterion such as the RFR or the NPV, which takes into account both the building and operational cost, and thus a global minimum or maximum can be found.

Since the result of a multi-criteria optimization is not uniquely defined, various methods can be applied to determine the set of optimal members. The most widespread one makes use of the concepts of "domination" and "Pareto optimality", the definitions of which for a maximization problem follow:

Let $\vec{x}_1,\ \vec{x}_2$ be two solutions which satisfy all constraints. Then, $\vec{x}_1$ dominates $\vec{x}_2$ if and only if $[f_i(\vec{x}_1) \geq f_i(\vec{x}_2)\ \forall\ i \in \{1,\dots n\}] \wedge [\exists\ j \in \{1,\dots n\}\ f_j(\vec{x}_1) > f_j(\vec{x}_2)]$ ($\vec{x}_1$ is at least as good as $\vec{x}_2$ in terms of all objective functions, with at least one strict inequality). Symbolically: $\vec{x}_1 \succ \vec{x}_2$.

A solution $\overrightarrow{x^*}$ is "Pareto optimal" if and only if $\nexists\, \vec{x} \succ \overrightarrow{x^*}$ ($\overrightarrow{x^*}$ is not dominated by any other solution).

The Pareto optimal solutions constitute the Pareto set, the graphical depiction of which is the Pareto front. As an example, the Pareto front of a random set of points for a two-criteria maximization problem is depicted in Figure 2-2[*].

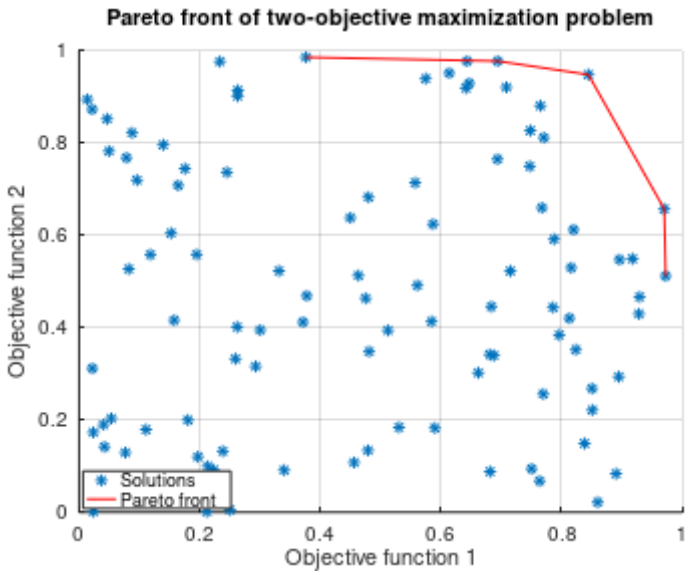

Figure 2-2. Pareto front of a random population for a two-objective maximization problem.

From the solutions belonging to the Pareto set, the selection of the optimum depends on the designer's preferences, the relative importance of each objective function etc.

In practice, the definition of ship design as a "generic optimization problem" which was presented in this chapter cannot be applied directly for the design of a new ship due to the complexity of the problem. Thus, the concept of ship design phases is utilized to decompose the problem into simpler ones, resulting in a multi-stage optimization system, in which each stage deals with different parameters of the problem.

For example, Papanikolaou et al. [16] have used a three-stage approach for the optimization of a SWATH passenger/car ferry. The first stage is a parametric study in order to determine the optimal capacity and speed for the vessel, using economic criteria. With given capacity and speed, the second optimization stage aims to find the main dimensions and principal characteristics of the lower hulls and struts that minimize the ship's resistance (basic design phase). Finally, the third stage deals with a local optimization of the hull form, further reducing the resistance for given principal characteristics.

[*] To be precise, the presented Pareto front corresponds to a continuous population of designs, some instances of which are those depicted by asterisks.

This could be followed for example by a structural optimization in order to determine the layout and scantlings of structural members that minimize the lightship weight while conforming to strength requirements.

Here it is assumed that local details do not interfere with global characteristics, i.e. that the optimal global characteristics which have been determined at a previous stage remain optimal after minor local modifications. This assumption is logical and in line with the traditional approach for solving complex problems, according to which the problem is decomposed into simpler ones using heuristic methodologies.

2.3. Parametric optimization in basic ship design

As mentioned already, by the end of the basic design all important characteristics of the ship have been reliably estimated. The traditional methodology followed during basic design regarding the main dimensions and the general characteristics of the ship is the "relational or empirical method". The designer acquires relevant information by studying one or more specific existing vessels, and/or diagrams and regression equations derived from the study of existing vessels, and bases the new design on it.

For the successful implementation of the "relational or empirical method", two assumptions must hold true:

1. Existing designs are, indeed, "near optimal", due to natural selection processes that take place in the shipping industry, meaning that "good" designs survive while "bad" ones are eliminated.
2. By studying "near optimal" ships the resulting ship is also "near optimal" – in other words, the objective functions are continuous and sufficiently flat around that "near optimal" point.

This approach results in a design which is feasible and – if the two assumptions hold true – also "near optimal".

The alternative to the "relational or empirical method" is the "parametric method", where a parametric model is constructed and used as the core of a formal optimization procedure in order to produce truly optimal designs [17]. In contrast with the manual process described above, a single model is constructed and used to examine different designs, in which all calculations are performed automatically.

Apart from greatly reducing the volume of manual design work, this method can result in improved designs, as the employed optimization algorithms are able to overcome possible local optima, in which the designer could be trapped during a manual procedure.

An indicative flowchart of the parametric optimization procedure as applied for the basic design of a ship is presented in Figure 2-3.

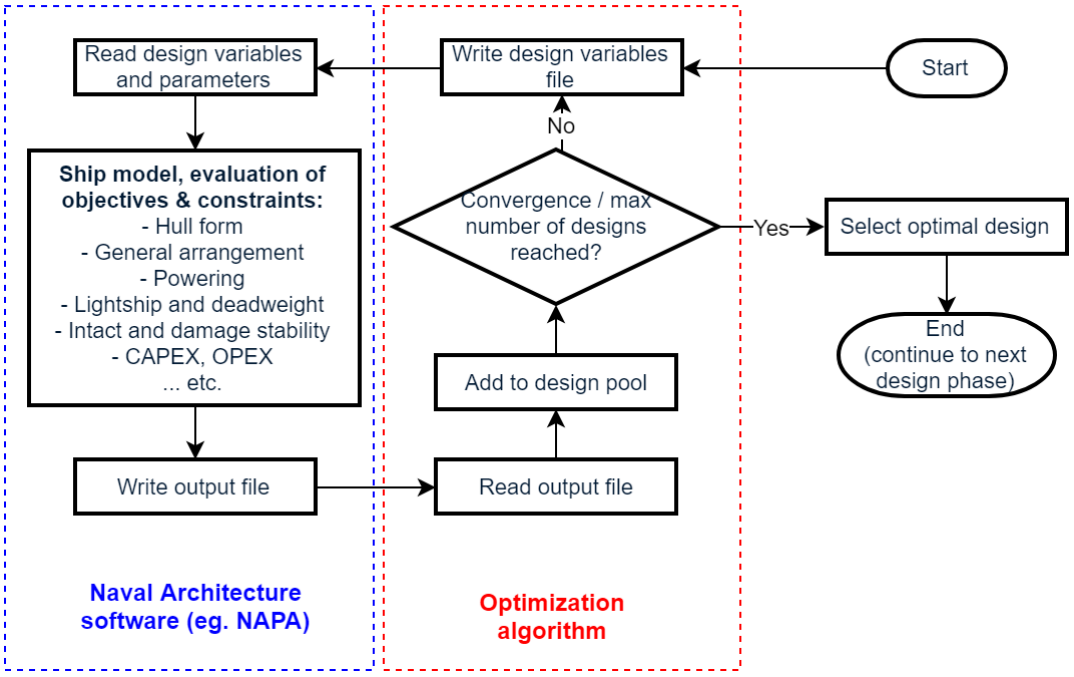

Figure 2-3. Illustration of the basic design parametric optimization procedure.

The use of parametric methods for basic ship design is by no means a new development. The first attempts at parametric optimization, using simplified / empirical models, can be traced back to the middle 1960s [18]. However, accelerating developments in computer hardware and software tools mean that parametric design methods are constantly evolving, enabling naval architects to assess more and more aspects of ship design with satisfactory accuracy at an early stage.

A parametric model gives a geometric representation of the ship, which is utilized within a series of related calculations. For a system as complex as a ship, building a parametric model is quite a challenging task: a “good” parametric model is simple, so as to avoid unnecessary complications and increase generality of application, but simultaneously realistic enough for the results to be of value [17].

The geometric representation depends on the breadth and complexity of required calculations, which, in turn, depend on the design phase and the required level of accuracy. In preliminary design, estimation formulas can be used, giving priority to fast calculations rather than high accuracy.

For basic design, a geometric model typically includes at least the hull surface, the main watertight boundaries (decks and bulkheads) and the most important compartments. These are sufficient for a good estimation of values of interest such as the payload, propulsion power, financial indices as well as the most important constraints (eg. stability). A hull surface can be fully parametric, with each curve being explicitly defined as a function of certain parameters, or partially parametric, meaning that a new hull is generated by imposing transformations on an existing one. The second alternative is simpler, but the first gives the designer more flexibility. As

an example, Figure 2-4 depicts two forebody design variants of a ro-pax, produced by a fully parametric hull model using the FRIENDSHIP-Modeler [19]. Such a model can be coupled with computational hydrodynamics software for calm water resistance or seakeeping calculations.

A more sophisticated model could include the structural representation of the ship rather purely topological information. The scantlings of the structural members can be determined according to the rules of a classification society or by first principles. Furthermore, structural parameters can be introduced to the problem, regarding for example the arrangement and dimensions of stiffeners, which can be optimized for minimum structural weight. Apart from the obvious advantage that the ship's structure is addressed at an early design stage, another major advantage of a parametric structural model is the direct calculation of the steel weight, which constitutes the largest percentage of the lightship, for each examined alternative design. An example of a parametric model including structural calculations and enabling the direct calculation of the steel weight is presented in Figure 2-5 [20].

Of course, the parametric modeling of ship's structure without even the main dimensions being fixed is not a simple task. A compromise would be to calculate the weight per running meter only in the midship region, add the weight of transverse structural members and use appropriate correlation coefficients from similar ships to calculate the final steel weight.

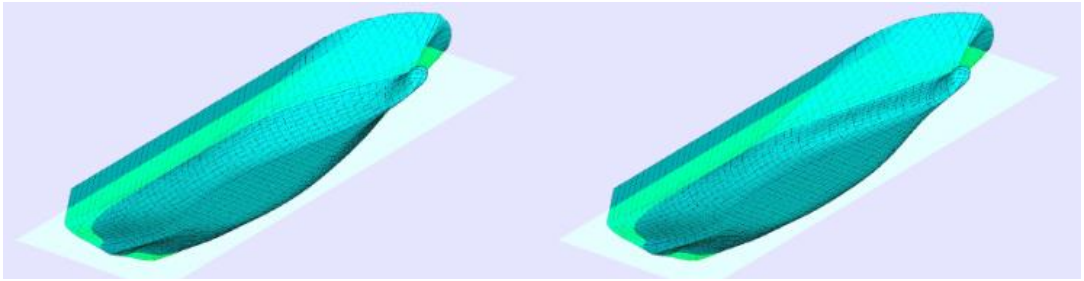

Figure 2-4. Forebody design variants generated from a parametric hull model [19].

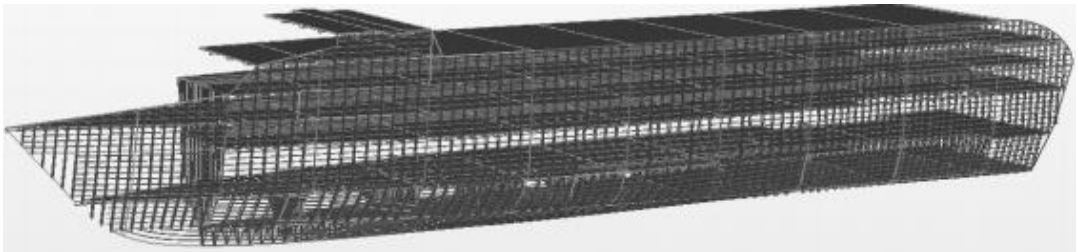

Figure 2-5. Parametric structural model of fast monohull ro-pax ship [20].

Table 2-1 presents some examples of calculation methods that can be implemented, starting from the simplest ones, which can be used in very early concept design and only give rough estimations, and gradually moving towards direct calculations, which are the most complex but most exact. The selected examples concern the calculation of steel weight, calm water resistance and stability.

Table 2-1. Examples of calculation methods for basic design.

Steel weight	**Calm water resistance**	**Stability (intact or damage)**
Empirical / statistical methods	Similar ships (eg. British Admiralty formula)	Empirical formulas
Volumes and areas (weight per m^3 or per m^2)	Empirical / statistical methods	Direct calculation of stability criteria
Lengthwise integration of transverse section weight per meter	Potential flow calculations combined with empirical methods	
Full structural layout	RANS calculations	

The accuracy of empirical methods can be improved if reference values from similar ships are used for calibration. Furthermore, if the selected design methodology involves computationally demanding calculations, these can be substituted by surrogate models (or response surfaces or metasurfaces). These models are based on data derived from exact evaluations for a series of designs and are therefore much more accurate than general empirical formulas, as they have been produced for a particular optimization problem.

2.4. Genetic algorithms

Various methods have been developed for the solution of an optimization problem, both deterministic and probabilistic, each one with different advantages and limitations. A simplistic and straightforward approach is the exhaustive search, referring to the sequential evaluation of many members of the design space (or all of members, if the design space is discrete). For multi-parametric and multi-objective problems however, exhaustive search is out of the question, especially if time-consuming calculations are involved and high accuracy is desired.

A widely used search method for such complex optimization problems is the use of genetic algorithms. These are probabilistic algorithms which mimic the evolution processes that take place in nature, introduced by Holland in 1975 [21]. As genetic algorithms have also been used in this project, this section briefly presents their general characteristics.

A genetic algorithm starts with an initial population within the search space and gradually produces new generations by imposing genetic operators on the previous one and keeping the “fittest” members that occur. The exact procedure varies from algorithm to algorithm, but an indicative flowchart is presented in Figure 2-6 below. A brief explanation of the various steps follows, referring only to binary coding for simplicity.

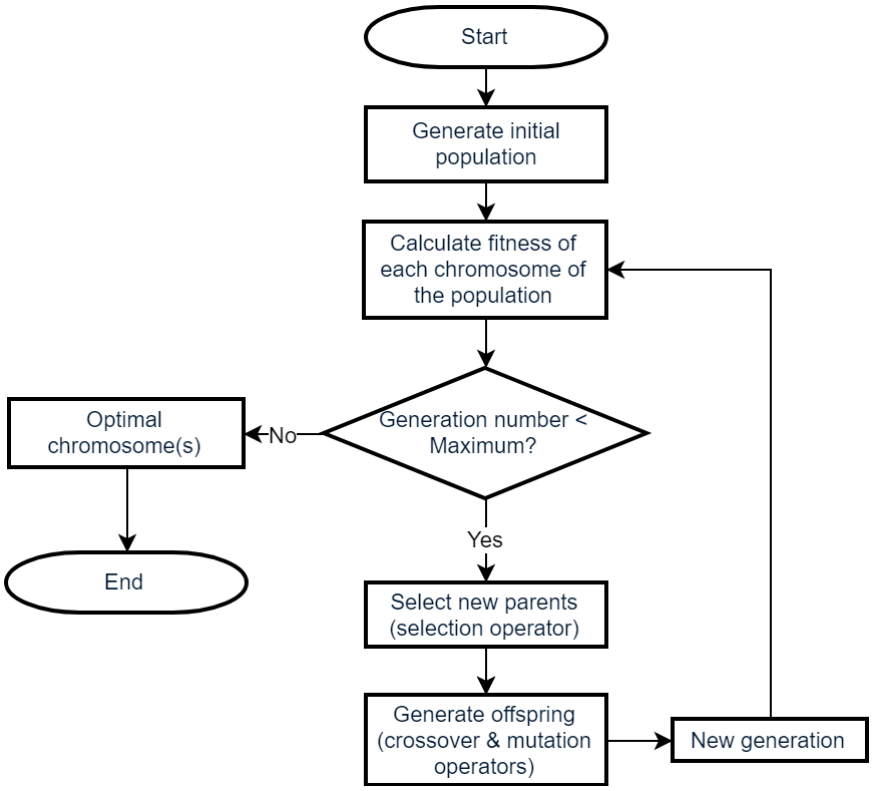

Figure 2-6. Basic steps of a genetic algorithm.

- **Initial population**
  The initial population can be selected randomly or quasi-randomly. Very often the quasi-random Sobol sequence is used, as it covers the search space more evenly in comparison with random sequences.
- **Evaluation of chromosomes**
  A genetic algorithm must be able to assign each "chromosome" (member of a generation) a value of "fitness", which is used to determine its probability of survival. In single-objective optimization, that is easy, as the evaluation function can be the same as the objective function. In multi-stage optimization however, due to the possibly contradicting objective functions, things are not as simple. One possibility is to classify the population in Pareto fronts and assign fitness values accordingly - the members of the first front have the highest fitness, etc. Between members of the same front, highest fitness can be assigned to those that are most "isolated" (furthest away from the others), in order to facilitate "exploration" of the search space, in contrast to "exploitation". This reduces the probability that the algorithm gets "stuck" at a local optimum due to not exploring the search space enough.
- **The selection operator**
  The selection operator selects pairs of chromosomes ("parents") which are used to produce the next generation ("offspring"). The selection is stochastic, based on the fitness of each member; members of higher fitness are assigned higher probability of being selected as parents. One method of choosing parents is the "roulette

wheel" selection: each member is assigned a part of a roulette wheel which is proportional to its fitness. Each time the roulette is spun, one parent is selected.

- **The crossover operator**

  The crossover operator is used on each pair of parents, typically with a large probability (eg. 70%), and produces two new offspring. This can be implemented in many ways, the simplest of which is the single-point crossover, where the parents' chromosomes are crossed over at one randomly selected point. If the crossover operator is not activated, the parents survive unchanged to the new generation.

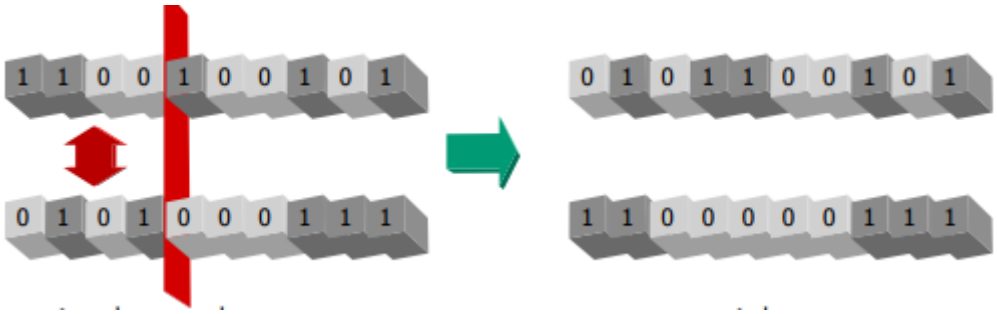

Figure 2-7. Example of a crossover operation (left: parents, right: offspring). The vertical plane symbolizes the crossover point [22].

- **The mutation operator**

  The mutation operator is usually applied with a very small probability (eg. 1%) to the offspring that result from the parents' crossover. When used on a chromosome, it randomly inverses the value of one of its bits (from 0 to 1 or vice-versa). The concept of mutation supports "exploration" of the search space, enabling the algorithm to overcome possible local minima / maxima.

Figure 2-8. Example of mutation of a chromosome (left: initial, right: mutated, red arrow: mutation point) [22].

- **Survival of the fittest**

  After selecting the parents and producing offspring as described above, a new generation is to be formed. One choice is for the new generation to consist of the produced offspring. Another methodology is to always pass the fittest members of a generation to the next one, so a generation is formed partly from the produced offspring and partly from their parents. This technique is called elitism and facilitates "exploitation" of regions of the search space where the members are of high fitness.

Chapter 3. The Geometric Model

Chapter 3 presents the developed geometric model. Section 3.1 is introductory. Section 3.2 refers to the generation of the hull form. Sections 3.3 to 3.6 constitute the main part of the chapter, presenting the parametric definition of the general arrangement.

3.1. Overview

The geometric model includes the hull surface and the general arrangement of the ship. A series of macros is developed in the well-known naval architectural software NAPA, the execution of which produces a ship model according to the values which have been assigned to the relevant parameters.

The developed model is capable of generating large ro-pax ship models within certain limits of main dimensions, as well as of global hull form characteristics (C_B and LCB). Parameters are also introduced to control certain properties of the general arrangement. Indicative upper and lower limits of the most important global parameters (which, under circumstances, can be exceeded) are presented in Table 3-1 below.

Table 3-1. Indicative limits of main dimension and hull form parameters.

Parameter	Lower limit	Upper limit
L_{PP}	165 m	225 m
B	26 m	33 m
C_B	0.55	0.62
LCB/L_{PP}	45%	48%

All designs are fitted with three trailer decks: the lower hold (deck 1), the main deck (deck 3) and the upper deck (deck 4). Hoistable platforms are arranged on top of the upper trailer deck, which can be lowered to convert the trailer deck into two private car decks (deck 4 and deck 5). The model extends to the superstructure, with four or five decks intended for passenger accommodation, including a large number of cabins, airseats and indoor and outdoor public spaces. It is also possible to arrange a ro-ro space for private cars occupying part of the lowest passenger deck, namely deck 6.

The main engines are always arranged in two engine rooms as a means of compliance with “safe return to port” regulation for passenger ships, as discussed in Chapter 1.4.

Regarding the design methodology which is followed, an important characteristic is that the framing system is decoupled from the main dimensions. This means that, rather than scaling the framing system along with the length to adjust the general arrangement to a modified ship size, the entire range of lengths between perpendiculars can be examined with any reasonable frame spacing specified by the user. This complicates the parametric design procedure but results in more realistic

models. By default, the frame spacing is set at 800 mm, while the web frame spacing at 3,200 mm (four times the ordinary frame spacing).

The modeling starts with the transformation of a parent hull in accordance with the supplied parameters. Subsequently, the geometric modeling is temporarily interrupted and the powering calculations (resistance, propulsion and selection of main engines) are carried out for the transformed hull form and at the specified service speed(s)[*]. This is in order to ensure that ample space is allocated to the engine rooms, according to the dimensions of the selected prime movers. Then the geometric modeling resumes with the definition of the main reference surfaces, which are afterwards used for the subdivision of the hull in watertight compartments and tanks. Finally, the ship is divided into main vertical zones and the main compartments of the superstructure decks are defined.

The above steps and the interaction of the geometric model with the relevant calculations are schematically presented in Figure 3-1.

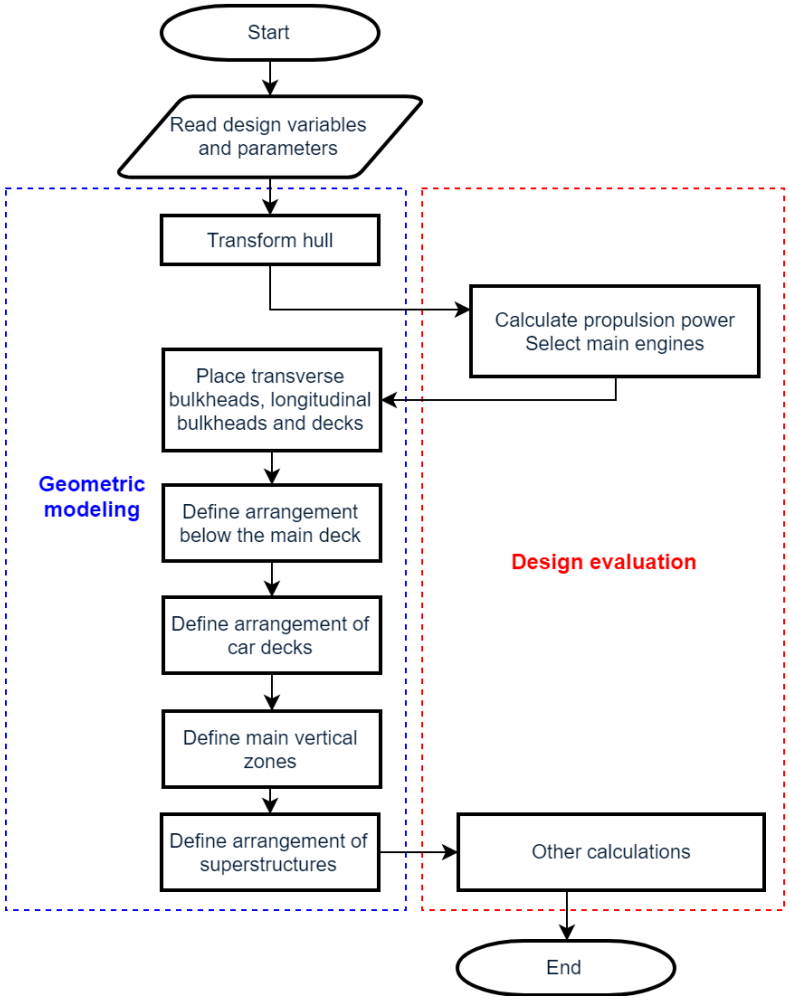

Figure 3-1. Flowchart of modeling process with emphasis on the geometric model.

[*] The option for different design speeds for day and night trips is included, if that suits the operational profile of the ship.

3.2. Hull form

The design of the hull form is partially parametric, using a parent hull which had already been modeled using CAESES and transferred to NAPA as part of a previous optimization study within the EU project HOLISHIP [17] [23]. It is a typical hull of a modern ro-pax ferry, with a flared bow and a goose-neck bulb, a very small parallel midbody and a buttock-flow stern with a skeg.

The transformation (TRANS) subtask of NAPA offers a pool of transformations which can be imposed on the parent hull to create variants. Affine transformations are utilized to produce hulls with different main dimensions (L_{PP}, B, T_D[*]), while displacement transformations are used to modify the block coefficient and LCB.

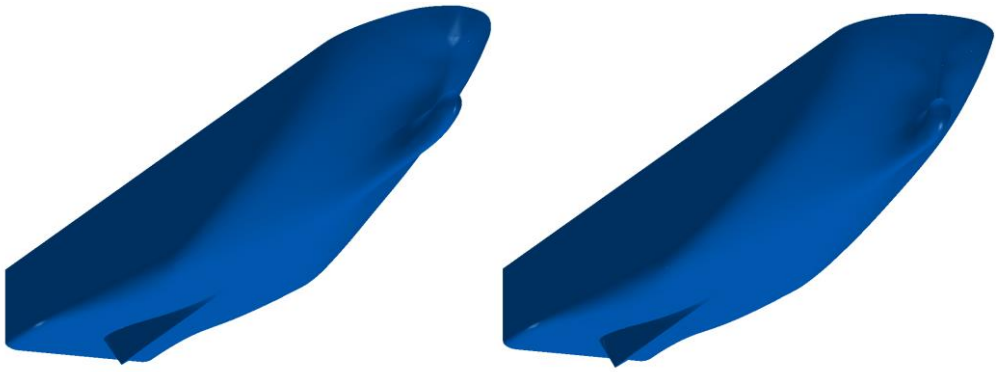

Figure 3-2. Two variants created from the parent hull through displacement transformations (left: C_B=0.55, LCB=0.46L_{PP}, right: C_B=0.62, LCB=0.48L_{PP} – all other parameters kept constant).

The resulting surface, the aft limit of which is still open, is then trimmed by an auxiliary surface that defines the stern, forming the duck tail and the transom.

3.3. Main reference surfaces

The region from the bottom up to the main ro-ro deck (deck 3) constitutes the lower region of the ship, which is characterized by a dense watertight subdivision and is mainly occupied by machinery and auxiliary spaces, various tanks and void spaces.

In all cases, the inner bottom (deck 0) is also the bottom of the main engine rooms, which vertically extend up to deck 3. Deck 1 is the floor of the lower hold. The lower hold also extends up to deck 3, in order to function as a trailer deck. Deck 2 is a platform deck around the main engine rooms, which houses auxiliary machinery rooms, the engine control room and various store rooms.

The first modeling step in this region is the definition of its main watertight boundaries, namely transverse bulkheads, decks and longitudinal bulkheads.

[*] At this stage, the design draft functions as a scale factor in the vertical direction for the linear transformation. The same value is later used for other purposes as well, for example to compute the ship's resistance. This implies that the given value must correspond to a representative loading condition of the ship. However, as the floating position of a volume carrier cannot be known a priori, an iteration might be required in order to obtain a realistic value.

An example set of reference surfaces is presented in Figure 3-3 below.

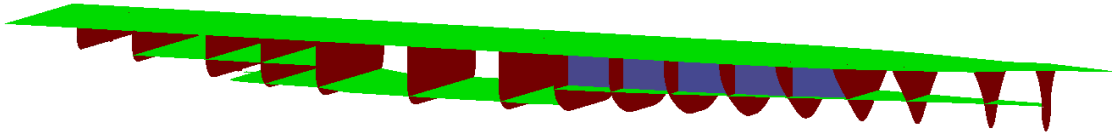

Figure 3-3. Main reference surfaces up to the main deck. For clarity, the extent of each surface has been restricted to the regions where it mainly functions as a compartment limit.

3.3.1. Main transverse bulkheads

As mentioned already, the general arrangement is to adapt to the main dimensions and the hull form without modifying the framing system. Thus, an algorithm is developed for determining the positions of transverse bulkheads as a function of the length between perpendiculars.

An initial set of bulkhead positions is assumed, corresponding to a "baseline design" with a length between perpendiculars of 180 m. For deviations from that reference length, compartments are gradually lengthened or shortened. Furthermore, for larger deviations, new bulkheads may be added or existing ones removed. The length of each engine room is determined by the length of the selected main engines, as the powering calculations have already taken place after the transformation of the hull (see Chapter 4.2).

The number of compartments to be lengthened / shortened and added / removed is calculated in order to comply with two constraints:

I. The aft engine room bulkhead remains within predefined limits as a percentage of L_{PP}. The main engine rooms cannot extend too far aft, as a minimum engine room height is required while the "buttock-flow" stern is elevated from the base plane. On the other hand, moving the engine rooms too far forward reduces lane capacity of the lower hold and increases the length of the shafting system. Default limits for the position of the aft engine room bulkhead are set to 26.5% and 28.5% of the length between perpendiculars, following a study of existing large ro-pax vessels, as shown in Figure 3-4 below.

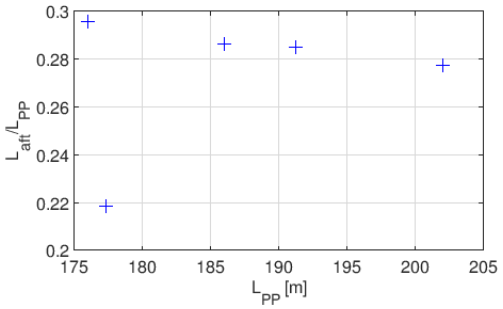

Figure 3-4. Aft engine room bulkhead positions (L_{aft}) of existing large ro-pax ships.

II. The collision bulkhead remains within the limits specified by SOLAS Convention, possibly with an extra user-defined margin. A parameter is introduced to control whether the collision bulkhead is placed towards the forward or the aft limit, in case more than one web frame is found within the allowable limits.

The basic steps of the algorithm are presented in Figure 3-5 below, followed by a brief description of the procedure.

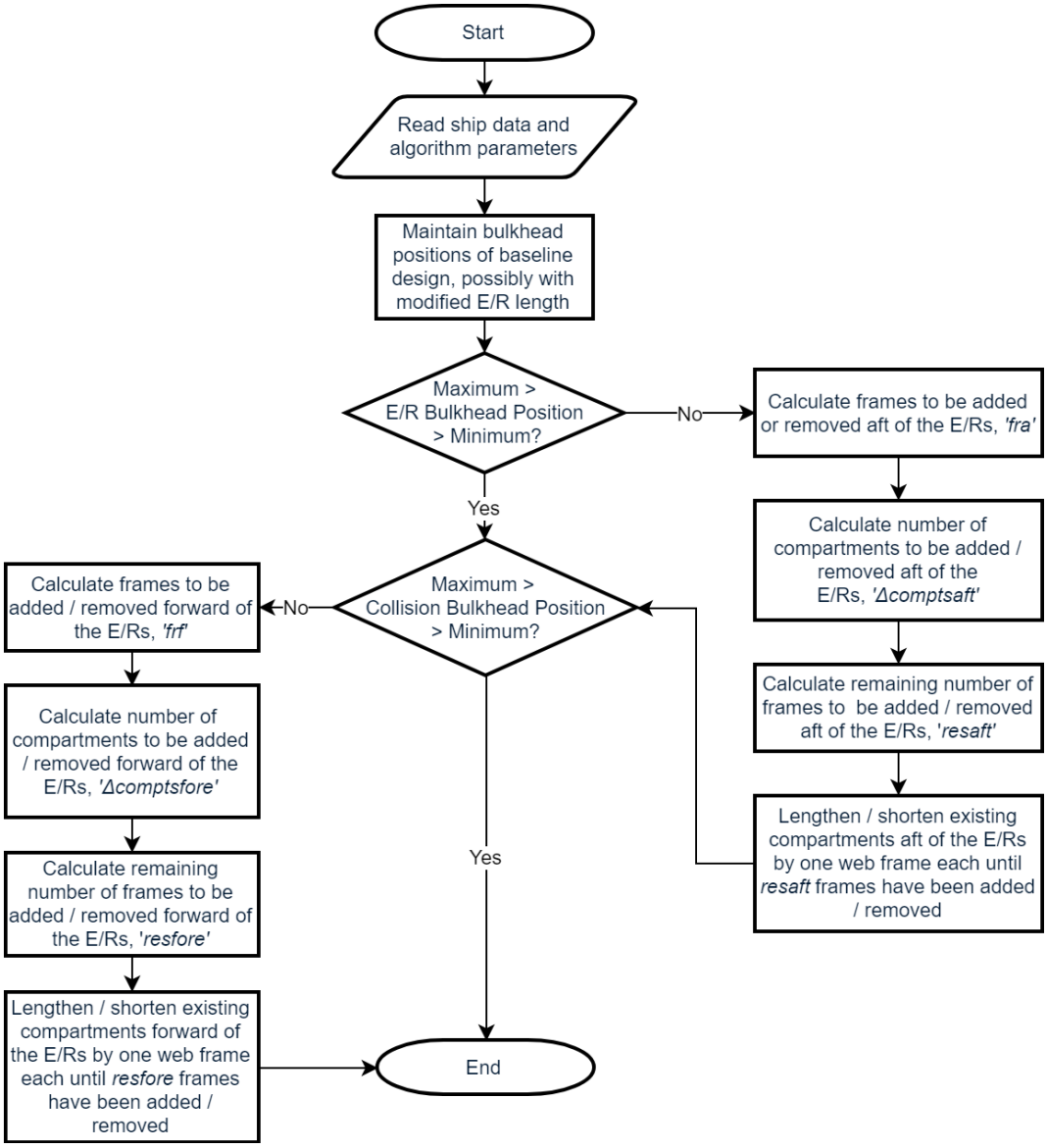

Figure 3-5. Flowchart of the basic steps of the transverse bulkhead position algorithm.

Starting with the subdivision of the baseline design and having selected the ship's main engines, the length of each main engine room is modified in order to account for the change in installed power. The length of all other compartments is temporarily kept as in the baseline design and compliance with constraint I is checked. In case of non-compliance, the subdivision of the aft part is modified. For smaller deviations, this is achieved by shifting existing bulkheads forward or aft by one web frame each.

In case this is not sufficient, a new bulkhead is added or an existing one is removed. All bulkheads from the engine rooms up to the collision bulkhead are also shifted forward or aft to make room for the modifications in the aft part. Then, compliance with constraint II is checked, taking into account the already modified bulkhead positions. If it is not satisfied, the same procedure is followed for the forward part of the ship, until the collision bulkhead reaches the required position.

Various calculation methods have been developed for the quantities that appear in Figure 3-5 regarding the inserted / removed compartments. For simplicity, only one is presented in detail below, which is considered to yield more realistic results and is used in all applications presented herein.

The equations presented below refer to the aft part of the ship (therefore, to assess compliance with constraint I) and for the case that elongation of the aft part is required in comparison with the baseline design. A similar procedure is followed for the forward part of the ship (constraint II), as well as in case shortening of existing compartments (compared to the baseline design) is required.

The required number of frames is calculated as follows:

$$fra = ceil\left(\frac{L_{aft,min} - L_{aft}}{FS}\right)$$

The number of new compartments in the aft region (in comparison with the baseline design) is:

$$\Delta comptsaft = floor\left[\frac{fra}{frperweb \cdot length(shiftorderaft)}\right]$$

In the above equation, $shiftorderaft$ is a vector containing indices of bulkheads aft of the engine rooms, which are to be shifted forward if needed.

Then, the number of existing compartments to be lengthened is calculated as:

$$shiftbhdaft = ceil\left(\frac{fra}{frperweb} - \Delta comptsaft \cdot webspercompt\right)$$

Thus, in this case constraint I is satisfied by adding $\Delta comptsaft$ compartments of $webspercompt$ web frames each at a predefined position aft of the engine rooms, as well as by shifting forward the first $shiftbhdaft$ elements of $shiftorderaft$ by one web frame each.

It has been observed that the desired range of lengths between perpendiculars can be achieved with a fixed number of compartments aft of the engine rooms, while compartments are added or removed in the forward part, corresponding to differences in the number of bulkheads compared to the baseline design $\Delta N_{BHD} \in \{-1,0,1,2\}$. Therefore, the rest of the modeling must be able to account for these four cases.

Figure 3-6 schematically presents the described procedure for a ship with L_{PP}=220 m. Aft of the engine rooms, an addition of three web frames is required, which is achieved by lengthening three compartments by one web frame each. In the forward part, nine web frames are added by inserting a new compartment of four web frames and elongating five existing ones by one web frame each.

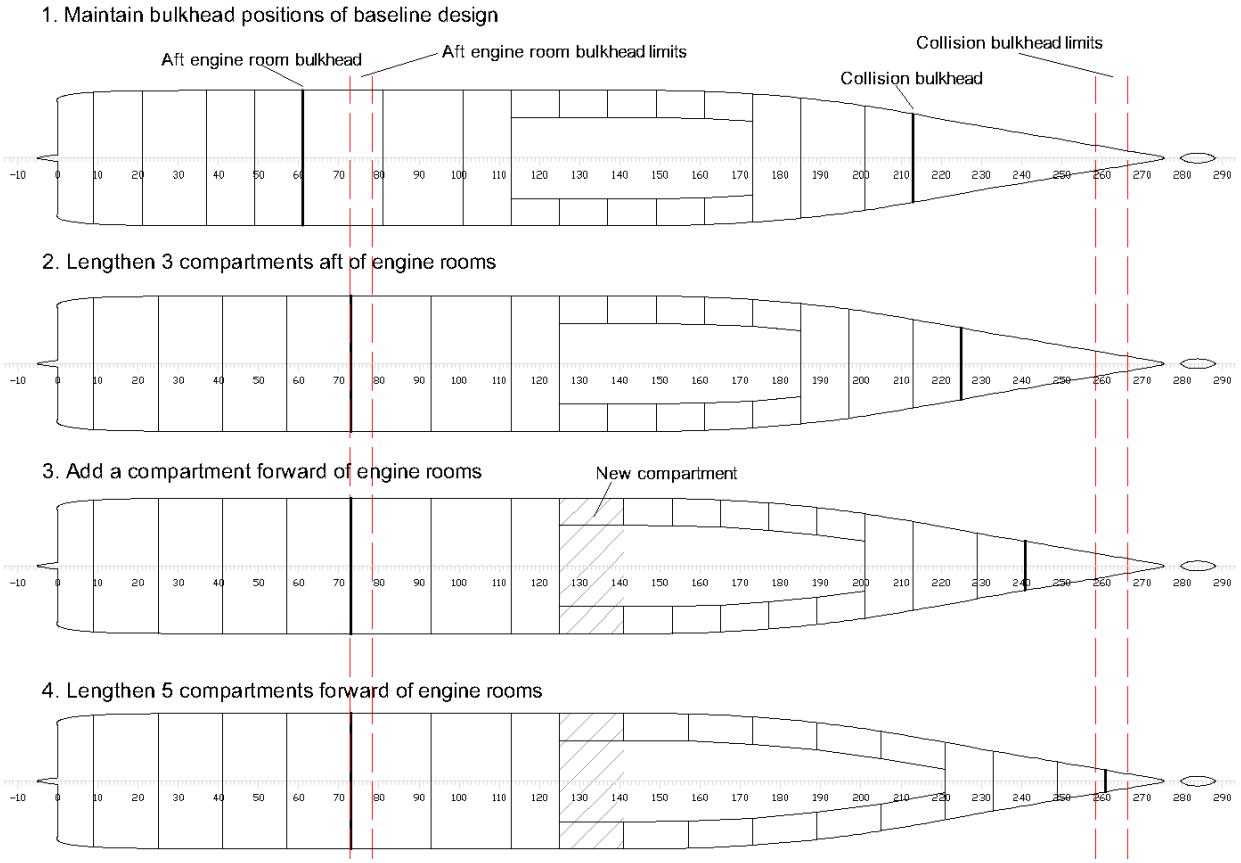

Figure 3-6. Application of transverse bulkhead positioning algorithm for a ship of L_{PP}=220 m.

3.3.2. Decks

The heights of all decks are parameters supplied by the user. Decks 1, 2 and 3 are generally flat horizontal surfaces, while the inner bottom might be stepped, lying at different heights at the engine rooms and at the regions forward and aft of them. Selected default values are presented in Table 3-2 below.

Table 3-2. Default deck heights (decks 0 - 3).

$h_{DB,aft}$	2.3 m
$h_{DB,E/R}$	1.7 m
$h_{DB,fwd}$	1.5 m
h_1	4.2 m
h_2	6.3 m
h_3	9.8 m

Subsequently, the specified positions are internally checked and if necessary modified in order to comply with certain constraints, related either to the general arrangement or relevant regulations:

- According to SOLAS convention, the minimum double bottom height is $\min\{\frac{B}{20}, 2m\}$, while the minimum height of the lower hold deck (deck 1) is $\min\{\frac{B}{10}, 3m\}$.
- A minimum distance of the inner bottom from the hull is required. This is important towards the stern where the hull surface is raised upwards, potentially causing problems with the various tanks in that region or with the installation of the reduction gear and/or the main engines.
- The height of the engine rooms, defined as the distance of the main car deck (deck 3) from the double bottom at the engine rooms (deck 0), should be in accordance with the height requirement of the main engines. The requirement is that the engine rooms must be at least as high as the main engines plus the required height for the removal of a piston, with an extra margin to account for the webs on top of the engine rooms.

Whenever a supplied value violates a constraint, the corresponding deck is moved up until the constraint is satisfied. The same holds for all decks above it, in order for the relative distances between all other decks to remain constant. In this sense, the deck heights defined in Table 3-2, or those that might be defined by the user, should be interpreted as the minimum heights acceptable for the particular design. Relevant warning messages are issued to inform the user about possible modifications of the supplied values.

3.3.3. Longitudinal bulkheads

As in most post-SOLAS ‘90 large ro-pax vessels, parts of the lower decks are subdivided into three transverse zones by two symmetric longitudinal bulkheads, which follow the hull form as it gets finer towards the bow. This was initially a measure of compliance with SOLAS ’90 damage stability regulations, which examined damages extending inwards up to one fifth of the ship’s breadth from the subdivision waterline. Therefore, by adopting longitudinal bulkheads at B/5 from the sides, the space in between was considered intact and could be utilized for large compartments such as lower holds. The probabilistic assessment method which has replaced these regulations examines damages with a maximum penetration limit of B/2 without requiring survival in all possible damage cases, however:

- SOLAS ’90 is still indirectly in place for ships designed to operate within EU waters, as the Stockholm agreement is based on it.
- A ship with an unprotected lower hold would be unlikely to satisfy the probabilistic assessment and the deterministic requirements that supplement it, as the large lower hold would be flooded after even minor side damage.

For these reasons, a "SOLAS '90 – inspired" design is followed, where the user can modify the distance of the bulkheads from the ship's shell* as a percentage of the beam, ranging from 15% (if the Stockholm agreement does not apply) to 25%. In general, as that percentage increases, the ship becomes safer but its vehicle capacity decreases. This will be discussed further in Chapter 3.4.

For simplicity, from now on these bulkheads will be referred to as the "B/5 bulkheads", even if their position is not necessarily at B/5 from the hull.

3.4. General arrangement – bottom to deck 3

Following the definition of the main reference surfaces, the next step is to create the general arrangement of the ship by subdividing its volume into compartments. The "parent design" mentioned in Chapter 3.2 has also been used as a reference ship for various parts of the general arrangement.

The main challenge concerning the parametrization of the general arrangement is to ensure the effective adaption of the internal geometry to the ship's shell within the entire design space, especially with regard to the lower decks. This is mainly due to two reasons:

- The hull form is not simply scaled in terms of the main dimensions, but global characteristics of its form, namely C_B and LCB, are also varied within certain limits.
- The limiting surfaces of a room may move discontinuously as the length of the ship varies. Longitudinally, compartments belong to watertight zones formed by transverse bulkheads, which, as has been explained, are lengthened or shortened by multiples of the web frame spacing. Furthermore, new bulkheads can be added, meaning that the number of rooms is not constant. Therefore, a given room is not always in the same dimensionless position within the hull, which may cause problems especially in the regions of the bow and stern.

Figure 3-7 presents an example arrangement of the lower decks, followed by a description of the arrangement and the methods used to parametrize it.

* As the subdivision draft is still unknown at this stage, the distance is measured at the design waterline, which is slightly below the subdivision waterline (and therefore the design is on the safe side).

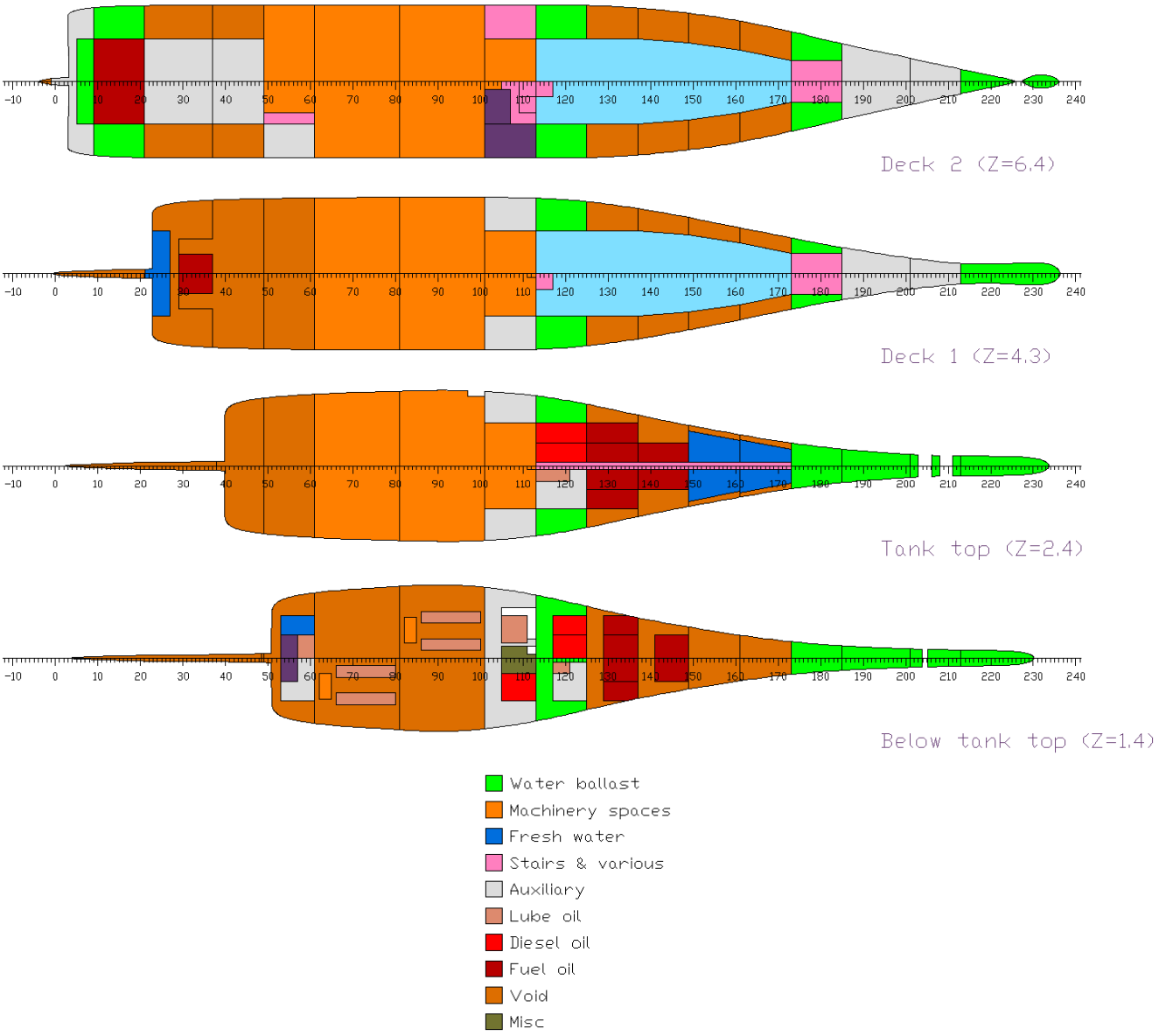

Figure 3-7. Lower decks.

Aft region

The aft region of the lower decks (zones* 1 to 8) is occupied mainly by the engine rooms and other machinery spaces (steering gear, engine control room, stabilizers room etc.). It also contains various tanks for water ballast, fuel oil etc., as well as store rooms. This part of the parametric model is partially static, as no transverse bulkheads are added or removed compared to the baseline design within the examined design space.

This area is sensitive to changes in the hull form, as a decrease of the block coefficient or movement of the LCB forward raises the hull upwards. This issue

* The term "zones" in this chapter refers to parts of the ship between two consecutive transverse bulkheads (or between a transverse bulkhead and the hull). These zones do not necessarily coincide with those formed, for example, for damage stability calculations (see Chapter 4.7).

particularly concerns zone 5, where various small tanks are located within the double bottom, and the main engine rooms (zones 6 and 7), where the main engines and the gearboxes are to be installed. As has been described in Chapter 3.3.2, the automatic adjustment of the double bottom height secures the required space, if needed. An example is depicted in Figure 3-8 below. Transversely, the B/5 bulkheads are used as limiting surfaces, which guarantees the adaption of the room limits to changes in the ship's beam.

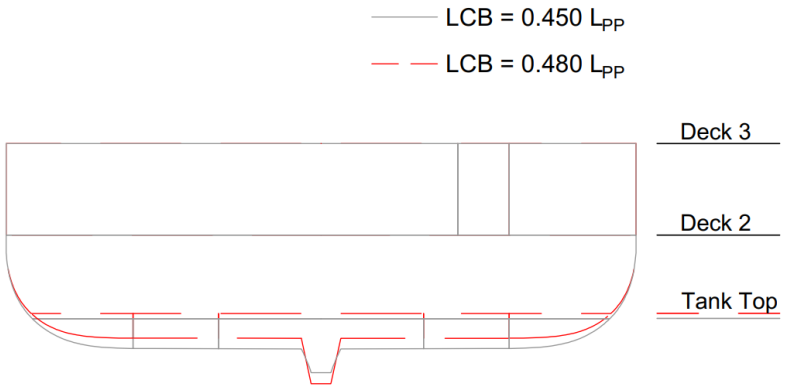

Figure 3-8. Section aft of the engine rooms (zone 5), showing the effect of the LCB on the general arrangement (adaption of double bottom height).

It is noted that various compartments in this region are connected by non-watertight doors or stairs. To take this into account in damage stability calculations, appropriate openings are defined.

Lower hold region

Forward of zone 8, four to seven zones are mainly occupied by the lower hold and constitute the region where watertight compartments are added or removed as the length of the ship changes.

In general, the lower hold extends from deck 1 to deck 3, between the B/5 bulkheads, and as far as possible towards the bow. The forward limit is determined by two factors. The first is that three watertight compartments must be reserved towards the bow up to the collision bulkhead for other purposes (stairs, pump room, bow thruster room). The second factor is that the breadth of the lower hold at its forward limit should not be less than a minimum value specified by the user (for example, the breadth required for the installation of a watertight door which leads to a staircase towards the upper decks for the drivers). If this criterion is not met, the maximum extent specified above is reduced and the corresponding compartments are replaced by void spaces. For example, the effect of the longitudinal bulkhead positioning on the lower hold arrangement is depicted in Figure 3-9.

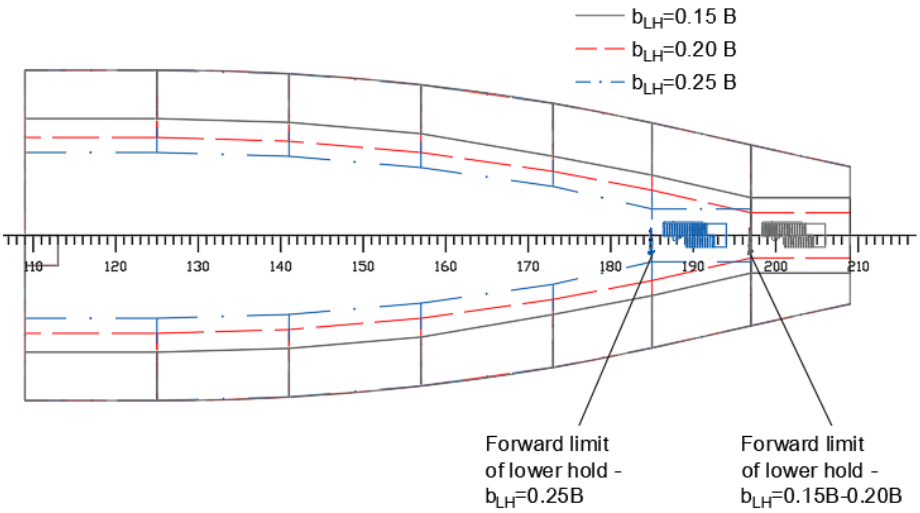

Figure 3-9. Effect of the longitudinal bulkhead position parameter on the lower hold (all other parameters kept constant).

Below deck 1, most of the space is occupied by diesel and fuel oil tanks, fresh water tanks and a pipe tunnel. The remaining volume, from the bottom up to deck 3, is occupied by one void space per zone. Apart from protecting the inner compartments in case of flooding, these void spaces enable instantaneous symmetrical flooding in order to avoid large heeling angles after minor side damages. This means that the movement of water from port to starboard side and vice versa must not be obstructed by other tanks in the region. An exception is the first lower hold zone (zone 9), where the heeling tanks are located, which must – by definition – be two separate symmetric tanks.

Depending on the number of transverse bulkheads, two or three zones are occupied by fuel oil tanks in this region. Each zone contains a maximum of two pairs of fuel tanks, with the outer ones extending up to the B/5 bulkheads. However, if the hull is not full enough at that level, one or even both of the pairs are not created[*]. The criterion is that the surrounding void space must allow the passage of water from one side to the other, as explained above. A relevant margin is introduced as a parameter, defining the minimum allowable distance of the fuel tanks from the ship's side.

[*] This means that the maximum bunker capacity of the ship is determined by the fullness of the hull in that region and the positioning of the longitudinal bulkheads. It has been shown however that, within the examined design space and for realistic values of design speed and required endurance, the resulting capacity easily exceeds the minimum requirement.

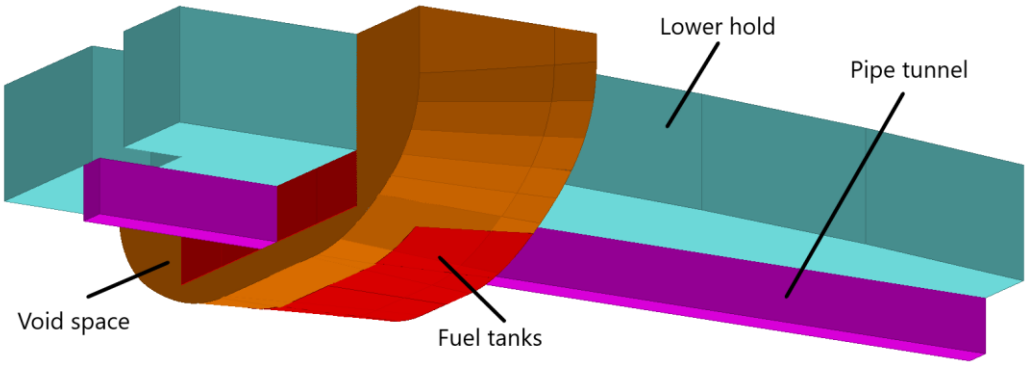

Figure 3-10. Arrangement of fuel tanks to enable instantaneous symmetrical flooding of surrounding void space.

Forward of the fuel tanks, one to three zones contain fresh water tanks, extending from the inner bottom up to deck 1. Generally, at this part of the ship the hull form is very fine, which is why a partial double hull arrangement is preferred. The inclined planes that serve as tank boundaries are defined parametrically so as to adapt to the surrounding shell. A parameter is introduced to define the minimum allowable distance from the hull. The slope of each plane in the vertical direction is the mean inclination of the hull in the region it extends, while two points – one at each of the limiting longitudinal positions – are found by imposing the specified minimum distance from the hull.

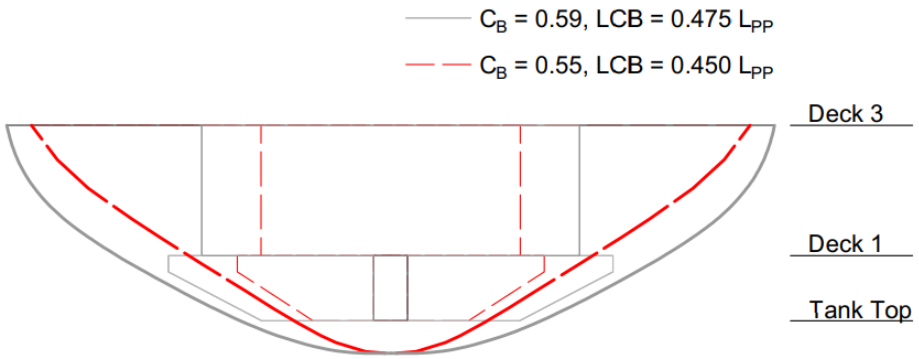

Figure 3-11. Transverse section towards the bow showing the adaption of rooms to the hull form (variation of C_B and LCB – all other parameters kept constant).

Forward region

The three foremost zones include the fore peak tank and other ballast tanks, as well as auxiliary machinery spaces (pump room and bow thruster room).

3.5. General arrangement – decks 3 to 5

Decks 3 to 5 are mainly occupied by ro-ro spaces. An indicative deck plan is shown in Figure 3-12 below.

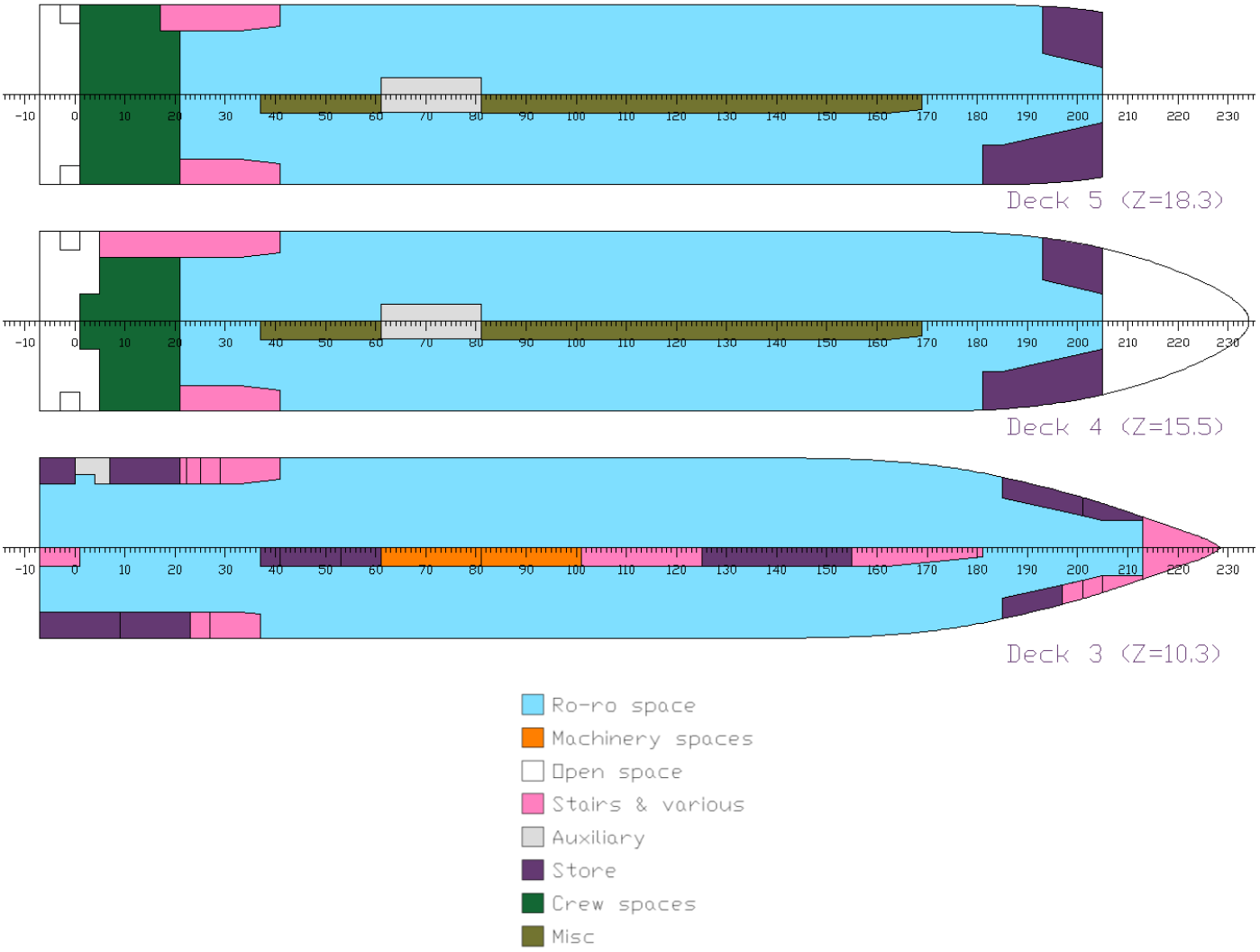

Figure 3-12. Main deck and upper ro-ro deck.

The main deck (deck 3) is intended mainly for the carriage of trucks and trailers. The ro-ro space covers the entire length of the ship up to the collision bulkhead, which according to SOLAS Chapter II-1 Reg. 12, shall be extended weathertight to the upper car deck. Loading and unloading of vehicles takes place through a stern and a bow door. The deck is equipped with a central casing for ventilation, access to lower decks and store rooms, as well as smaller side casings at the forward and aft parts, intended mainly for the embarkation and disembarkation of passengers and for store rooms.

Moving upwards, the next deck is the upper ro-ro deck (deck 4). Access to the upper deck takes place via the main ro-ro deck through an internal ramp. The volume between deck 4 and deck 6 is normally intended for trucks and trailers. However, it

can be split by a hoistable deck, creating two decks (deck 4 and deck 5) for private cars. The central and side casings extend to these decks as well. At the bow and the stern, parts of deck 4 are reserved for mooring equipment.

The aft region of decks 4 and 5 may also house crew spaces, as in Figure 3-12. This is determined by the selected superstructure arrangement (see Chapter 3.6).

The position of the central casing automatically adapts to the ship's beam, in order to maximize truck capacity. If the number of lanes is odd, it is positioned symmetrically to the center plane, while if the number of lanes is even it is offset in the transverse direction. This adaption is depicted in Figure 3-13 below. The width of all casings is approximately constant (independent of the ship's beam).

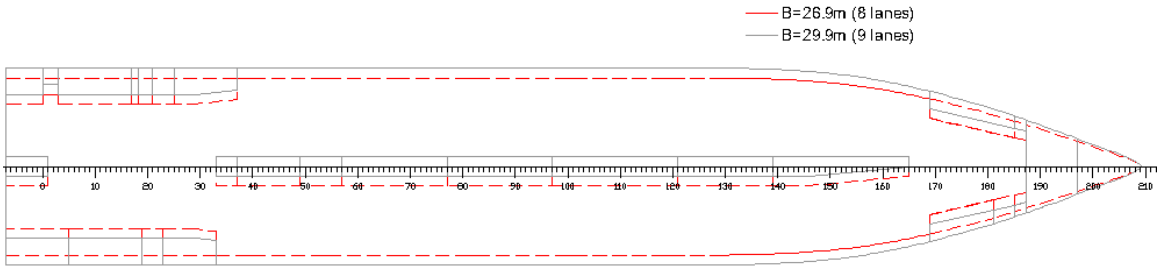

Figure 3-13. Effect of the ship's beam on the main deck arrangement. Notice the effect on the central casing position.

3.6. General arrangement of superstructure

3.6.1. Longitudinal limits and main fire divisions

The subdivision of the ship into main vertical zones concerns its entire length and height, but is of particular interest for the design of the superstructure. As has been mentioned, minimization of structural barriers within accommodation area is desired, not only because it allows for the design of large public spaces but also due to the increased weight, building cost and complexity resulting from an increased number of fire zones.

According to SOLAS Chapter II-2 Regulation 9.2, the maximum allowable length of a main vertical zone is 48 m, provided that the area of a zone on any deck is not more than 1600 m^2. Generally, the limits are to be aligned with the main transverse watertight bulkheads.

Within the parametric model, the main vertical zones are defined as follows: Starting from the aft limit of the ship and moving forward, main vertical zone limits are placed as far as possible from each other, provided that the SOLAS requirement is satisfied and the position of the limit coincides with that of a transverse bulkhead.

The aft limit of the enclosed superstructure is set forward to that of the hull (default position: frame 1), allowing for the creation of small open decks at the stern. The maximum forward limit is equal to that of the upper ro-ro deck. However, deviations from that limit are possible in case the length of the forward fire zone within the

superstructure is less than a user-defined value. In this case, the forward zone is considered to offer little accommodation area while requiring an extra fire zone; therefore, the forward limit of the superstructure is moved aftwards, reducing the number of fire zones within the superstructure.

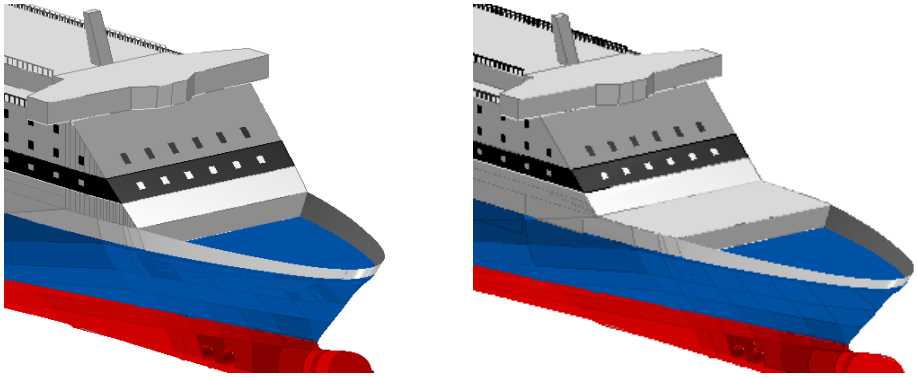

Figure 3-14. Adaption of forward superstructure limit to decrease the number of fire zones within accommodation area. Left: L_{PP}=205m, right: L_{PP}=229m (all other parameters kept constant).

Finally, in order to deal with possible lack of space issues in the forward zone of the wheelhouse/sun deck, the inclination of the forward limiting surface may also be internally modified. Both the initial (minimum) and the maximum allowable inclinations are user-defined parameters.

3.6.2. Internal layout

Three possible superstructure arrangements have been included in the developed macros, depending mainly on the specified number of decks (10 or 11). In the case of 10 decks, four decks (6 to 9) are allocated for passenger accommodation, including the sun deck, while the lower crew cabins are placed on decks 4 and 5.

Alternatively, the ship can be extended the ship vertically by one deck. The additional deck is utilized mainly for passenger cabins. In this case, some additional lane capacity is also obtained by moving the crew cabins from the upper car deck to the superstructure.

Finally, flexibility between passenger and vehicle capacity can be provided by replacing the cabins on deck 6 by another large ro-ro space for private cars. In that case, deck 6 is occupied by that ro-ro room, the reception and airseat areas.

An example superstructure arrangement is shown in Figure 3-15, followed by a summary of the three configurations in Table 3-3.

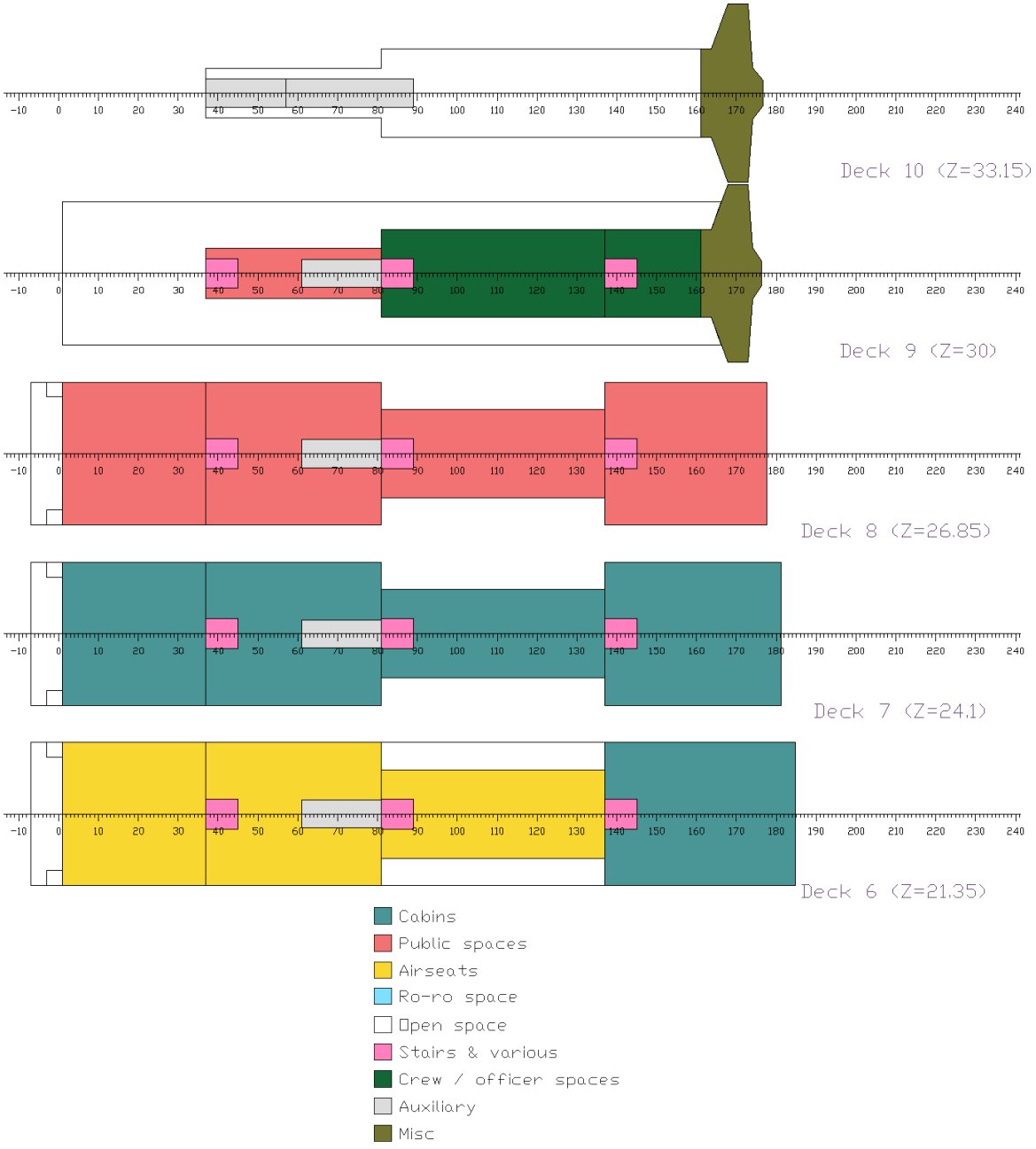

Figure 3-15. Superstructure decks – arrangement with ten decks.

Table 3-3. Possible superstructure configurations.

Number of decks	**10**	**11**	
Cars on deck 6	**No**	**No**	**Yes**
Deck 6	Airseats and passenger cabins	Airseats and passenger cabins	Airseats and private cars
Deck 7	Passenger cabins	Crew cabins and passenger cabins	
Deck 8	Public spaces	Crew cabins and passenger cabins	
Deck 9	Sun deck, officer cabins and wheelhouse	Public spaces	
Deck 10	Funnel and auxiliary spaces	Sun deck, officer cabins and wheelhouse	
Deck 11		Funnel and auxiliary spaces	

Other than the spaces presented in Table 3-3, the preliminary superstructure model includes staircases and the engine casing. One staircase is placed at the aft limit of each main vertical zone, with the exception of the aftmost zone, where there are two external staircases on the open decks.

Below the wheelhouse / sun deck (deck 9 or deck 10), accommodation areas generally extend to the ship's sides, with the exception of one fire zone, where the life-saving appliances are to be fitted. On the wheelhouse / sun deck, the enclosed superstructure remains narrower forward of the life-saving appliances zone, in order to create open spaces for passengers at the sides of the ship.

3.7. 3-D model

An additional NAPA macro is developed which constructs an external 3-D model of the ferry, as shown in Figure 3-16 below. The model is based on the ship's "gross hull", created by combining all enclosed rooms, as required in order to calculate its gross tonnage. Extra features (railings, windows, lifeboats etc.) can be added for illustration.

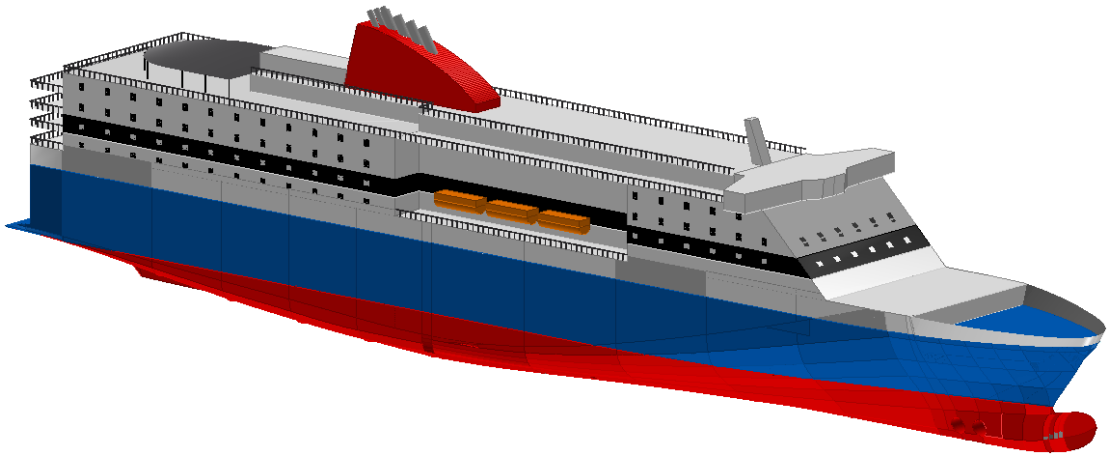

Figure 3-16. External ship model.

Chapter 4. Evaluation Methods

This chapter presents the selected calculation methods for the evaluation of various quantities of practical interest. These include the ship's powering, payload and lightship weight, intact and damage stability, energy efficiency, building and operational cost.

4.1. Overview

Figure 4-1 presents the series of calculations which are presented in this chapter, as well as how these interact with the geometric modeling process.

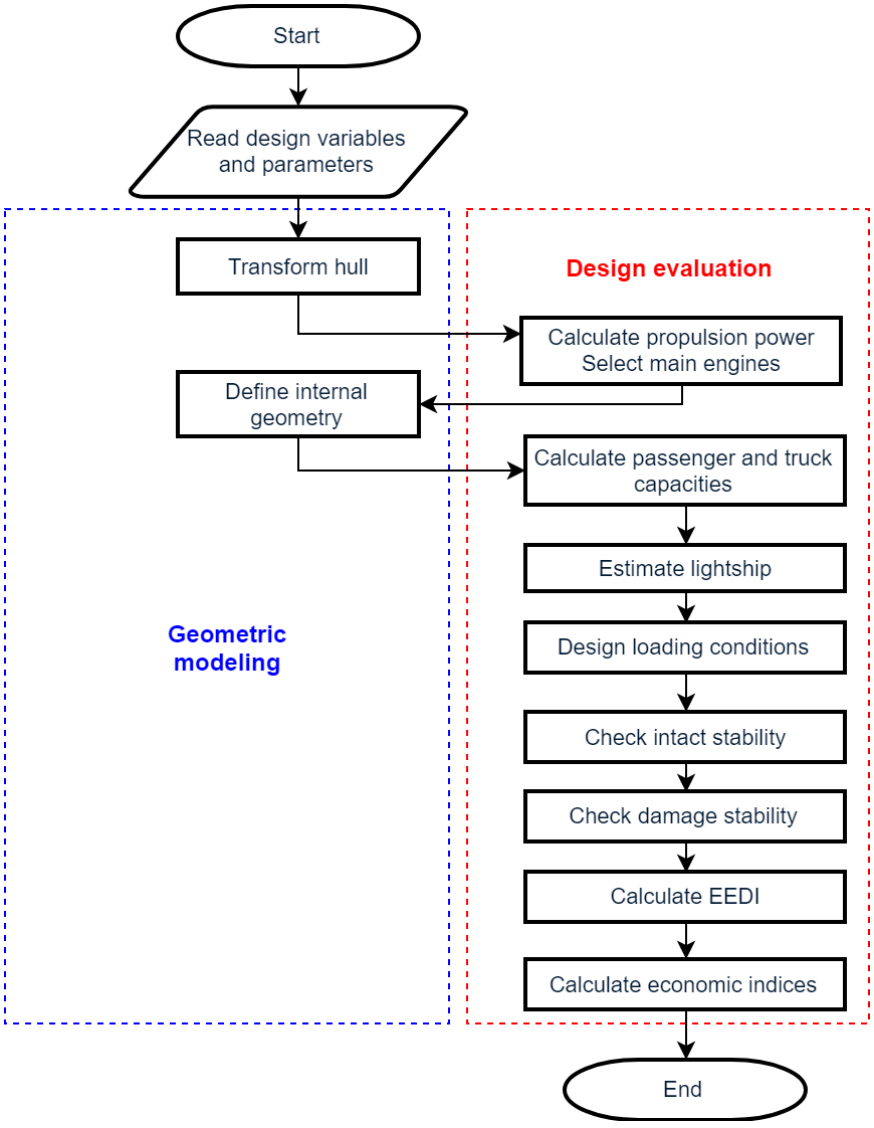

Figure 4-1. Flowchart of calculations and interaction with geometric modeling.

4.2. Powering

4.2.1. Towing resistance

Resistance and propulsion calculations take place immediately after the transformation of the parent hull, as the dimensions of the selected main engines affect the internal compartmentation.

Three alternative methods for the estimation of the towing resistance and effective horsepower have been included. The first option is the Holtrop method [24], a statistical method that builds up the resistance through various components: frictional resistance, viscous pressure resistance, wavemaking and wave breaking resistance, additional pressure resistance of bulbous bow near the water surface, additional pressure resistance of immersed transom stern, resistance of appendages and model-ship correlation resistance. The resistance is calculated for a range of speeds around the design speed(s). The method is included in the ship hydrodynamics (SH) subtask of NAPA, and therefore all calculations are performed automatically. A prediction method for the wind resistance is also available within NAPA, which is used to supplement Holtrop's method. It is recognized that the Holtrop method, like other empirical methods, provides a rough estimate and likely overestimates the resistance, as it is based on older and not necessarily optimized hull forms. However, it encompasses the impact of all relevant parameters (main dimensions, C_B and LCB), making it useful for optimization studies. Furthermore, inaccuracies can be greatly reduced if data from reference ships are available (see Chapter 4.2.2).

The second option is the direct input of the resistance through the input file, along with the design variables. This has been included for the case when the resistance is calculated using an external method and is then input to NAPA.

The third option is the use of a response surface, developed on the basis of the results of some CFD runs performed in FINE™/Marine for a particular optimization problem which is solved in Chapter 6. The effect of the length and the beam on the bare hull towing resistance is examined within the following limits:

$$L_{PP} \in [200\,m, 210\,m], \qquad B \in [26.9m, 27.7m]$$

The calculations have been carried out for constant design draft (6.6 m), hull form (C_B=0.55, LCB=0.46L_{PP}) and design speed (27 knots, same for day and night trips).

A simple two-degree polynomial surface has been fitted to the obtained data points, using the least squares method:

$$R(L_{PP}, B) = \alpha_1 L_{PP}^2 + \alpha_2 L_{PP} B + \alpha_3 B^2 + \alpha_4 L_{PP} + \alpha_5 B + \alpha_6$$

$$\alpha_1 = -0.77938\,kN/m^2\,, \alpha_2 = 0.798139\ kN/m^2\,, \alpha_3 = -94.2280\,kN/m^2\,,$$
$$\alpha_4 = 303.381\,kN/m\,, \alpha_5 = 5034.50\,kN/m\,, \alpha_6 = -99819.5\,kN$$

The response surface along with the calculated data points are presented in Figure 4-2 below.

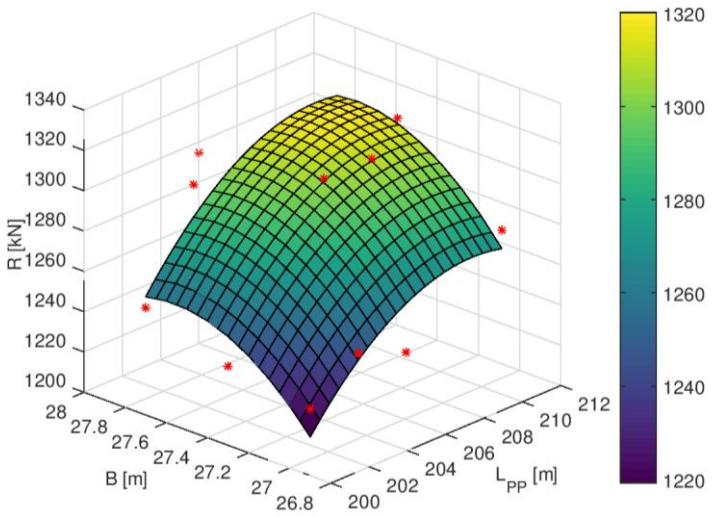

Figure 4-2. Calculated values of bare hull resistance and fitted surface.

Although the behavior of the dataset is not always captured correctly, a simple surface has been favored over a higher-degree one in order to avoid overfitting. In all cases, the deviation of the approximated values from the actual ones does not exceed 2%.

Regarding the second and third methods, it is noted that the input values of resistance refer to the bare hull towing resistance. The effect of appendages and wind are included by percentile increases, default values of which are selected as 7% and 5% respectively.

4.2.2. Propellers and propulsion power

Next, the propulsion calculations take place. The ship-propeller interaction factors, w, t and η_R, are estimated according to Holtrop's method as well. The diameter of each propeller is calculated taking into account the hull form and leaving a margin to ensure that class requirements are satisfied, vibration levels are acceptable and the propellers remain submerged in lighter conditions. All propellers are assumed to be four-bladed, while the expanded blade area ratio is calculated according to Keller's criterion in order to avoid cavitation problems. Finally, the pitch of the propellers is optimized in order to maximize their open water efficiency at the design speed, assuming Wageningen B-series propellers. This procedure is also implemented automatically in NAPA's hydrodynamics subtask. It is noted that the objective is not to design the actual propellers of the ship (which would be wake-adapted and controllable-pitch), but only to estimate their open water efficiency. In reality, the use of first principles for propeller design would be beneficial for the open water efficiency, but the larger hub diameter of a controllable pitch propeller would limit that increase.

Finally, by assuming a constant shafting system efficiency (default value: 0.97), the required propulsion power is obtained:

$$SHP_0 = PC \cdot EHP = \frac{1-t}{1-w}\eta_0\eta_R\eta_s EHP$$

If reliable data from similar ships are available, a correction coefficient can be used to correct the accuracy of the used methods (including both towing resistance and propulsion calculations):

$$SHP = SHP_0 \cdot \lambda_{SHP}$$

This method has been applied for an existing large ro-pax, the propulsion power of which is available. A ship with the same main dimensions, C_B, LCB, and design speed has been created through the parametric model, and the results of the Holtrop method and B-series open water efficiency polynomials have been compared with the actual propulsion power of the ship. The calculated value of the correction coefficient is $\lambda_{SHP} = \frac{SHP}{SHP_0} = 0.906$, showing that the approximate methods do indeed overestimate the propulsion power by about 10%. This result is set as a default value and can be used if there is no better estimate available.

4.2.3. Selection of main engines

Four 4-stroke Diesel engines are selected as prime movers of the vessel, with their maximum continuous rating determined based on the calculated SHP, the maximum consumed power of the shaft generators and a power margin:

$$MCR = \sum_{i=1}^{4} MCR_i = roundup\left[SHP(1+PM) + P_{shaftgen}\right]$$

The power of the shaft generators and the power margin are user-defined parameters.

In order to cover the specified limits of ship particulars for a range of design speeds, various models are included as potential main engines. These are presented in Table 4-1 below.

The manufacturer can either be selected by the user or left free. If the manufacturer is left free and two alternatives with the same rated power are found, minimization of the specific fuel oil consumption is used as a selection criterion. Furthermore, the user has the option to force the selection of four identical engines or allow the selection of two pairs of different ones, in order to achieve an installed power as close as possible to the minimum required and to increase the flexibility of the system. In the second case however, care is taken so that the two engines will be of the same manufacturer[*].

[*] Another option which could be implemented in the future would be to only allow the selection of two different engines of the same model, i.e. differing only in terms of cylinder number.

The weight, length, height (including that required for the removal of a piston) and specific fuel oil consumption of each selected engine are also included, as they are required for engine room dimensioning, weight calculations and economic assessment.

Table 4-1. Main engine models included in the powering macro.

Manufacturer	Model	Cylinders	RPM	MCR [kW]	SFOC [g/kWh]	L_{ME} [m]	H_{ME} [m]	W_{ME} [t]
MAN	V32/44CR	14	750	8,120	173	7.97	4.57	79
MAN	V32/44CR	16	750	9,600	172	8.60	4.57	87
MAN	V32/44CR	18	750	10,800	172	9.23	4.57	96
MAN	V32/44CR	20	750	12,000	172	9.86	4.57	104
MAN	V48/60CR	12	500	14,400	173	10.79	5.50	189
MAN	V48/60CR	14	500	16,800	173	11.79	5.50	213
MAN	V48/60CR	16	500	19,200	173	13.14	5.50	240
Wärtsilä	V31	14	750	8,540	167.7	8.54	4.63	84.6
Wärtsilä	V31	16	750	9,760	167.7	9.13	4.63	93.3
Wärtsilä	V46F	12	600	14,400	175	10.15	5.62	173
Wärtsilä	V46F	14	600	16,800	175	11.73	6.06	216
Wärtsilä	V46F	16	600	19,200	175	12.78	6.06	233

Validation of the powering calculations can be achieved by using the parametric model to recreate existing ships, the installed engines of which are known. Such examples are presented in Figure 4-3 below.

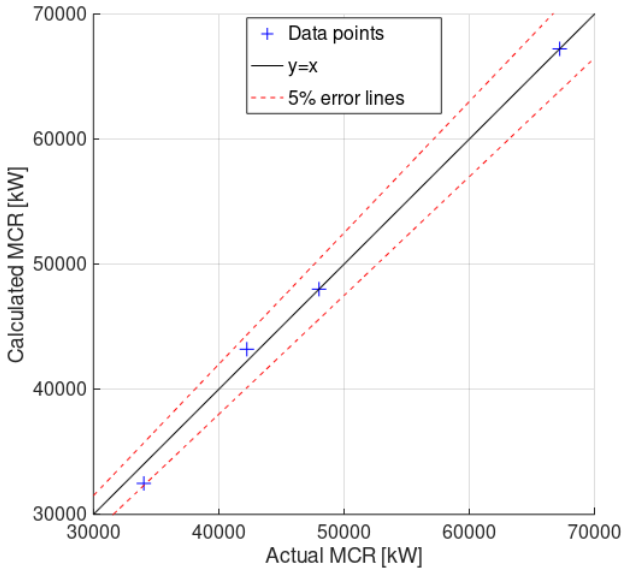

Figure 4-3. Validation of powering calculations.

The variables set equal to those of the existing ships in order to recreate them have been the main dimensions (length between perpendiculars, beam, design draft), the block coefficient, the design speed, and, when available, the LCB. The Holtrop method has been used to calculate the resistance, while the propulsion power obtained from the empirical methods has been calibrated with the coefficient (λ_{SHP}) calculated in Chapter 4.2.2. The shaft generator power has been taken equal to 3,000 kW, while

a power margin of 25% has been selected. In all four cases, it is shown that the calculated values are very close (or equal) to the actual ones.

4.3. Cargo and passenger capacity

A NAPA macro developed at NTUA-SDL is used to calculate the vehicle capacity of the ship. The macro receives as input the geometry of the ro-ro rooms, the dimensions and weight of the trucks, the web height at the sides of the ro-ro decks and the required margins from the webs and the casings, and calculates the lane meters and truck capacity for each ro-ro deck, along with the corresponding weights and their centers.

For the upper ro-ro deck, where a hoistable car deck is arranged, the private car capacity is estimated using the calculated number of trucks and an assumed private car – truck projected area ratio. The same calculation is performed for deck 6, in case part of it is reserved for private cars.

Selected default values for the various parameters are presented in Table 4-2 below.

Table 4-2. Default values of parameters for truck and car capacities.

Web height on main deck side	0.8 m
Margin of lanes from web	0.3 m
Margin of lanes from casing	0.3 m
Truck length	16 m
Truck lane beam	3 m
Truck height	4 m
Truck weight	25 t
Car length	4.5 m
Car lane beam	2.3 m
Car height	2 m
Car weight	1.5 t

Regarding the passenger capacity, the superstructure model is utilized along with assumed area coefficients (passengers / m^2). Default values which have been derived by studying existing large ro-pax ships are:

- 0.170 pax/m^2, airseats in reception zone
- 0.330 pax/m^2, other airseat zones
- 0.185 pax/m^2, cabin zones

The coefficient for cabins assumes a roughly equal distribution between 2-bed and 4-bed cabins. The user has the option to adjust the accommodation quality by supplying different weight values. All coefficients refer to the entire area of the zone in question, including corridors, toilets etc., rather than the net area intended for accommodation.

In a similar way, the maximum number of crew members that can be accommodated is calculated using area coefficients, default values of which have been selected as 0.10 persons/m^2 for lower crew and 0.05 persons/m^2 for officers. It is noted that the

developed model assigns spaces for crew cabins irrespective of the required crew number. However, as the general arrangement has been based on similar ships and the crew synthesis does not significantly vary with the size of the ship, the allocated space is expected to be close to that actually required. Attaining the required space for the crew is not considered to be a hard constraint that determines the feasibility of the design, as possible minor shortage can be covered at a later design stage with no significant effect on the general arrangement.

4.4. Lightship weight

The reliable estimation of the lightship weight is important for the correct determination of the ship's floating position and stability, but also for its building cost.

As a substitute of a more detailed method, empirical methods which have been found to be suitable for large ro-pax ships are used. The lightship is subdivided into four categories – steel, outfitting, accommodation and machinery:

$$LS = W_{ST} + W_{OT} + W_{ACC} + W_M$$

The vertical center of the lightship is also calculated by estimating the vertical center of each category:

$$KG_{LS} = \frac{W_{ST}KG_{ST} + (W_{OT} + W_{ACC})KG_{OT\&ACC} + W_M KG_M}{LS}$$

A simplified formula is used for the longitudinal center of the lightship, which is estimated as a fraction of the length between perpendiculars:

$$LCG_{LS} = C_{LCG}L_{PP}, \;\; C_{LCG} = 0.425$$

The selected calculation methods for the lightship components are presented below.

4.4.1. Steel weight

The steel weight is calculated according to Watson's method [25], as a function of an older formulation of the equipment numeral:

$$W_{ST} = KE_N^{1.36}\left[1 + 0.05\left(C_{B,0.8h_6} - 0.7\right)\right], \;\; K = 0.031 \pm 0.006$$

$$E_N = \underbrace{L_{PP}(B + T_{max}) + 0.8L_{PP}(h_6 - T_{max})}_{E_{N,hull}} + \underbrace{+ 0.85 \sum_{i=6}^{n_{decks}-1} (h_{i+1} - h_i)l_i + 0.75h_{n_{decks}}l_{n_{decks}}}_{E_{N,supst}}$$

A default value of K=0.0296 has been selected after calibration with available data from existing ships. The maximum draft, which is unknown at this stage as it depends

on the lightship weight, is estimated based on the design draft, for example 25 cm larger.

In order to calculate the vertical center of the steel weight, the resulting value is split into hull and superstructure weights as follows:

$$W_{HULL} = W_{ST}\frac{E_{N,hull}}{E_N},\ \ W_{SUPST} = W_{ST}\frac{E_{N,supst}}{E_N}$$

$$KG_{ST-hull} = C_{KG-hull}h_6,\ \ C_{KG-hull} = 0.47$$

$$KG_{ST-supst} = h_6 + C_{KG-supst}\left(h_{n_{decks}} - h_6\right),\ \ C_{KG-supst} = 0.35$$

4.4.2. Outfitting and accommodation weights

The outfitting and accommodation weights are calculated according to Schneekluth and Bertram [26]:

$$W_{OT} = W_{RAMPS} + W_{OT-rest} = W_{RAMPS} + C_{OT}W_{ST}^{2/3},\ \ C_{OT} = 1.1$$

$$W_{ACC} = C_{ACC}A_{ACC},\ \ C_{ACC} = 0.180\ t/m^2$$

$$KG_{OT\&ACC} = C_{KG-OT\&ACC}h_4,\ \ C_{KG-OT\&ACC} = 1.15$$

The weight of internal and external ramps is calculated as a function of their length and breadth according to Papanikolaou [5]. The dimensions of the ramps are taken equal to those of an existing large ro-pax and are assumed constant, while their number depends on whether a ro-ro deck for private cars is arranged on deck 6.

4.4.3. Machinery weight

The machinery weight is subdivided into two sub-categories, taking advantage of the fact that the main engines' weight is precisely known:

$$W_M = W_{ME} + W_{REST}$$

$$W_{REST} = C_{GEAR}MCR + C_{REST}MCR^{r_{REST}},$$
$$C_{GEAR} = 0.003, C_{REST} = 0.830, r_{REST} = 0.70$$

$$KG_M = C_{KG-M}h_4,\qquad C_{KG-M} = 0.50$$

In order to validate the selected methods and calibrate the various coefficients, existing ships, for which precise data are available, have been recreated using the developed model. This means that, in each case, a design with the same main dimensions, C_B, LCB, number and heights of decks has been generated. Figure 4-4 presents a comparison between actual and calculated weights, showing very good agreement in all cases, despite the simplicity of the methods.

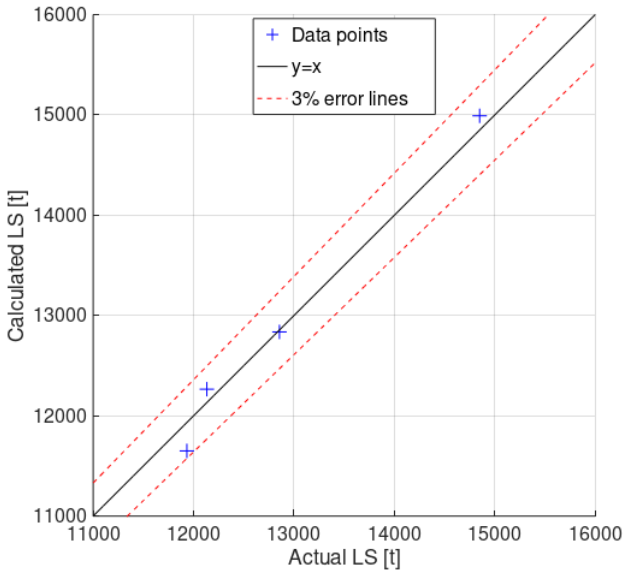

Figure 4-4. Validation of lightship calculation methods by comparison with existing ships.

The results for the vertical and longitudinal center of the lightship weight are also in agreement with available values for two existing ships, with the deviations not exceeding ±2%.

4.5. Loading conditions

Utilizing the developed compartment model and having calculated the lightship weight, the design of the loading conditions takes place.

The following representative loading conditions are defined:

- LDS01, LDS02: Full load departure, full load arrival
  The three trailer decks are fully loaded with trucks of the maximum weight, and the car deck –if applicable– fully loaded with private cars. The ship is also fully loaded with passengers.
- LDS03, LDS04: Only passenger departure, only passenger arrival
  The ship is fully loaded with passengers but without any vehicles, as specified in IMO's intact stability code.
- LDS05, LDS06: Light load departure, light load arrival
  These conditions are based on LDS01 and LDS02 respectively, but with reduced truck weights by 70% on the lower hold and by 50% on the main and upper car decks.
- LDS07, LDS08: Summer full load departure, summer full load arrival
  The upper trailer deck is converted into two car decks by lowering the hoistable platforms, and the two car decks are fully loaded with private cars. The other ro-ro decks are also fully loaded and the number of passengers is the maximum possible, as in LDS01 and LDS02.
- LIGHT: Lightship condition (not seagoing)

In departure conditions, the filling percentage of fuel tanks is calculated based on the ship's design operational profile (range and desired number of trips without bunkering), including also an appropriate safety margin. In arrival conditions, the filling percentage is 10% of the above.

Finally, all conditions include some ballasting in order to attain satisfactory stability and / or trim. It is noted that the optimization of loading conditions in terms of floating position and stability is not included in the parametric model. Firstly, this means that, for specific values of parameters, the required fuel is split between the various tanks proportionally to their volumes. Furthermore, for a specific loading condition, predefined ballast tanks are loaded up to a specific percentage, irrespective of the values given to the parameters. In reality, the distribution of fuel between the various tanks could also be a way to reduce trim, while the optimal ballasting could be parametrically calculated in order to attain the required stability characteristics. For the examined design space however, it has been observed that this partially static model is sufficient.

4.6. Intact stability

The intact stability of the ship is calculated according to IMO's intact stability code (Resolution MSC. 267(85)), for each of the design loading conditions.

The relevant criteria are:

- The general criteria, regarding the properties of the righting lever curve.
- The severe wind and rolling criterion (weather criterion).
- Special criteria for passenger ships, specifying maximum heeling angles due to crowding of passengers and due to turn.

The procedure is organized by a NAPA Macro, while the core of the calculations (generation of GZ curves, calculation of heeling angles etc.) is performed automatically by NAPA.

The intact stability of the ship is assessed by the intact VCG margin, expressing the minimum distance of the ship's vertical center of gravity from the maximum allowed position, taking into account all loading conditions and relevant stability criteria:

$$\Delta KG_{intact} = \min_{i=1,\dots,n_{LC}} \{KG_{max,i} - KG_i\}, \; KG_{max,i} = \min_{j=1,\dots,n_{CR}} \{KG_{max,ij} - KG_i\}$$

4.7. Damage stability

4.7.1. General

In order for the damage stability calculations to take place, the hull is subdivided into transverse, longitudinal and horizontal zones. This procedure is parametrically programmed in order to account for the various possible numbers of transverse bulkheads. The subdivision should be dense enough for the model not to be overly conservative, meaning that all important watertight boundaries of the ship are

included, but not too dense, in order for the calculation time to be acceptable. In general, longitudinal zones are limited by the main transverse bulkheads, transverse zones by the B/5 bulkheads and horizontal zones by the decks. In some cases, other relatively important limits are taken into account, eg. some tank sides or the upper limit of the skeg.

Another measure taken in order to speed up the calculation is that the damages are assumed only on the port side of the ship. The effect of this simplification is considered negligible, as the general arrangement is to a very high degree symmetric.

Damage stability calculations are conducted for the three initial conditions which are defined in SOLAS Chapter II-1 Regulation 2. These are: the full load condition, with the ship at its subdivision draft d_s and even keel, the light service draft d_l with 0.2 m trim by stern, and the partial service draft, $d_P = 0.6d_S + 0.4d_l$ with even keel. The metacentric heights of these loading conditions are determined by those of the previously designed loading conditions.

All lost buoyancy calculations are automatically performed by NAPA, while the procedure is organized by NAPA macros developed at NTUA-SDL and HSB.

4.7.2. SOLAS regulations 6 & 7

Regulations 6 and 7 of SOLAS Chapter II-1 prescribe the application of a probabilistic model to assess a ship's damage stability. The main requirement is $A \geq R$, where A is the "attained subdivision index", expressing the probability that a ship survives after collision, and R the "required subdivision index", which is the minimum allowed probability of survival.

The required subdivision index R is a function of the number of persons on board [27], as shown in Figure 4-5. This amended formulation included in SOLAS 2020 generally returns significantly higher values for R in comparison with the older SOLAS 2009 index.

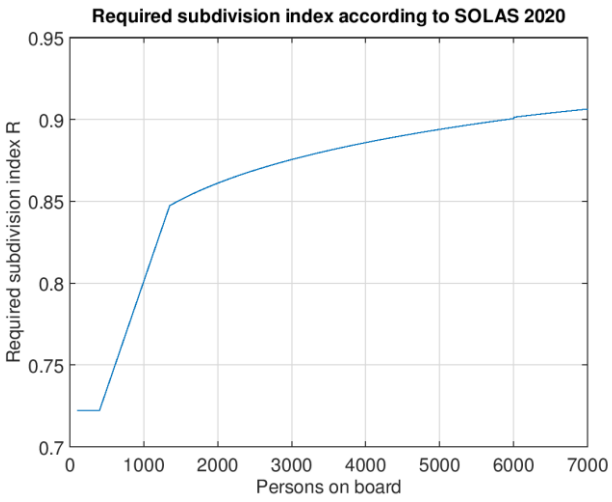

Figure 4-5. Required subdivision index R.

The attained index is a weighted average of three partial indices, A_d, A_p and A_l, referring to the three aforementioned loading conditions, with weights equal to 0.4, 0.4 and 0.2 respectively.

Each partial index is defined as $A_c = \sum_i p_i v_i s_i\,,\ \ c = d, p, l$, where:

- i is the damage zone (compartment or group of compartments) under consideration, as defined by transverse and longitudinal watertight boundaries.
- p_i is the probability that only the damage zone i is flooded after a damage.
- v_i is the probability that spaces above the horizontal subdivision are not flooded.
- s_i is the probability that the ship survives the examined damage (does not sink or capsize).

The probabilities p_i and v_i are calculated using specific probability density functions, while the probabilities s_i according to the properties of the GZ curve in the damaged condition. SOLAS 2020 rules also take into account the possible impact of ro-ro deck flooding, prescribing stricter parameters for the calculation of the s-factor when an examined damage impacts ro-ro spaces.

In addition to the requirement that $A \geq R$, each partial index must also be at least 90% of R: $A_c \geq 0.9R,\ \ c = d, p, l$.

An appropriate macro developed at NTUA-SDL is used for the assessment. Damages of up to five adjacent zones are taken into account.

4.7.3. SOLAS regulations 8 & 9

The probabilistic model is supplemented by some deterministic requirements for passenger ships, defined in SOLAS Chapter II-1 Regulations 8 and 9:

- Regulation 8.1: Passenger ships carrying 400 persons or more must survive breaching of all compartments within 8% of the subdivision length from the forward perpendicular (survival probability: s_i=1).
- Regulation 8.2-3: Passenger ships carrying 36 persons or more must survive side shell damages of a certain extent with a probability $s_i \geq 0.9$.
- Regulation 9: Ships with an unusual double bottom arrangement must be able to survive raking damages of a certain extent with probability s_i=1.

Compliance with the first two requirements (regulation 8) is assessed using a NAPA macro developed at HSB.

The examined designs are actually subject to regulation 9 as well, due to the partial double hull arrangement in the forward region. However, it is considered that such large ships are not expected to face problems after raking damage of small vertical extent.

4.7.4. Stockholm agreement

For ships sailing in the European Union, the Stockholm agreement sets further damage stability criteria in addition to IMO's requirements. It demands that, for damages including the first ro-ro deck above the waterline, damage stability requirements according to SOLAS '90 Regulation II-1/B/8.2.3 be satisfied with that ro-ro deck flooded up to a certain height, even if the deck remains entirely above the equilibrium waterline. The height of the "water on deck" ranges between 0 and 0.5 m, depending on the residual freeboard after the damage and the significant weight height in the region the ship operates [13].

Once again, the calculations are performed automatically using a macro developed at HSB.

4.8. Energy efficiency design index

The EEDI is calculated taking into account the ship's propulsion and auxiliary power, including shaft generators. For ro-pax ships with conventional diesel propulsion and disregarding efficiency technologies, the general EEDI formula is simplified as follows [14]:

$$EEDI = \frac{1}{f_c\, DWT\, V_{ref}}\left[f_j\, 0.75 C_{FME} SFOC\left(MCR - P_{shaftgen}\right) + P_{shaftgen,EEDI} C_{FME} SFOC + P_{AE,EEDI} C_{FAE} SFOC_{AE}\right]$$

The numerator expresses the total rate of CO_2 emissions, while the denominator expresses the rate of transport work produced by the ship. Thus, the EEDI is actually an inverse efficiency factor, expressing the produced emissions for a given transport work rate.

The various terms are calculated as follows:

$$P_{shaftgen,EEDI} = \min\{P_{shaftgen},\ 0.025MCR + 250kW\}$$

$$P_{AE,EEDI} = 0.025MCR + 250kW - P_{shaftgen,EEDI}$$

$$C_{FME} = C_{FAE} = 3.206$$

$$f_j = \min\left\{\frac{1}{Fn_L^{2.5}\left(\frac{L}{B}\right)^{0.5}\left(\frac{B}{d_s}\right)^{0.75}\left(\frac{L}{\nabla^{1/3}}\right)}, 1\right\}$$

$$f_c = \begin{cases}\left(\dfrac{\frac{DWT}{GT}}{0.25}\right)^{-0.8}, & \dfrac{DWT}{GT} \le 0.25 \\ 1, & \dfrac{DWT}{GT} > 0.25\end{cases}$$

As can be observed in the above equations, the auxiliary power is calculated as a function of the installed power of the main engines and is not linked to the actual auxiliary power of the ship. With regard to the correction coefficients, f_j aims to take into account the speed of the ship, while f_c its volumetric capacity as opposed to just the deadweight.

The calculation of the maximum speed is approximate, based on the design speed and assuming that, for small deviations from a reference condition, propulsion power is proportional to $V^3\nabla^{2/3}$, where displacement volume is in turn proportional to the draft:

$$V_{ref} = V\left[\frac{0.75\left(MCR - P_{shaftgen}\right)}{SHP}\right]^{\frac{1}{3}}\left(\frac{T_d}{d_s}\right)^{\frac{2}{9}}$$

The required EEDI for each application phase is calculated as follows:

$$EEDI_{req} = \left(1 - \frac{X}{100}\right) DWT^{-0.381} \cdot \begin{Bmatrix} 752.16, & phase < 2 \\ 902.59, & phase \geq 2 \end{Bmatrix}$$

$$X = \begin{cases} 0, & phase\ 0\ (2013 - 2015) \\ 5, & phase\ 1\ (2015 - 2019) \\ 20, & phase\ 2\ (2020 - 2024) \\ 30, & phase\ 3\ (2025 +) \end{cases}$$

It is noted that the above formula yields higher values for phase 2 compared to phase 1. This is due to a recent 20% increase of the reference line for ro-pax ferries from phase 2 onwards, as the original baseline was proved to have been overly optimistic [28].

4.9. Economic indices

In order to assess the economic performance of the ship, the building cost as well as the yearly income and operational expenses are estimated.

The building cost is estimated based on unit cost coefficients for the lightship components. Another coefficient is introduced to cover non-weight costs. The cost of the scrubber, if applicable, is supplied separately:

$$K_{build} = (K_{ST} + K_{OT\&ACC} + K_M)(1 + C_{K-rest}) =$$
$$= [C_{K-ST}W_{ST} + C_{K-OT\&ACC}(W_{OT} + W_{ACC}) + C_{K-M}W_M + K_{SCRUB}](1 + C_{K-rest})$$

Default values for the cost coefficients have been selected according to Watson [25], adjusted to 2019 values: $C_{K\text{-}ST}$ = 4,500 \$/t, $C_{K\text{-}OT\&ACC}$ = 18,000 \$/t, $C_{K\text{-}M}$ = 16,000 \$/t, $C_{K\text{-}rest}$ = 10%. Regarding the cost of the scrubber, a default value of \$3,000,000 has been selected. It is emphasized that these values are not meant to be accurate but mostly to provide a basis for comparison between different designs – however, the various coefficients may be modified by the user if more precise data are available.

The building cost is then increased by a percentage (default value: 5%) to obtain the newbuilding price.

The yearly income IN_t comes from the passenger and vehicle tickets. Default ticket prices have been selected based on current (2019) prices for the Patras – Ancona route, which can be modified according to the route under consideration. An additional income per passenger from on-board services can be added. Mean yearly occupancies for passengers, cars and trucks are also given as parameters. VAT and other charges are then deducted from the gross income.

Measures are taken in order to ensure that ships only modestly benefit from economies of scale, meaning that a given percentile increase in capacity does not bring about an equal increase in transported passengers and freight. This applies to ships with larger capacity than the specified owner's requirements, which are supposed to represent a reference demand for transport work. In other words, the given occupancies refer to ships with the exact capacity required by the owner; for larger ships, the passenger occupancy is multiplied by the factor N_{PAXeff}/N_{PAX} etc.

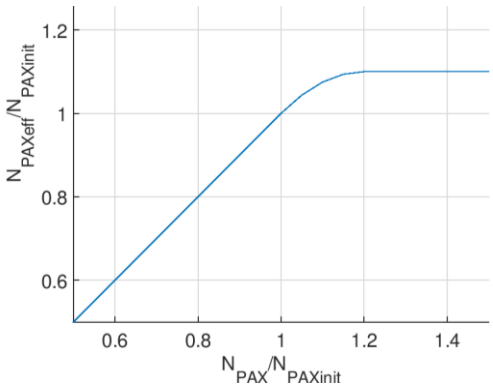

Figure 4-6. Actual versus effective passenger capacity of the ship. Similar relations apply to car and truck capacities.

The fuel oil and diesel oil costs per trip are calculated based on the defined operational profile and the selected main engines:

$$K_{fuel} = \left[SFOC_{eff} \cdot SHP_{eff} \cdot t_{trip} + SFOC_{AE,eff} \cdot P_{AE} \cdot t'_{trip}\right] C_{fuel}$$

The specific fuel oil consumption of the engines is corrected for different fuel in comparison with ISO conditions, using the ratio of lower calorific values of the two fuels. To obtain the "effective" propulsion power, the calculated power demand is increased by a percentage representing an average increase due to adverse weather conditions and fouling. Auxiliary power is estimated empirically, assuming a reference value, 60% of which remains constant and 40% increases proportionally to $L_{PP} \cdot B$. In all cases, the main and auxiliary engines are supposed to use the same fuel, which is either heavy fuel oil if the ship is equipped with a scrubber or low-sulfur fuel oil otherwise.

The cost of lubricant oil is estimated as a fraction of the total fuel cost.

After bunker costs, the second major operational expense is the crew cost, which is estimated using a mean monthly value per person, including salary but also insurance, provisions etc. Yearly insurance and maintenance costs of the ship are estimated as fractions of the building cost. The total operational cost is derived as the sum of the above, including also a percentile increase to account for various other costs.

Finally, assuming an interest rate and a lifetime of the investment, the net present value of the investment is calculated:

$$NPV = -K_{ship} + \sum_{t=1}^{lifetime} \frac{IN_t - OUT_t}{(1+r)^t} + \frac{K_{final}}{(1+r)^{lifetime}}$$

As with the building cost of the ship, the calculated net present value is not meant to be accurate, as highly uncertain parameters are involved in the calculation. The results are mainly intended to serve as a basis of comparison between different designs in terms of profitability.

Chapter 5. Example Design

This chapter presents a design example. Realistic values are assigned to the various parameters and some indicative results are presented.

5.1. General particulars

The selected values of some global parameters which affect the entire design loop are presented in Table 5-1. Of course, the design is governed by many more parameters with local effect, which will be presented later in the relevant sections.

Table 5-1. Selected values of global parameters.

L_{PP}	207.00 m
B	29.90 m
T_D	7.000 m
C_B	0.560
LCB/L_{PP}	0.455
V	28.0 kn
V_{return}	28.0 kn
FS	0.800 m
Decks	11
Cars on deck 6	No
h_{DB} / $h_{DB,E/R}$ / $h_{DB,aft}$	1.50 m / 1.70 m / 2.30 m
h_1	4.20 m
h_2	6.30 m
h_3	9.80 m
h_4	15.40 m
h_5	18.20 m
h_6	21.25 m
h_7	24.00 m
h_8	26.75 m
h_9	29.90 m
h_{10}	33.05 m
h_{11}	35.75 m

5.2. Hull form and powering

Figure 5-1, Figure 5-2 and Figure 5-3 present the transformed hull, the hydrostatic diagram of the ship and the cross curves of stability respectively.

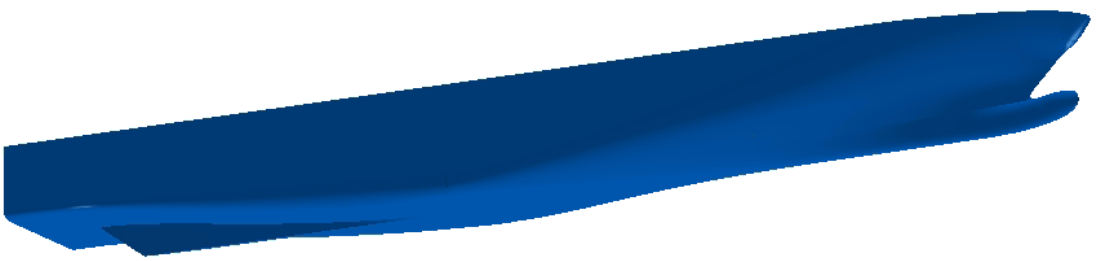

Figure 5-1. Hull of the ship.

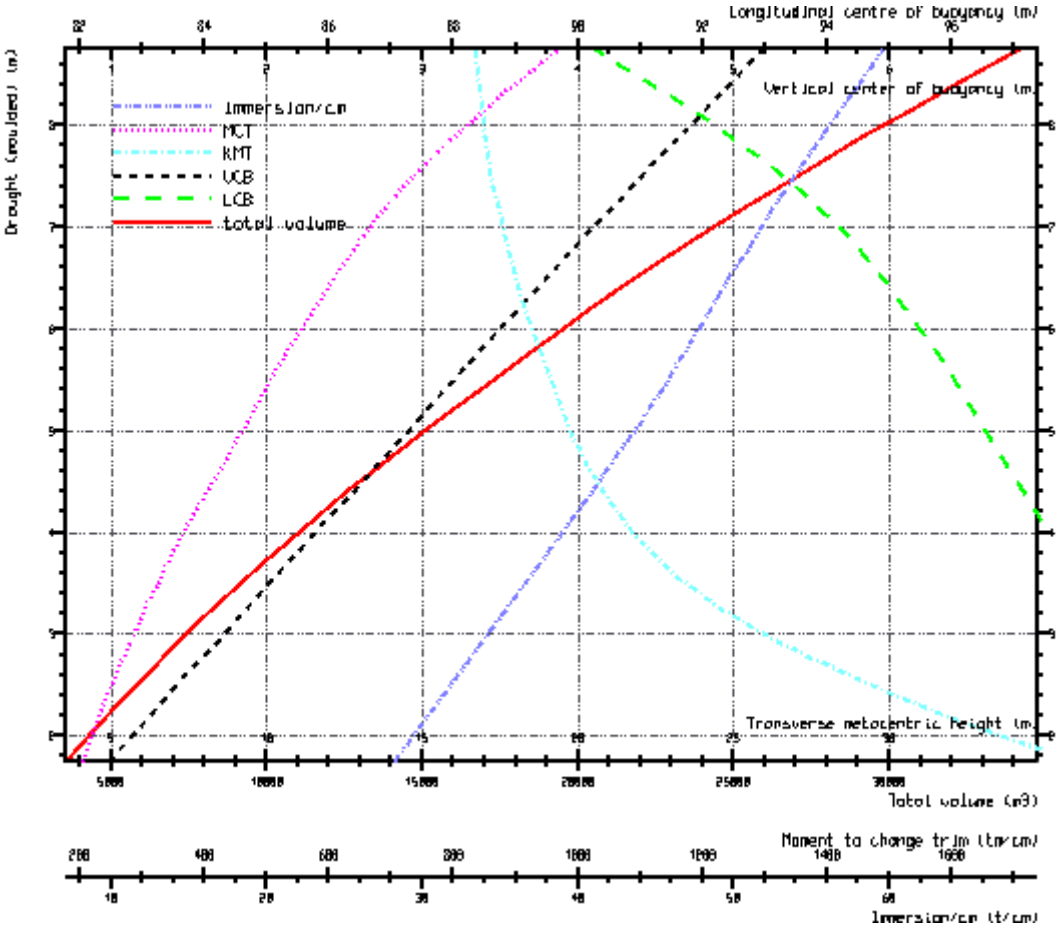

Figure 5-2. Hydrostatic diagram.

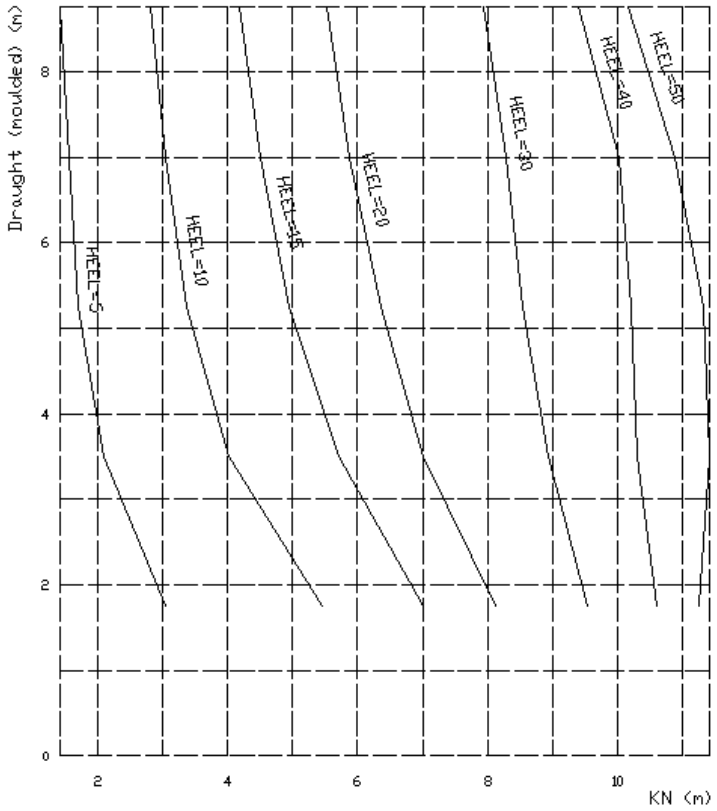

Figure 5-3. Cross curves of stability.

Next, Table 5-2 lists the values of the parameters affecting stern form and the powering of the ship, while Table 5-3 presents the results of the calculations.

Table 5-2. Parameters regarding the stern of the ship and the powering calculations.

Hull end	#-7
Length of duck tail aft of hull end	5 m
Resistance calculation method	Holtrop
Position of propellers	#5
PM	0.25
η_s	0.97
λ_{SHP}	0.906
Engine manufacturer	Both
Allow different engines	Yes
$P_{shaftgen}$	3,000 kW

Table 5-3. Results of powering calculations.

Froude number	0.309
Effective horsepower	29.36 MW
Propeller diameter	5.39 m
Number of blades	4
Expanded area ratio	0.787
Wake fraction	0.086
Thrust deduction factor	0.100
Relative rotative efficiency	0.976
RPM	168.78
Pitch – diameter ratio	1.140
Propulsive coefficient	0.641
SHP_0	45.77 MW
SHP	41.46 MW
Engine models	4 x MAN 12V48/60CR
Engine MCR	4 x 14,400 kW
Engine weight	4 x 189 t
Engine length	10.79 m
Engine height	5.50 m
Specific fuel oil consumption (ISO conditions)	173 g/kWh
MCR	57,600 kW
SHP_{max}	54,600 kW

5.3. General arrangement and 3-D model

The values of parameters which govern the general arrangement of the ship are presented in Table 5-4.

Table 5-4. Selected values of relevant parameters.

Required engine room length in excess of main engine length	5 m
Required engine room height in excess of main engine height	1 m
Collision bulkhead margin from extreme values	1 m
Position of collision bulkhead (forward or aft)	Aft
Minimum position of aft E/R bulkhead [% L_{PP}]	26.5
Maximum position of aft E/R bulkhead [% L_{PP}]	28.5
Minimum acceptable lower hold breadth	3.5 m
Longitudinal bulkheads position [% B]	20
Bunkers margin from hull side	1 m
Fresh water margin from hull side	1 m
Width of open deck for life-saving appliances	5.5 m
Initial inclination of bow superstructure surface	0.96
Maximum allowed inclination of bow superstructure surface	2
Minimum acceptable fire zone length in superstructure	17 m
Half breadth of staircases in superstructure	3 m
Half breadth of enclosed superstructure on sun deck	5 m

The resulting number of bulkheads is equal to that of the baseline design (16), while the ship is subdivided into six fire zones, the last of which is entirely outside the superstructure. The positions of the relevant divisions are presented in Table 5-5 and Table 5-6 respectively.

Table 5-5. Positions of transverse bulkheads and resulting compartment lengths.

i	1	2	3	4	5	6	7	8	9	10	11	12	13	14	15	16	17
Bulkhead i position [#]	9	25	41	57	69	89	109	121	137	153	169	185	201	217	233	245	
Compt. length aft of bulkhead i [m]	17.8	12.8	12.8	12.8	9.6	16	16	9.6	12.8	12.8	12.8	12.8	12.8	12.8	12.8	9.6	22.3

Table 5-6. Positions of main fire divisions and resulting fire zone lengths.

i	1	2	3	4	5	6
Fire division position [#]	41	89	137	185	245	
Fire zone length aft of fire division i [m]	43.39	38.40	38.40	38.40	48.0	22.29

Next, the general arrangement is presented in Figure 5-4 and Figure 5-5, followed by some views of the external ship model in Figure 5-6.

Subsequently, all compartments with their properties and the internal openings (non-watertight connections between rooms) are listed in Table 5-7 and Table 5-8 respectively.

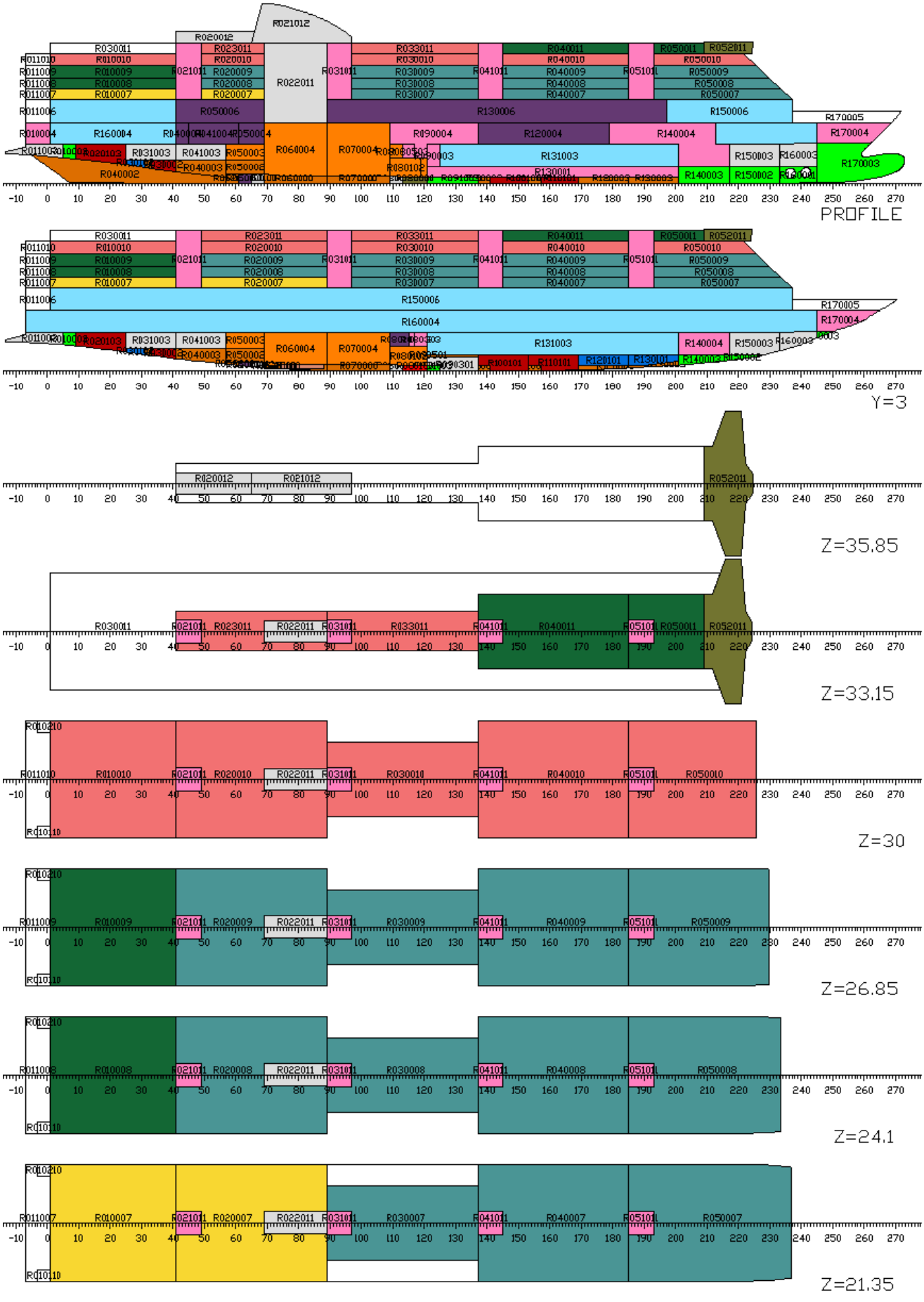

Figure 5-4. Profile, longitudinal section and superstructure decks (open decks are also modeled as rooms).

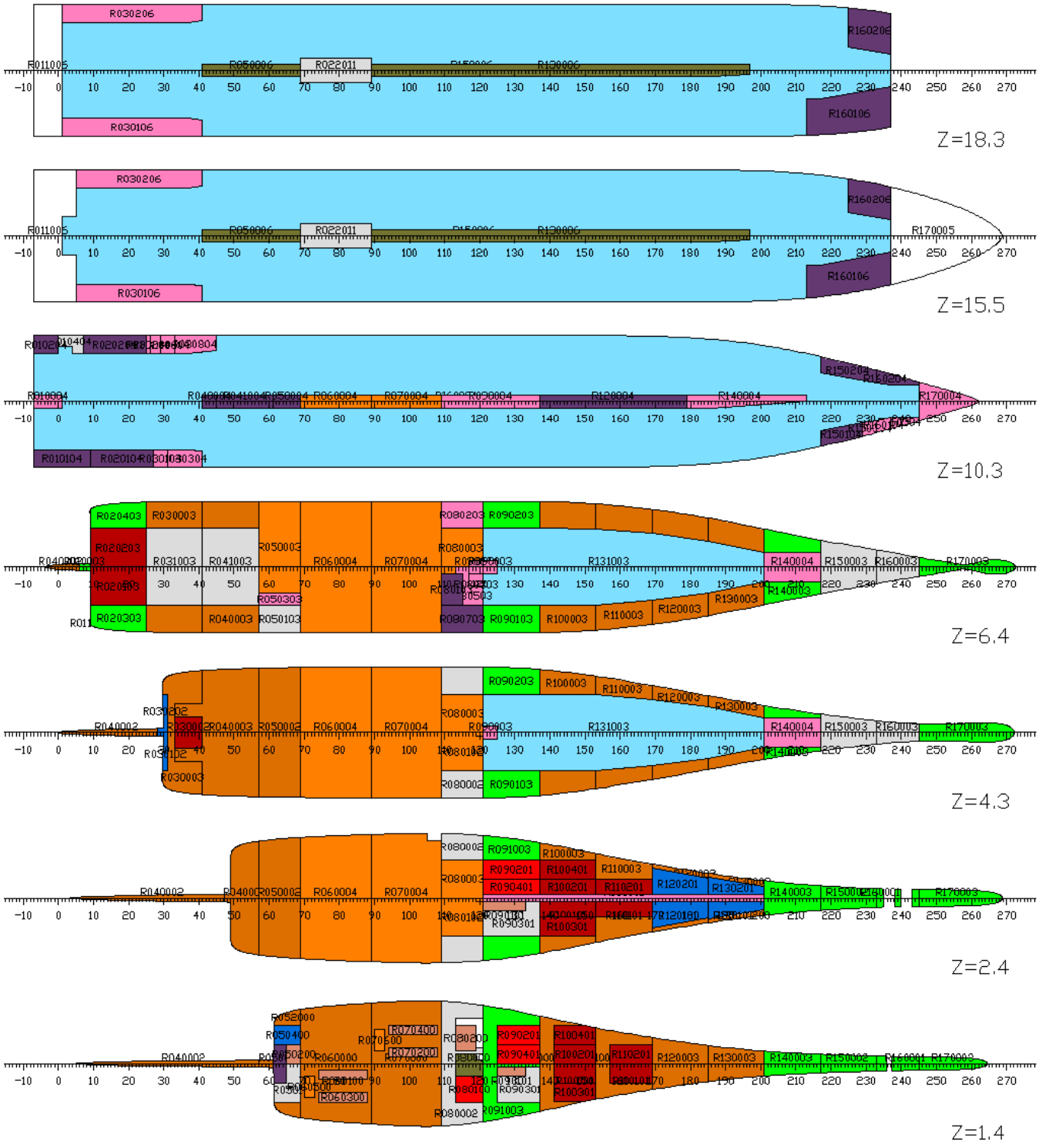

Figure 5-5. Ro-ro decks and lower decks.

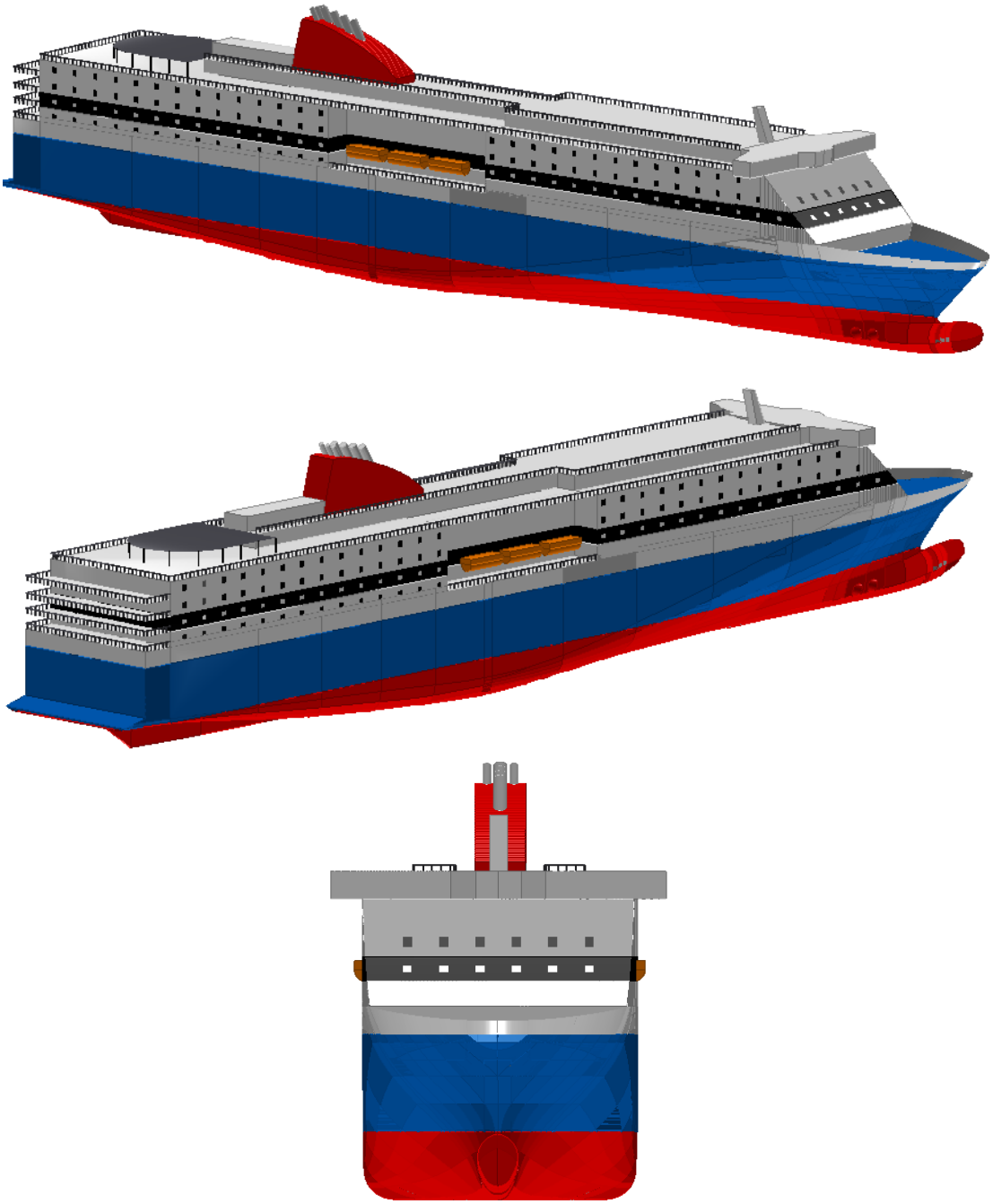

Figure 5-6. Views of the 3-D model.

Table 5-7. Table of compartments and their basic properties.

NAME	DESCRIPTION	V_{NET} [m^3]	FRMIN	FRMAX	LCG [m]	VCG [m]
Accommodation						
R011007	Open deck	462.9	-7	1	-2.57	22.62
R011008	Open deck	462.9	-7	1	-2.57	25.37
R011009	Open deck	530.3	-7	1	-2.57	28.32
R011010	Open deck	530.3	-7	1	-2.57	31.47
R010007	Airseats	2,578.6	1	41	16.8	22.62
R020007	Airseats	2,749.3	41	89	51.62	22.62
R030007	Cabins	1,852.4	89	137	91.29	22.62
R040007	Cabins	2,990.8	137	185	129.35	22.62
R050007	Cabins	3,118.3	185	237	168.57	22.61
R010008	Crew cabins	2,578.6	1	41	16.8	25.38
R020008	Cabins	2,749.3	41	89	51.62	25.38
R030008	Cabins	1,852.4	89	137	91.29	25.38
R040008	Cabins	2,990.8	137	185	129.35	25.37
R050008	Cabins	2,894.6	185	233.41	167.17	25.36
R010009	Crew spaces	2,953.6	1	41	16.8	28.32
R020009	Cabins	3,149.2	41	89	51.62	28.33
R030009	Cabins	2,121.9	89	137	91.29	28.33
R040009	Cabins	3,425.8	137	185	129.35	28.32
R050009	Cabins	3,036.9	185	229.83	165.65	28.3
R010010	Public spaces	2,953.6	1	41	16.8	31.47
R020010	Public spaces	3,149.2	41	89	51.62	31.47
R030010	Public spaces	2,121.9	89	137	91.29	31.48
R040010	Public spaces	3,425.8	137	185	129.35	31.47
R050010	Public spaces	2,736.1	185	225.72	164.01	31.45
R023011	Public spaces / various	677.4	41	89	50.48	34.4
R033011	Public spaces / various	914.5	89	137	92.18	34.4
R030011	Sun deck	5458	1	137	42.03	34.4
R040011	Officer cabins	1,818.8	137	185	129.69	34.4
R050011	Officer cabins	858.6	185	209	158.36	34.4
SUBTOTAL		**67,143.0**			**87.22**	**28.14**
Auxiliary machinery spaces						
R011003	Steering gear room	1,077.7	-13.24	9	-1.11	8.33
R031003	Compressors room	861.5	25	41	26.4	7.84
R041003	Auxiliary machinery	861.5	41	57	39.2	7.84
R050103	Auxiliary machinery	228.3	57	69	50.4	7.84
R080002	Auxiliary machinery	735.1	109	121	91.54	3.14
R150003	Pump room	783	217	233	179.53	7.41
R160003	Bow thruster room	384.8	233	245	190.88	7.57
R010404	Ventilation machinery	97.3	0	7	3.12	12.6
R022011	Engine casing	1,786.9	69	89	63.2	25.57
R021012	Funnel	957	65	97	63.08	39.66
R020012	Auxiliary machinery	300.8	41	65.93	42.59	37.16
SUBTOTAL		**8,074.0**			**66.21**	**16.27**
Ro-ro spaces						
R131003	Lower hold	5,240.3	121	201	125.36	7
R160004	Main roro deck	26,768.9	-7	245	90.83	12.62
R150006	Upper roro deck	27,345.9	1	237	94.8	18.33
SUBTOTAL		**59,355.1**			**95.71**	**14.75**
Diesel oil tanks (ρ=0.9 t/m^3)						
R080100	Diesel oil tank	55	113	121	93.6	0.75
R090201	Diesel oil tank	169	121	137	103.73	1.9
R090401	Diesel oil tank	153.4	121	137	103.84	1.79
SUBTOTAL		**377.4**			**102.3**	**1.69**

Fresh water tanks (ρ=1 t/m^3)						
R030102	Fresh water tank	57.8	25	31	22.59	5.16
R030202	Fresh water tank	57.8	25	31	22.59	5.16
R050400	Dist. FW tank	31.5	61	69	52.25	1.72
R120101	Fresh water tank	185.3	169	185	141.16	3
R120201	Fresh water tank	185.3	169	185	141.16	3
R130101	Fresh water tank	119.1	185	201	153.77	3.04
R130201	Fresh water tank	119.1	185	201	153.77	3.04
SUBTOTAL		**755.9**			**123.29**	**3.29**
Grey water tanks (ρ=1 t/m^3)						
R050100	Grey water tank	51.5	61	69	52.79	1.64
R090301	Grey water tank	250.3	121	137	104.15	1.88
SUBTOTAL		**301.8**			**95.39**	**1.84**
Heavy fuel oil tanks (ρ=0.98 t/m^3)						
R020103	HFO tank	458.8	9	25	14.01	7.69
R020203	HFO tank	458.8	9	25	14.01	7.69
R030002	HFO tank	108.8	33	41	29.78	4.68
R100101	HFO tank	185.1	137	153	116.53	2.15
R100201	HFO tank	185.1	137	153	116.53	2.15
R100301	HFO tank	185.6	137	153	116.22	2.45
R100401	HFO tank	185.6	137	153	116.22	2.45
R110101	HFO tank	180.7	153	169	129.28	2.2
R110201	HFO tank	180.7	153	169	129.28	2.2
SUBTOTAL		**2,129.1**			**70.02**	**4.73**
Lubricating oil tanks (ρ=0.9 t/m^3)						
R050200	Lube oil tank	19.9	65	69	53.64	1.53
R060100	Lube oil tank	24	74	88	64.8	1.21
R060300	Lube oil tank	24	74	88	64.8	1.21
R070200	Lube oil tank	24	94	108	80.8	1.2
R070400	Lube oil tank	24	94	108	80.8	1.2
R080200	Dirty oil tank	41.3	113	119	92.8	0.75
R090101	Lube oil tank	61.8	121	133	102.13	1.92
SUBTOTAL		**219.2**			**83.1**	**1.35**
Miscellaneous						
R050000	Bilge tank	33.6	61	65	50.45	1.61
R050300	Gear S	3.4	57	61	47.2	2.05
R050600	Gear P	3.4	57	61	47.2	2.05
R080000	Sludge tank	44.7	113	121	93.41	0.75
R050006	Casing upper car deck	375	41	69	44	18.32
R130006	Casing upper car deck	1,431.4	89	197	113.98	18.33
R052011	Wheelhouse	944.7	209	224.62	173.22	34.55
SUBTOTAL		**2,836.2**			**123.22**	**23.22**
Machinery spaces						
R050003	ECR	782.3	57	69	50.4	7.84
R060500	Gear	8.7	70	73	57.12	1.68
R060004	Main engine room	4,052.2	69	89	63.28	6.27
R070600	Gear	4.6	90	93	73.2	1.5
R070004	Main engine room	4,111.1	89	109	79.19	6.21
R080102	Separator room	394.6	109	121	91.97	3.92
R080003	Aux. room	700.1	109	121	91.9	5.66
SUBTOTAL		**10,053.7**			**71.9**	**6.22**
Stairs & various						
R050303	ECR corridor	109.9	57	69	50.4	7.84
R090004	Stairs & lift	399	109	137	98.14	12.23
R080303	Stairs	32.7	117	121	95.2	8.05
R080503	Corridor	106.3	113	121	93.79	8.05
R080203	Generator room	208	109	121	92	8.05

R090003	Stairs	52.3	121	125	98.4	7
R130001	Pipe tunnel	252.3	121	201	128.8	2.85
R140004	Stairs	843.1	179	217	162.13	9.37
R170004	Bow door	707.7	245	268.67	202.26	13.31
R010004	AHU room	104.4	-7	1	-2.39	12.6
R030104	Bunker station S	71.7	27	31	23.2	12.6
R030304	Stairs	175.9	31	41	28.75	12.6
R030204	Escape	22.2	25	26.24	20.49	12.6
R030404	Crew lav.	49.5	26.24	29	22.09	12.6
R030604	Bunker station PS	71.7	29	33	24.8	12.6
R030804	Ventilation machinery	202	33	45	31.03	12.6
R150304	Escape trunk	93.2	229	233	184.79	13.06
R160104	Escape trunk	88.6	233	237	187.98	13.12
R160304	Staircase	140	237	245	192.56	13.31
R030206	Side casing port	709.5	1	41	17.46	18.4
R030106	Side casing stb	709.5	1	41	17.46	18.4
R010110	Staircase	113.3	-3	1	-0.8	27.15
R010210	Staircase	113.3	-3	1	-0.8	27.15
R021011	Staircase	556.8	41	49	36	28.5
R031011	Staircase	556.8	89	97	74.4	28.5
R041011	Staircase	556.8	137	145	112.8	28.5
R051011	Staircase	556.8	185	193	151.2	28.5
SUBTOTAL		**7,603.2**			**92.64**	**17.85**
Stores						
R080103	Dry provision store room	122.6	109	115	89.6	8.05
R080703	Refrigerating room	208	109	121	92	8.05
R010104	Various store	286.4	-7	9	0.81	12.6
R010204	Various store	125.2	-7	0	-2.79	12.6
R020104	Fire station	322.6	9	27	14.4	12.6
R020204	Store	322.6	7	25	12.8	12.6
R040004	Store	52.3	41	45	34.4	12.6
R041004	Store	209.3	45	61	42.4	12.6
R050004	Store	104.7	61	69	52	12.6
R120004	Store	549.4	137	179	126.4	12.6
R150204	Store	383.7	217	233	179.93	13.01
R150104	Store	290.7	217	229	178.37	12.99
R160204	Store	228.6	233	245	190.78	13.23
R170005	Mooring equipment & stores	1,178.1	237	271.8	200.16	16.87
R160206	Side casing port	506.1	225	237	184.84	18.46
R160106	Side casing stb	970.9	213	237	180.26	18.43
R011006	Mooring	1,306.6	-7	5	-1.7	18.1
SUBTOTAL		**7,167.8**			**110.35**	**15.36**
Void spaces						
R040002	Skeg	206	-5.05	57	20.65	2.75
R030003	Void space	971.4	25	41	26.83	6.74
R040003	Void space	1,914.5	33	57	39.06	5.37
R052000	Void space	105.5	57	69	49.74	1.8
R050002	Void space	975.8	57	69	50.42	4.12
R060000	Void space	488.8	69	89	63.53	1.1
R070000	Void space	649.6	89	109	79.25	0.86
R090501	Cofferdam S	70.5	121	137	103.2	3.85
R090601	Cofferdam P	70.5	121	137	103.2	3.85
R100003	Void space	1,139.2	137	153	115.47	5.87
R110003	Void space	1,242.4	153	169	128.46	5.63
R120003	Void space	1,017.8	169	185	141.56	6.21
R130003	Void space	986.4	185	201	154.41	6.56
SUBTOTAL		**9,838.4**			**85.8**	**5.05**

Water ballast tanks (ρ=1.025 t/m^3)						
R010003	Water ballast tank	179.3	5	9	5.62	8.17
R020303	Water ballast tank	310.7	9	25	13.99	7.76
R020403	Water ballast tank	310.7	9	25	13.99	7.76
R090103	Heeling tank S	483.6	121	137	103.17	6.68
R090203	Heeling tank P	483.6	121	137	103.17	6.68
R091003	Water ballast tank	402.3	121	137	101.81	1.88
R140003	Water ballast tank	973.2	201	217	166.69	5.96
R150002	Water ballast tank	232	217	233	179.67	2.49
R160001	Water ballast tank	98.8	233	245	191.04	2.34
R170003	Fore peak tank	542.6	245	272.87	204.42	5.18
SUBTOTAL		**4,016.8**			**120.53**	**5.71**
TOTAL		**179,871.5**			**90.57**	**18.71**

Table 5-8. Arrangement of openings.

Opening	Frame	x [m]	y [m]	z [m]	Room 1	Room 2
DOOR0501	#63	50.40	8.760	5.880	R050103	R050303
DOOR0502	#63	50.40	5.840	5.880	R050303	R050003
STAIRS05	#57	45.60	8.760	5.880	R050003	R050002
DOOR0801	#115	92.00	6.935	6.300	R080103	R080503
DOOR0802	#117	93.60	2.920	6.300	R080303	R080503
DOOR0803	#113	90.40	0.000	6.300	R080003	R080503

5.4. Payload and lightship

All parameters regarding passengers and vehicles, as well as the lightship weight coefficients, have been assigned their default values as these have been presented in Chapter 4. The results regarding passenger, truck and car capacities are shown in Table 5-9, with the lightship weight calculation results following in Table 5-10.

Table 5-9. Passenger, car and truck capacities of the ship.

Lanes	9
Lane meters	3,071.1
Lane meters – deck 1	242.3
Lane meters – deck 3	1,437.7
Lane meters – deck 4	1,391.0
Trucks	187
Trucks – deck 1	13
Trucks – deck 3	88
Trucks – deck 4	86
Cars – decks 4 & 5 (no trucks)	797
Cars – deck 6	0
Passengers	2,458
Passengers in cabins	1,969
Passengers in airseats	489
Passengers – deck 6	1,035
Passengers – deck 7	720
Passengers – deck 8	703
Max. officers and upper crew	50
Max. lower crew	93

Table 5-10. Lightship and its components.

	Weight [t]	**LCG [m]**	**VCG [m]**
Hull	8,862		9.99
Superstructure	2,292		27.05
Outfitting	763		17.71
Accommodation	3,870		
Machinery	2,713		7.70
Total lightship	**18,500**	**88.91**	**13.70**

5.5. Loading conditions and intact stability

Before the loading calculations take place, some more parameters are assigned values, as shown in Table 5-11. These are needed to calculate the weight of people on board and filling percentage of fuel tanks, using the method that has been described in Chapter 4.5. A summary of all loading conditions is presented in Table 5-12.

Table 5-11. Parameters regarding the loading conditions.

Weight per passenger – incl. luggage [kg]	85
Weight per crew – incl. luggage [kg]	85
One-way distance [nm]	500
Time at port [h]	3
Trips before bunkering (incl. return)	2
Fuel safety factor	1.3

Table 5-12. Presentation of loading conditions.

Condition	**Draft [m]**	**Draft aft [m]**	**Draft fwd [m]**	**Trim [m]**	**DWT [t]**	**Displacement [t]**	**GM [m]**	**ΔKG_{intact} [m]**
LDS01	7.297	7.675	6.913	-0.755	8,351	26,851	4.94	2.19
LDS02	7.228	7.690	6.767	-0.923	8,068	26,569	4.75	2.07
LDS03	6.499	7.102	5.895	-1.207	4,284	22,784	6.10	2.83
LDS04	6.148	6.893	5.402	-1.491	2,625	21,125	5.65	1.97
LDS05	7.044	7.454	6.635	-0.820	6,997	25,497	5.74	2.65
LDS06	7.096	7.031	7.161	0.130	6,785	25,286	4.98	2.74
LDS07	7.215	7.516	6.915	-0.601	7,809	26,310	5.09	2.56
LDS08	7.076	7.326	6.825	-0.501	6,981	25,482	5.23	2.33
LIGHT	5.542	6.700	4.384	-2.317	0	18,500	5.88	

The resulting floating positions confirm that the chosen design draft (7 m) is appropriate. The resulting range of trims is also acceptable, although – as has been mentioned already – the optimization of loading conditions is not included in the routines. In cases where the trim may be considered excessive (for example, the only-passenger conditions LDS03 and LDS04), it may be corrected by redistribution of fuel oil or ballast water along the ship.

Furthermore, it is shown that all conditions easily comply with intact stability criteria. This is attributed mainly to the large beam of the ship.

The detailed presentation of the full load departure condition (LDS01) follows.

Table 5-13. Loading components of LDS01.

Name	Mass [t]	Fill %	x [m]	y [m]	z [m]	FSM [t m]
Concentrated loads						
PAX	208.9	0.0	106.19	0.00	24.63	0.00
CREW	10.2	0.0	75.60	0.00	26.75	0.00
OWNER	10.0	0.0	89.63	0.00	21.57	0.00
PROV	40.0	0.0	137.86	0.00	19.82	0.00
TRAILERS-DK1	448.3	0.0	127.23	0.00	6.00	0.00
TRAILERS-DK3	2,659.8	0.0	87.52	0.00	11.60	0.00
TRAILERS-DK4	2,573.4	0.0	94.98	0.00	17.20	0.00
SUBTOTAL	**5,950.7**	**0.0**	**94.71**	**0.00**	**14.16**	**0.00**
Diesel oil						
R080100	55.0	41.4	93.60	5.84	0.31	93.69
R090201	169.0	41.4	104.48	-6.52	0.91	79.05
R090401	153.4	41.4	104.76	-2.20	0.77	45.75
SUBTOTAL	**377.4**		**103.00**	**-2.96**	**0.77**	**218.5**
Fresh water						
R030102	57.8	100	22.59	4.33	5.16	0.00
R030202	57.8	100	22.59	-4.33	5.16	0.00
R050400	31.5	100	52.25	-6.57	1.72	0.00
R120101	185.3	100	141.16	3.60	3.00	0.00
R120201	185.3	100	141.16	-3.60	3.00	0.00
R130101	119.1	100	153.77	2.64	3.04	0.00
R130201	119.1	100	153.77	-2.64	3.04	0.00
SUBTOTAL	**755.9**		**123.29**	**-0.27**	**3.29**	**0.00**
Heavy fuel oil						
R020103	186.3	41.4	14.58	4.33	6.43	688.64
R020203	186.3	41.4	14.58	-4.33	6.43	688.64
R030002	44.2	41.4	30.04	0.00	3.96	199.26
R100101	75.1	41.4	117.27	2.25	0.94	49.81
R100201	75.1	41.4	117.27	-2.25	0.94	49.81
R100301	75.3	41.4	116.58	6.32	1.39	82.58
R100401	75.3	41.4	116.58	-6.32	1.39	82.58
R110101	73.3	41.4	129.96	2.19	1.01	49.81
R110201	73.3	41.4	129.96	-2.19	1.01	49.81
SUBTOTAL	**864.3**		**70.59**	**0.00**	**3.48**	**1,941.0**
Lube oil						
R050200	17.6	98.0	53.64	-1.98	1.52	0.00
R060100	21.2	98.0	64.83	2.56	1.20	0.00
R060300	21.2	98.0	64.83	7.67	1.20	0.00
R070200	21.2	98.0	80.80	-2.55	1.19	0.00
R070400	21.2	98.0	80.80	-7.66	1.19	0.00
R080200	36.4	98.0	92.80	-5.84	0.74	0.00
R090101	54.5	98.0	102.14	1.82	1.88	0.00
SUBTOTAL	**193.3**		**83.11**	**-0.77**	**1.33**	**0.00**
Water ballast						
R090103	150.0	30.3	103.11	11.75	4.49	250.45
R090203	150.0	30.3	103.11	-11.75	4.49	250.45
R160001	101.3	100.0	191.04	0.00	0.00	0.00
SUBTOTAL	**401.3**		**125.30**	**-0.00**	**3.95**	**500.9**
Miscellaneous						
R080000	44.7	100.0	93.41	0.51	0.75	0.00
SUBTOTAL	**44.7**	**100.0**	**93.41**	**0.51**	**0.75**	**0.00**
DWT	**8,351.0**		**96.14**	**-0.09**	**10.99**	**2,660.4**

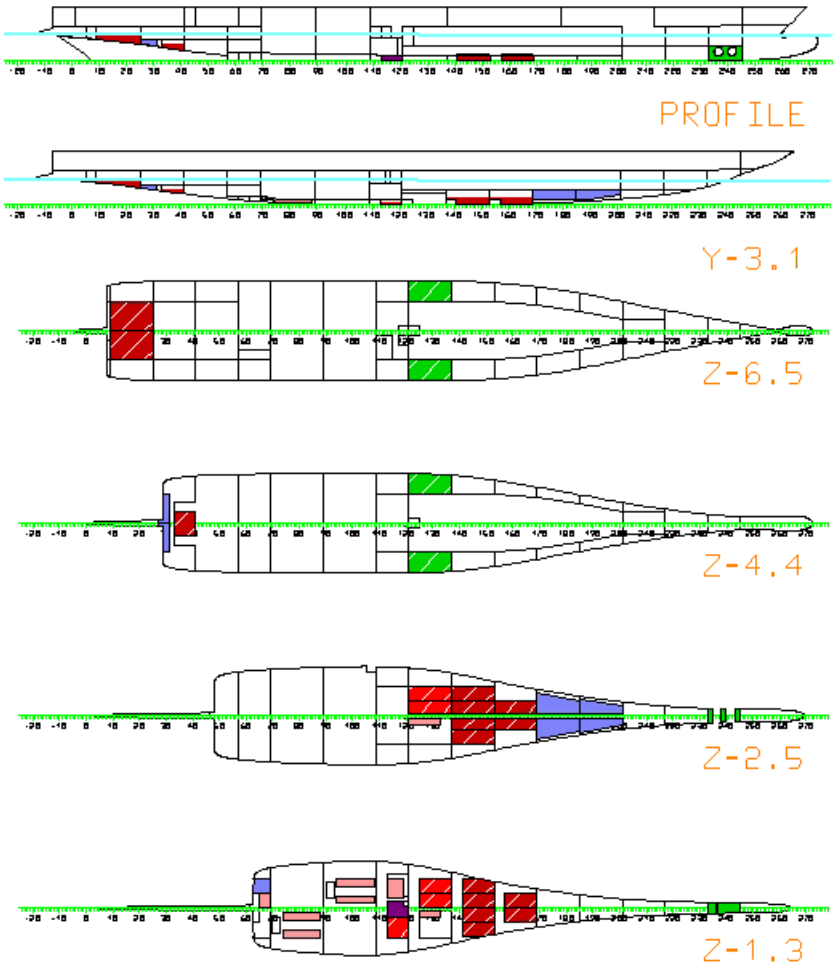

Figure 5-7. Loaded tanks and floating position of LDS01.

Table 5-14. Stability criteria check for LDS01.

Criterion	**Required value**	**Attained value**	**Status**
Area under GZ curve between 0 – 30 deg	0.055 m rad	0.519 m rad	OK
Area under GZ curve berween 0 – 40 deg	0.09 m rad	0.822 m rad	OK
Area under GZ curve between 30 – 40 deg	0.03 m rad	0.303 m rad	OK
Max GZ	0.2 m	1.778 m	OK
Max GZ angle	25 deg	32.87 deg	OK
GM	0.15 m	4.937 m	OK
Max heel due to crowding of passengers	10 deg	1.112 deg	OK
Weather criterion	1	3.716	OK
Max heel due to turning	10	2.140	OK

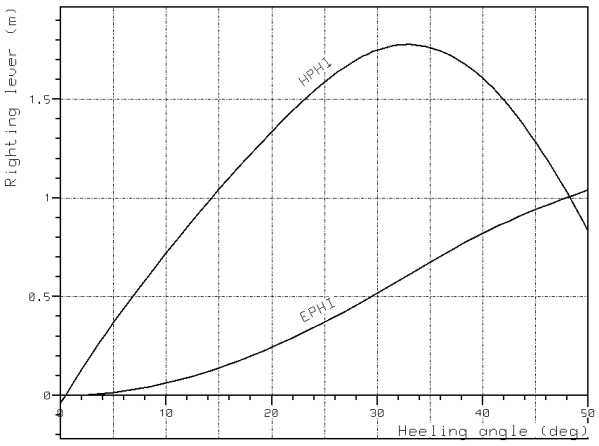

Figure 5-8. GZ curve of LDS01.

5.6. Damage stability

First of all, the properties of the initial conditions and the subdivision of the ship are presented in Table 5-15 and Figure 5-9 respectively.

Table 5-15. Initial conditions for damage stability calculations.

Initial Condition	T [m]	GM [m]
d_l	6.148	5.020
d_p	6.837	4.602
d_s	7.297	4.602

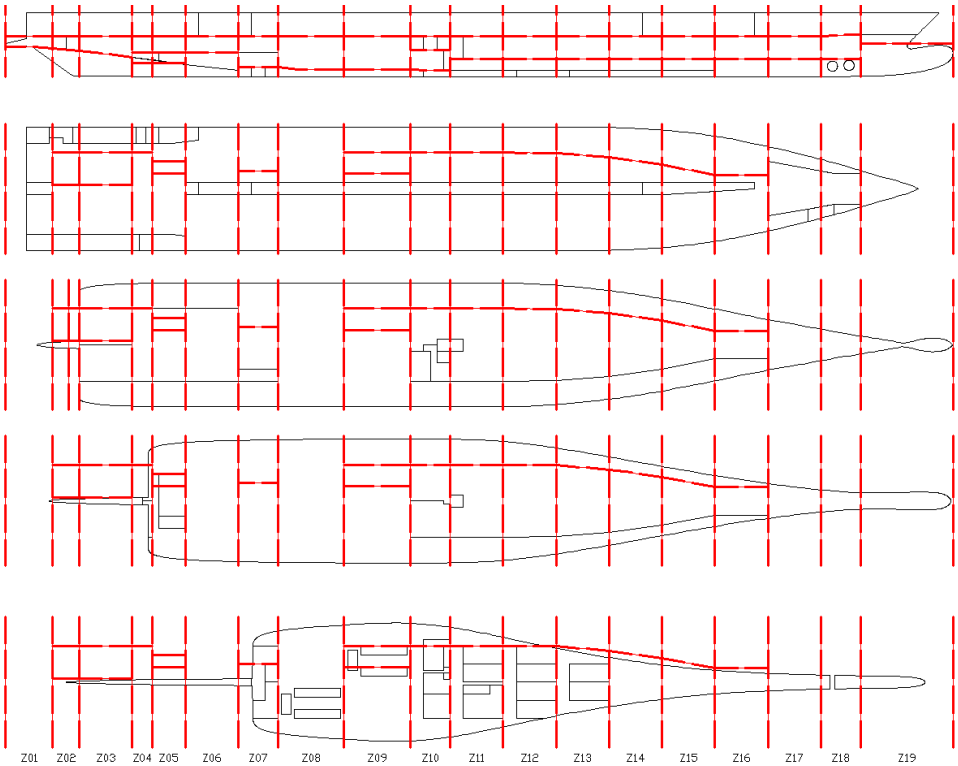

Figure 5-9. Subdivision of the ship for damage stability calculations.

The results of the calculations follow in Table 5-16. The water on deck regulation is to be satisfied for a significant wave height of 4 m.

Table 5-16. Results of damage stability calculations.

Init. Cond.	**A**	**R**	**Reg. 6/7 status**	**Reg 8.1 min GM**	**Reg 8.1 status**	**Reg 8.2/3 min GM**	**Reg 8.2/3 status**	**WOD min GM**	**WOD status**
d_l	0.979	0.783	OK	1.080	OK	2.400	OK	2.329	OK
d_p	0.927	0.783	OK	1.673	OK	2.595	OK	2.409	OK
d_s	0.832	0.783	OK	2.614	OK	3.243	OK	3.597	OK
Total	0.899	0.870	OK						

Two damage cases are selected to be presented as examples. The first concerns the water on deck regulation. It is the most severe examined damage, with the two engine rooms flooded and with an imaginary accumulation of water on the main deck. The floating position is depicted in Figure 5-10. All criteria are satisfied, as is required for each examined damage in order to fulfill the deterministic requirements.

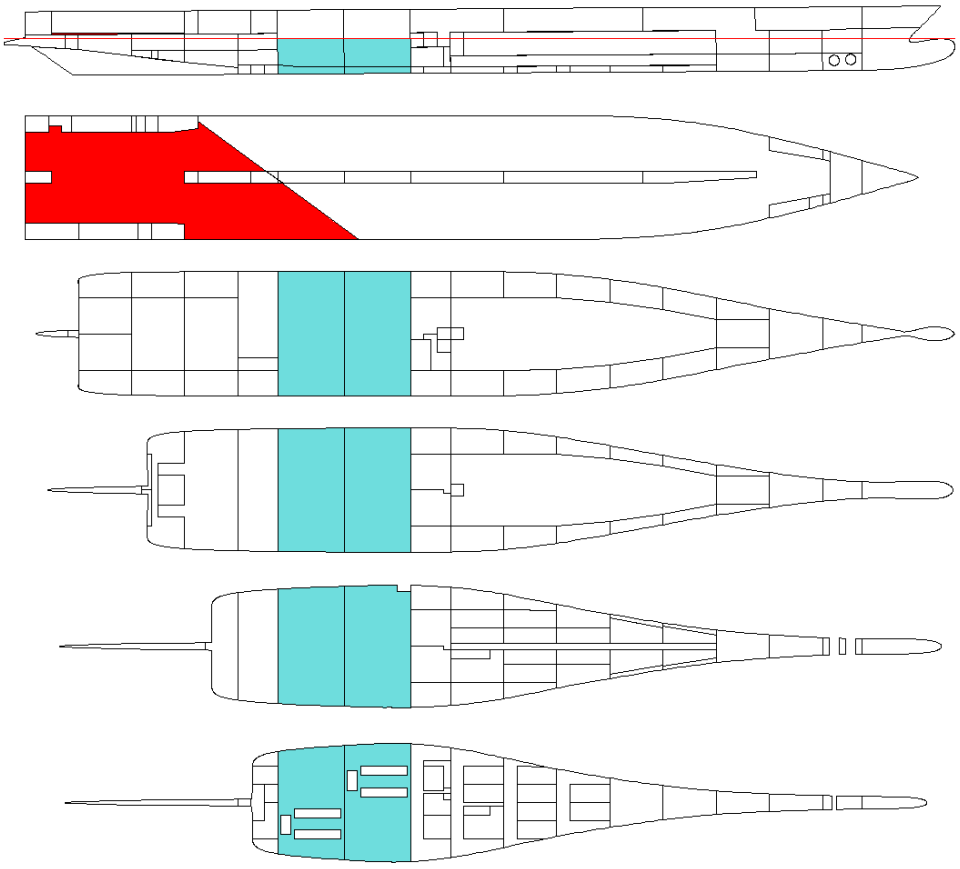

Figure 5-10. Example damage case for water on deck regulation.

The second example is a very severe three-zone damage case, with the lower hold and a large part of the main deck flooded, generated for compliance assessment with SOLAS regulations 6 and 7. As seen in Figure 5-11, the upper deck edge is marginally not submerged in this case. According to IMO's model, the corresponding probability (with the ship at its subdivision draft) is less than 1%, while survival probability is around 16%.

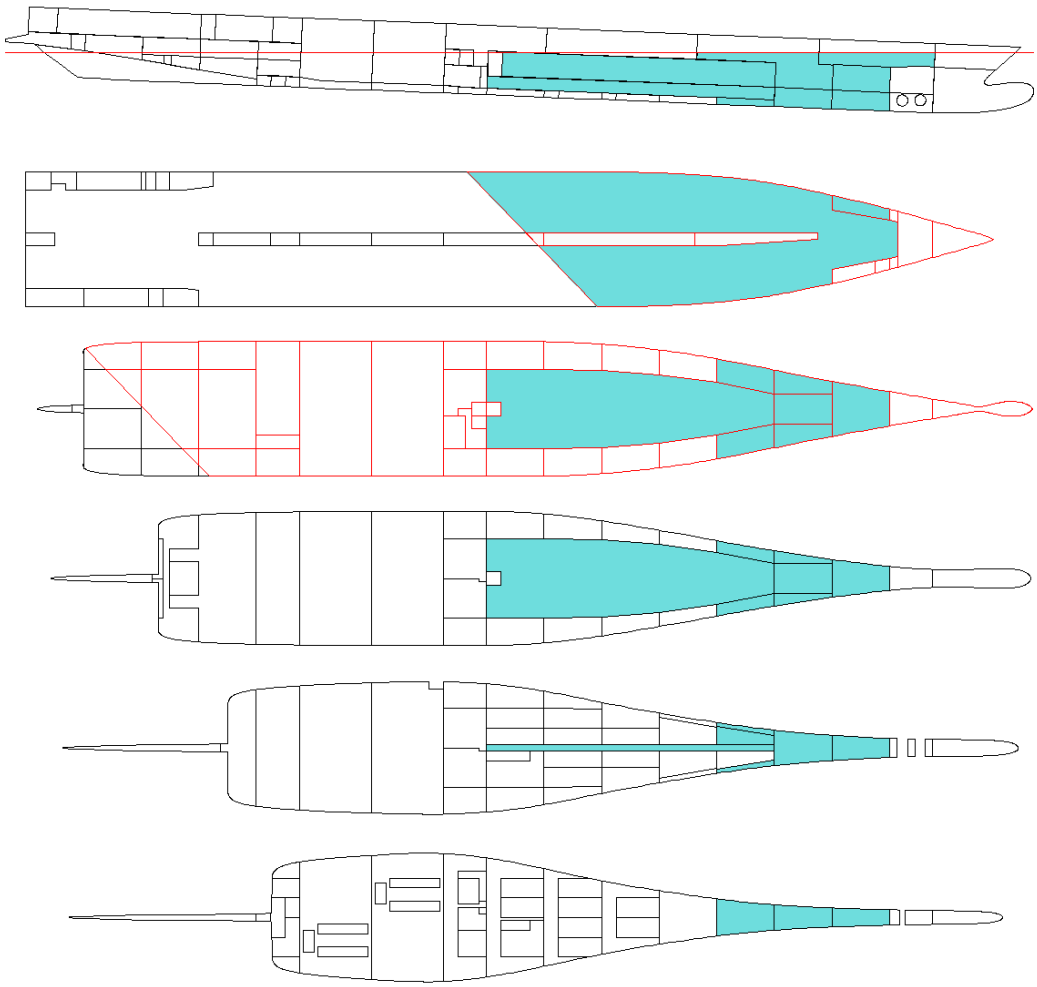

Figure 5-11. Example damage case for the probabilistic assessment.

5.7. Energy efficiency design index

The attained EEDI of the ship is 25.53 g/tm, calculated at the "EEDI condition" which corresponds to an estimated speed of 27.63 knots. The required EEDI values for the various implementation phases are presented in Table 5-17.

Table 5-17. Required EEDI values and compliance status.

Phase	$EEDI_{req}$ [g/tm]	Status
0	24.11	NOT OK
1	22.90	NOT OK
2	23.14	NOT OK
3	20.25	NOT OK

The design does not seem to comply with any phase of EEDI. Of course, more detailed calculations of the required horsepower and the lightship weight would be required to determine whether this is indeed the case. Furthermore, local hydrodynamic hull optimization can be conducted at a later design phase to reduce resistance. If, however, the required EEDI is still not achieved, reduction of speed might be necessary.

5.8. Financial assessment

The values of parameters defining the operational profile of the ship as well as the various cost coefficients are listed in Table 5-18, while the relevant results follow in Table 5-19.

It is shown that the net present value of the investment is very high, despite the also very high newbuilding price. It is also noted that passengers are by far the most important source of income, while the fuel cost is the largest fraction of the yearly expenses.

Table 5-18. Operational and financial parameters.

Reference number of passengers	2,400
Reference lane meters	3,000
Mean propulsion power increase during operation [%]	10
Low season duration [weeks]	25
High season duration [weeks]	25
Passenger occupancy	0.60
Truck occupancy	0.70
Car occupancy	0.60
Trips per week – low season (one-way)	4
Trips per week – high season (one-way)	6
Basic freight [$]	90
Airseat freight multiplier	1
Cabin freight multiplier	2.111
Car freight multiplier	1.333
Truck freight multiplier	7.778
Extra income per passenger [$ / trip]	5
VAT and other charges [% of ticket price]	35
Mean crew cost [$ / person per month]	3,000
Yearly insurance cost [% of building cost]	1
Yearly maintenance cost [% of building cost]	1.5
Various yearly costs [% of other costs]	5
Resale price [fraction of building cost]	0.15
Existence of scrubber	Yes
Lifetime [years]	20
Interest rate	0.05
HFO price [$/ton]	450
LSFO price [$/ton]	650
Mean electric load [kW]	3,461
$SFOC_{AE}$ [g/kWh]	185.8

Table 5-19. Calculated operational and financial values.

Trip duration [h]	17.86
Trip duration – return [h]	17.86
Mean occupied lane meters	2146.8
Mean passengers in cabins	1,180
Mean passengers in airseats	293
Newbuilding price [million $]	188.99
Income from passengers per year [million $]	41.91
Income from trucks per year [million $]	15.26
Total income per year [million $]	57.18
M/E fuel cost per year [million $]	17.07
A/E fuel cost per year [million $]	1.54
Lube oil cost per year [million $]	1.86
Crew cost per year [million $]	4.32
Port fees per year [million $]	0.34
Insurance cost per year [million $]	1.89
Maintenance cost per year [million $]	2.83
Other expenses per year [million $]	1.49
Final year income [million $]	28.35
Net present value [million $]	143.72

Chapter 6. Optimization Case Study

Chapter 6 presents the solution of a ship design problem using the developed parametric model. Realistic owner's requirements are assumed and the optimization problem is formally defined. The problem is then solved using design space exploration and optimization algorithms available in CAD/CAE software CAESES.

6.1. Owner's requirements – optimization problem formulation

Using the developed parametric model, a vessel is to be designed for the Patras – Ancona route. The assumed owner's requirements are the following:

- Capacity: 1,800 passengers, 2,300 lane meters for trucks.
- Service speed (calm sea, clean hull, 80% MCR): 27 knots.
- Compliance with all relevant regulations for ships built in 2020. Water on deck regulation is to be satisfied for the maximum possible significant wave height, i.e. 4 m, and a scrubber is to be fitted for compliance with MARPOL Annex VI.

Unless otherwise stated, the various parameters are assigned their default values, as presented in Chapter 4 and Chapter 5.

Several test runs are conducted in order to define an appropriate design space. It is observed that the required capacity can be achieved with ten decks (four passenger decks, including the sun deck), in the region of L_{PP}=200 m and with 8 lanes for trucks, corresponding to a minimum beam of 26.9 m. An equivalent longer and narrower solution (seven lanes for trucks), namely L_{PP}=225 m and B=23.9 m, is out of the question for stability reasons. A shorter and beamier ship with L_{PP} around 180 m and B=29.9 m (nine lanes) would be another option. However, this would correspond to an L/B ratio around 6, which is low for such large ships and would probably lead to increased resistance (and possible problems with EEDI compliance). Nonetheless, it is noted that this solution would operate at a Froude number around 0.33, which is considered favorable in terms of bow – stern wave interference; therefore, it could also be studied in the future.

Considering the above, the first two design variables are introduced:

- The length between perpendiculars, ranging from 200 m to 210 m. The length of the ship is the most important design variable and must obviously be optimized, as it affects virtually all values of interest.
- The beam, ranging from 26.9 m to 27.7 m. The beam could have been kept constant at 26.9 m (minimum for 8 trailer lanes), as deviating from that minimum is expected to lead to increased propulsion power and building cost, while increasing only the passenger capacity with negligible effect on lane capacity. However, small deviations from the minimum beam are examined, first and foremost as a means of overcoming possible stability problems, and secondly to

examine whether the increase in passenger capacity could possibly outweigh the increased building and operational costs.

In order to increase accuracy, the resistance response surface based on the results of CFD simulations (see Chapter 4.2.1) is used. The C_B and LCB are kept constant at 0.55 and 46% L_{PP} respectively, so as to minimize the required number of CFD runs for a good representation of the design space. These relatively low values are chosen to ensure compliance with EEDI regulation. Obviously, the assumption of constant C_B and LCB is a simplification, especially with regard to the hydrodynamic performance of the ship. It is noted however that, unlike in other ship types, the effect of the block coefficient on the payload is negligible.

Some further test runs are conducted within the specified region with regard to L_{PP} and B, and for fixed C_B and LCB, to estimate the maximum draft (Figure 6-1). It is seen firstly that the maximum draft takes values within a very narrow range (less than 15 cm), and additionally that no clear trends are apparent as the main dimensions are varied. In reality, the subdivision draft as a function of length and beam is a discontinuous function, as the draft abruptly increases whenever for example a truck is added to the payload. For these reasons, the design draft is also kept fixed at 6.6 m.

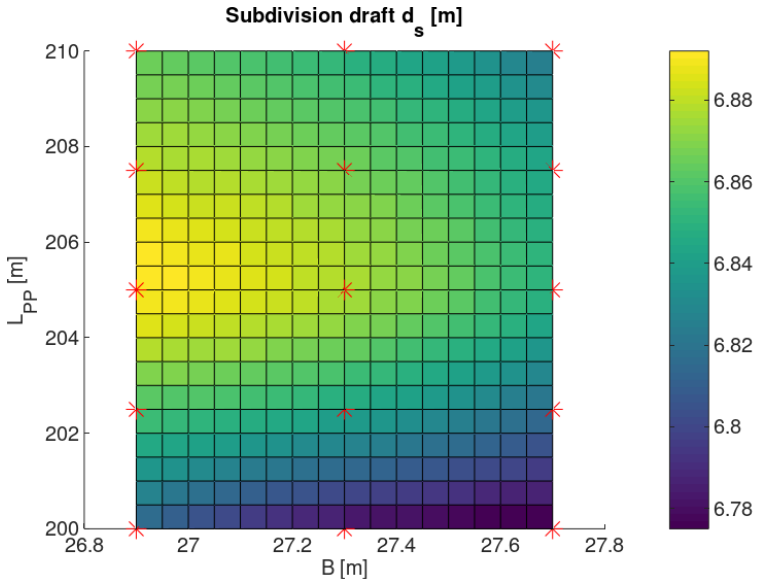

Figure 6-1. Subdivision draft as a function of the ship's length and beam (calculated points and fitted cubic surface).

Two additional design variables affecting the general arrangement of the ship are introduced. The third design variable is the total depth of the ship, controlled by varying the height of deck 1 above the double bottom, and thus of all decks above it. This is mainly a means of varying the height of the main deck, which considerably affects both intact and damage stability.

The fourth design variable is the position of the “B/5” longitudinal bulkheads, also as a means of overcoming possible damage stability problems.

Considering the above, the optimization problem is defined as follows:

- Objective: $\max_{\vec{x}}\{NPV(\vec{x},\vec{p})\}$
- Design variables: $\vec{x} = \left\{L_{PP}, B, \frac{b_{LH}}{B}, h_1 - h_{DB,E/R}\right\}$
  $L_{PP} \in [200m, 210m]$, $B \in [26.9m, 27.7m]$
  $b_{LH}/B \in [0.20, 0.23]$, $h_1 - h_{DB,E/R} \in [2m, 3m]$
- Parameters: $\vec{p} = \{T_d = 6.6m, C_B = 0.55, LCB = 0.46L_{PP}, n_{decks} = 10\}$ *
- Constraints:
  $N_{PAX} \geq 1{,}800, lane\ meters \geq 2{,}300$
  $\Delta KG_{intact} \geq 0.3m$, $\Delta KG_{R8.1} \geq 0.3$, $KG_{R8.2-3} \geq 0.3m$, $\Delta KG_{WOD} \geq 0.3m$
  $\Delta A = A - R \geq 0.01$, $\Delta A_c = \min_{c=d,p,l} A_c - 0.9R \geq 0.01$
  $\Delta EEDI = EEDI_{req} - EEDI \geq 0.3\ g/tm$
  $errors = 0$ (no errors encountered during the design procedure in NAPA)

6.2. Design of experiment (DoE)

A design of experiment is conducted in order to explore the design space and discover interesting correlations (or lack thereof) between the values of interest. This is achieved by linking NAPA with CAD / CAE software CAESES, where a Sobol sequence generator is available. Based on the Sobol sequence, values are assigned to the design variables and the relevant input file which is to be read by NAPA is written. Then, the NAPA project is run in batch mode and produces an output file which contains the value of the objective function, the constraints as well as other quantities of interest. This file is read by CAESES, the results are saved and the process continues with the next design, until the generation of 80 variants.

The covered range of design variables as well as of the output values of interest are presented in Table 6-1.

This is followed by a series of scatter diagrams, presenting relationships between the various technical and economical values of interest, along with some relevant comments. Circles denote feasible designs, while crosses designs which violate at least one constraint and are therefore infeasible.

* $\vec{p}$ also includes all other parameters which are assigned their default values, as have been presented in the previous chapters.

Table 6-1. Characteristics of ships generated by the Sobol sequence.

	Minimum	Average	Maximum	Compliance percentage
L_{PP} [m]	200.15	204.94	209.84	
B [m]	26.91	27.29	27.69	
Long. bulkhead parameter	0.200	0.215	0.230	
Deck 1 above tank top [m]	2.02	2.51	2.99	
NPV [m $]	38.31	43.92	51.19	
Building cost [m $]	138.45	142.99	147.50	
Passengers	1,796	1,869	1,956	99%
Lane meters	2,274.5	2,359.2	2,442.1	89%
Lightship [t]	14,920	15,434	15,972	
DWT [t]	6,362	6,700	7,114	
Gross tonnage	42,687	44,415	46,309	
Propulsion power [kW]	29,206	30,408	31,216	
MCR [kW]	40,800	42,240	43,200	
ΔKG_{intact}	0.439	0.935	1.433	100%
$\Delta KG_{R8.1}$	1.086	1.698	2.242	100%
$\Delta KG_{R8.2\text{-}3}$	0.125	0.541	1.168	79%
ΔKG_{WOD}	-0.025	0.679	1.363	91%
ΔA	0.0350	0.0691	0.0978	100%
ΔA_c	0.0002	0.0930	0.1452	99%
$\Delta EEDI$	1.130	1.890	2.735	100%
Errors	0	0	0	100%

Figure 6-2 and Figure 6-3 present the influence of the length and beam on the net present value and the building cost respectively. The length of the ship is positively correlated with the net present value of the investment. This is due to economies of scale, despite the reduced percentile occupancies on which larger ships are supposed to operate, the increased building cost and propulsion power. The building cost is also positively correlated with the beam – although not as strongly –, while the effect of the beam on the net present value is not clear.

Next, passenger and lane capacities are plotted against the main dimensions in Figure 6-4 and Figure 6-5. Obviously, the length positively affects both passenger capacity and lane meters. The beam is positively correlated with the passenger number as well, while its impact on the lane meters is negligible. It is worth noticing the clear formation of four straight lines on the beam-passenger capacity scatter diagram. These are attributed to the discontinuous relationship between ship length and superstructure length, with each straight line corresponding to a range of ship lengths for which the superstructure length is constant.

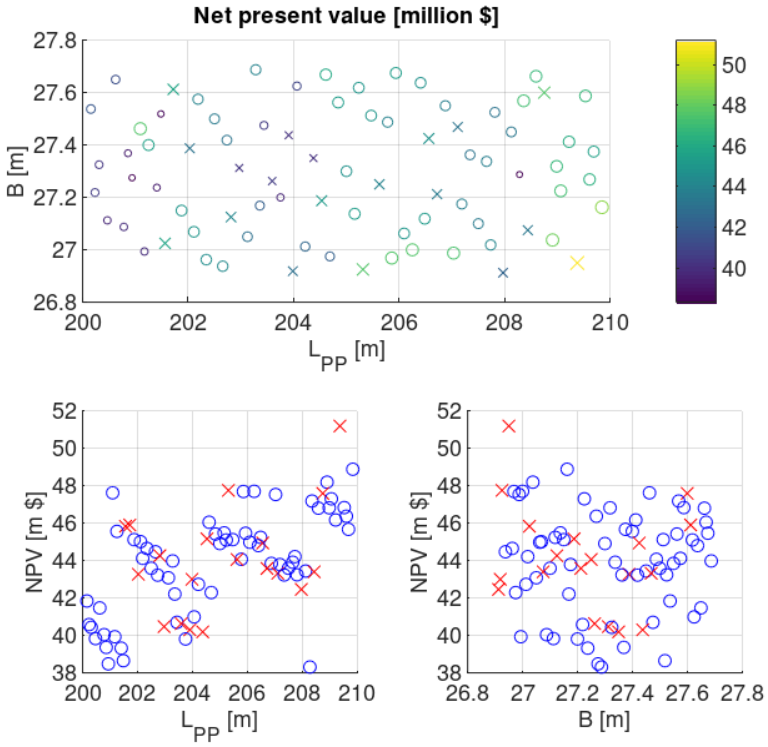

Figure 6-2. NPV scatter diagrams.

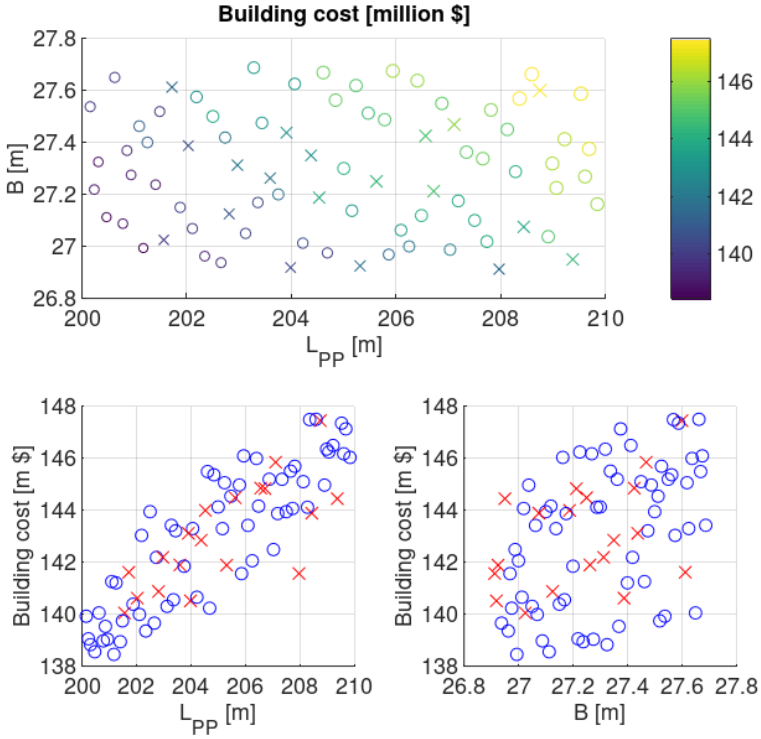

Figure 6-3. Building cost scatter diagrams.

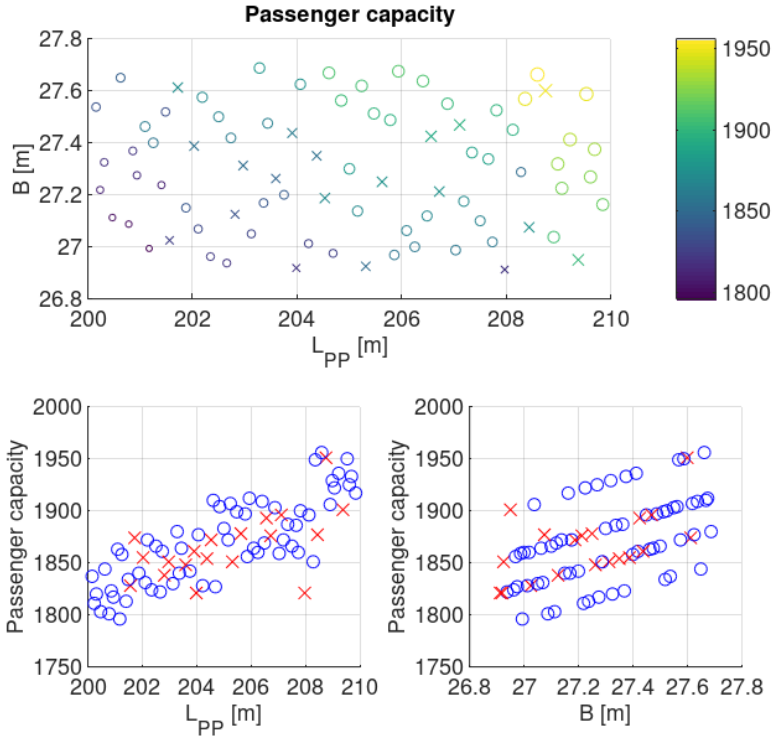

Figure 6-4. Passenger capacity scatter diagrams.

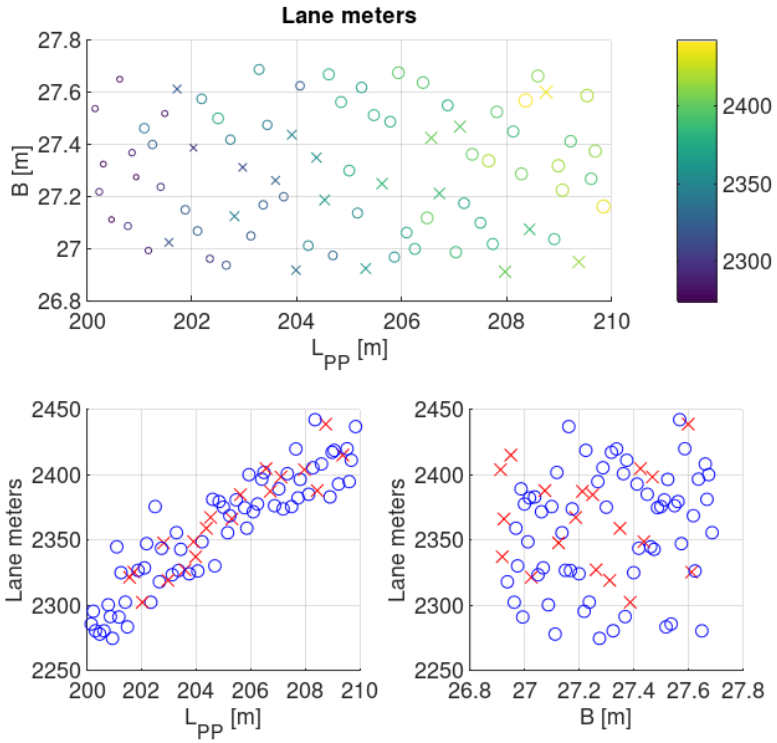

Figure 6-5. Lane meters scatter diagrams.

Both the length and beam are positively correlated with the lightship weight (Figure 6-6). The influence of the length is more significant, confirming that the length is “the most expensive dimension of the ship” [5].

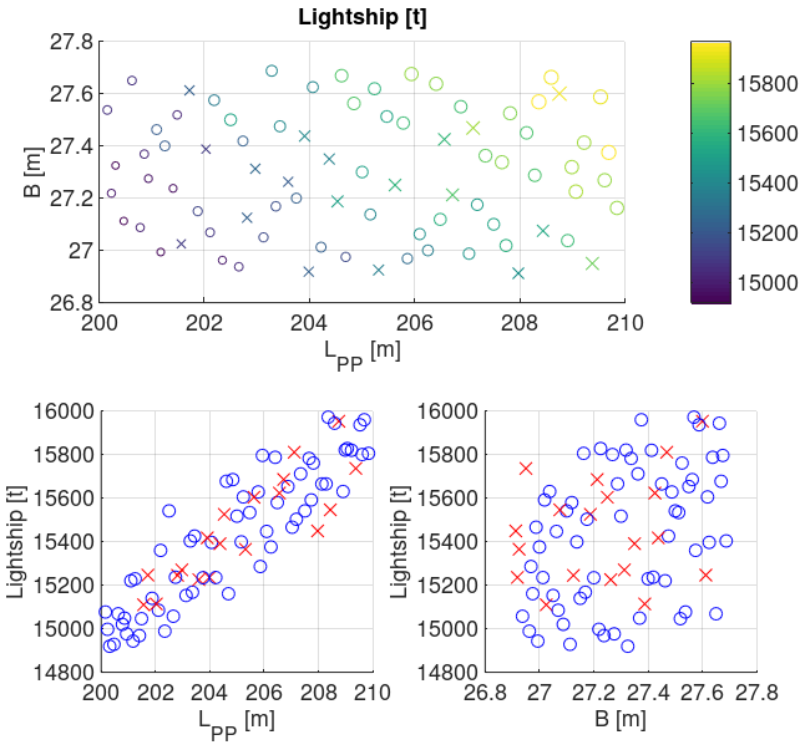

Figure 6-6. Lightship weight scatter diagrams.

The propulsion power is positively correlated with both main dimensions, as shown in Figure 6-7. This can largely be deduced by the resistance response surface presented in Chapter 4.2.1.

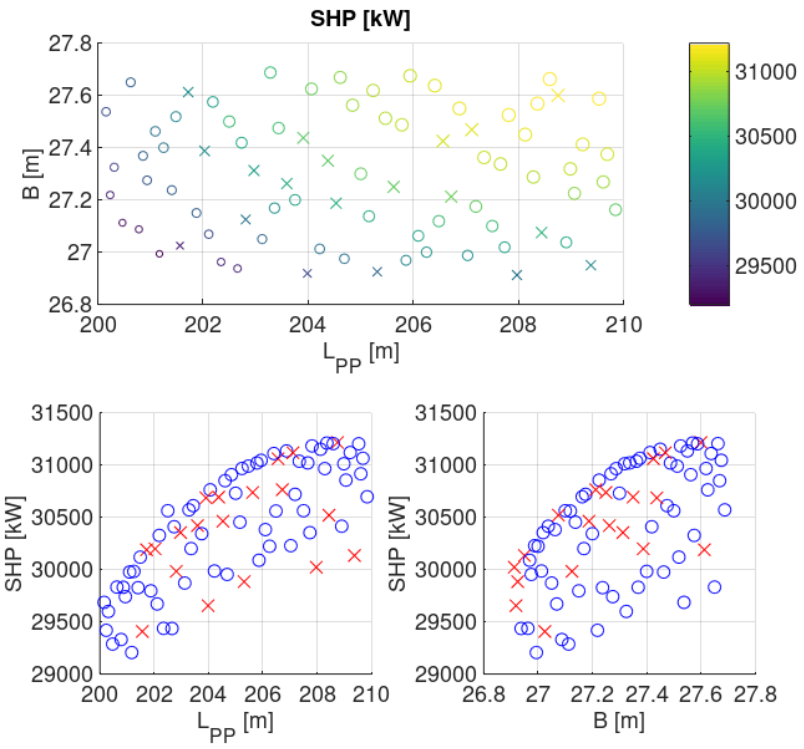

Figure 6-7. Propulsion power scatter diagrams.

Some additional interesting scatter diagrams which show the correlations between various calculated quantities follow.

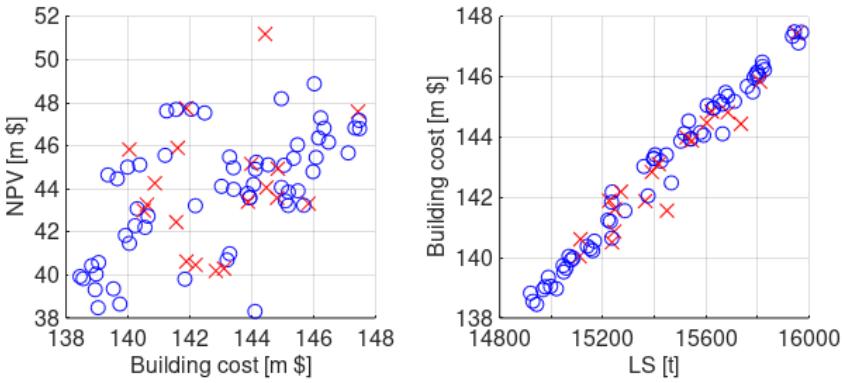

Figure 6-8. Building cost – NPV and lightship weight – building cost scatter diagrams.

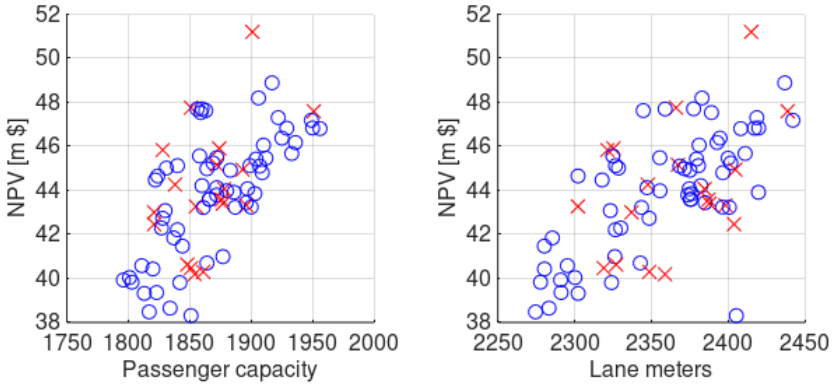

Figure 6-9. Passenger number – NPV and lane meters – NPV scatter diagrams.

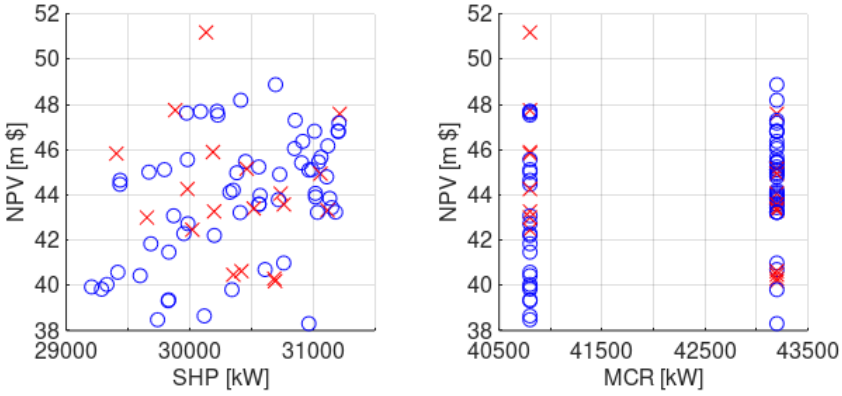

Figure 6-10. Propulsion power – NPV and installed power – NPV scatter diagrams.

Due to economies of scale, the NPV is positively correlated with the building cost, which in turn varies almost linearly with the lightship weight. Passenger capacity and lane meters also positively affect profitability.

Ships with larger propulsion power generally have a larger NPV due to their size, as also observed earlier. However, an exception is present: the ship with the largest NPV requires lower propulsion power. That ship is long but narrow, so its power demands

can be covered by smaller engines than wider ships of the same length – meanwhile, its small beam does decrease passenger capacity but not its lane meters. The net result is a higher net present value than long and wide ships. Nonetheless, that design happens to be infeasible for stability reasons.

In terms of stability, the scatter diagrams presented in Figure 6-11 below present the stability margins against the relevant design variables. It is clear from Figure 6-11 (and in accordance with basic ship theory) that increased beam comes with substantially improved stability. The longitudinal bulkhead position only affects the A index margin, which is not a critical criterion for the examined problem, as all designs easily achieve the required index. Increasing the height of deck 1 considerably worsens intact stability by raising the ship's center of gravity. Its effect on damage stability is not as clear: the increase of VCG has a negative impact, however the increase of freeboard to the main ro-ro deck is obviously beneficial.

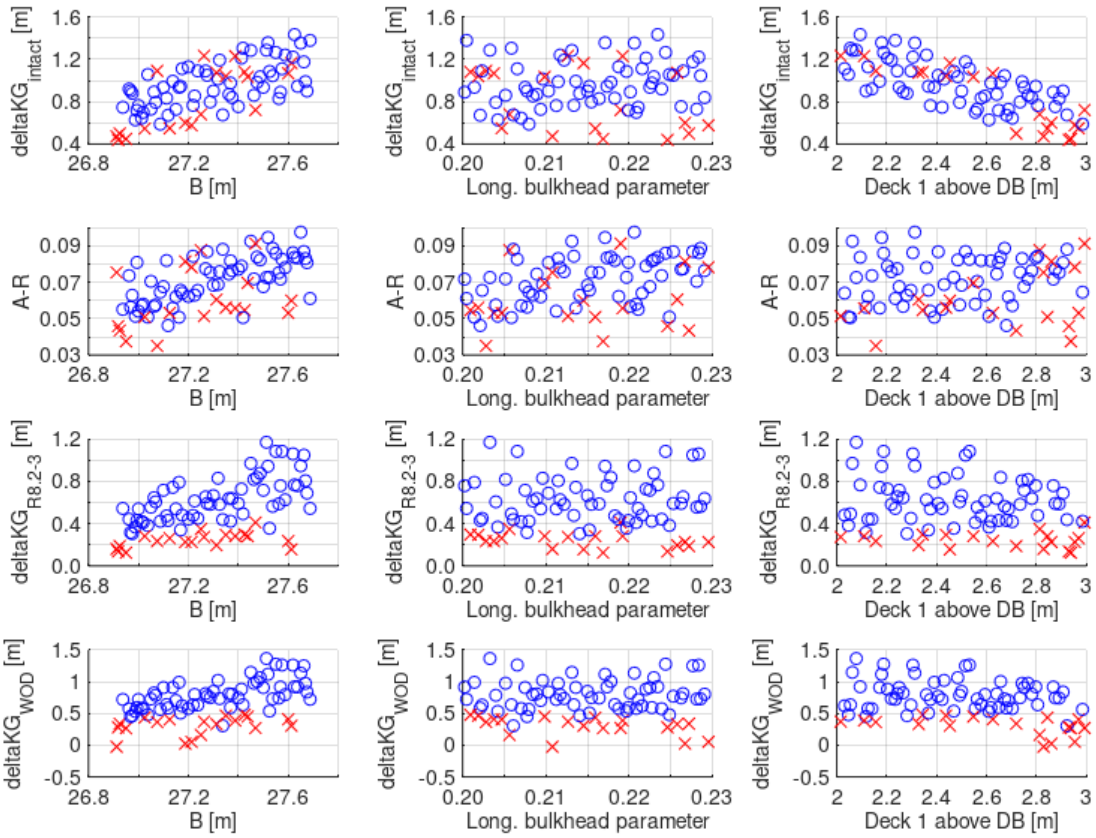

Figure 6-11. Stability scatter diagrams - influence of design variables on stability constraints.

Figure 6-12 below shows that, although the various stability criteria are generally positively correlated with each other, this is not always the case: for example, several designs which are well above the required subdivision index might fail the deterministic criterion of regulations 8.2-3.

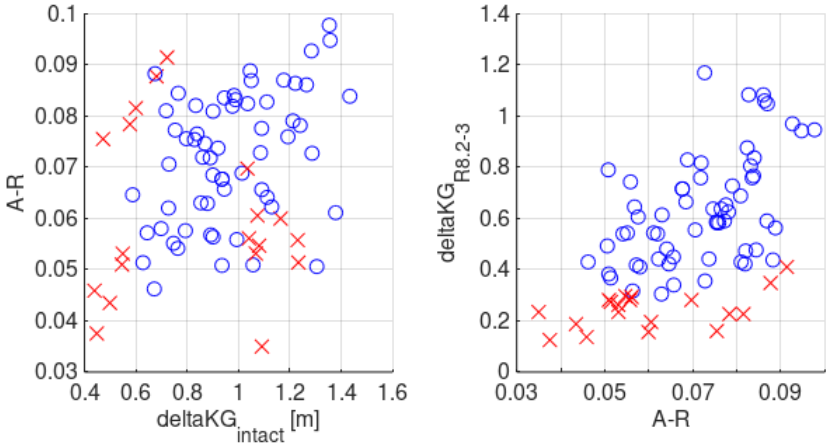

Figure 6-12. Scatter diagrams showing the correlation between different stability criteria.

Regarding EEDI, it is shown in Figure 6-13 that all ships within the design space easily pass the criterion, with larger margins corresponding to shorter ships. The situation becomes clearer if the designs are grouped according to their installed power (Figure 6-14): ships with smaller engines exhibit increased EEDI margins. Between ships with the same engines however, the declining trend is still present. This is mainly attributed to the f_j coefficient, which is strongly dependent on the Froude number. For given installed power, the maximum attainable speed decreases with the size of the vessel while the reference length increases, resulting to a decrease in the Froude number and therefore an increase of f_j. This trend is reversed towards the upper limit of L_{PP}, which is attributed to the flattening of the resistance surface in that region. Of course, this is a result that should be treated with caution, as the resistance prediction cannot be considered completely reliable.

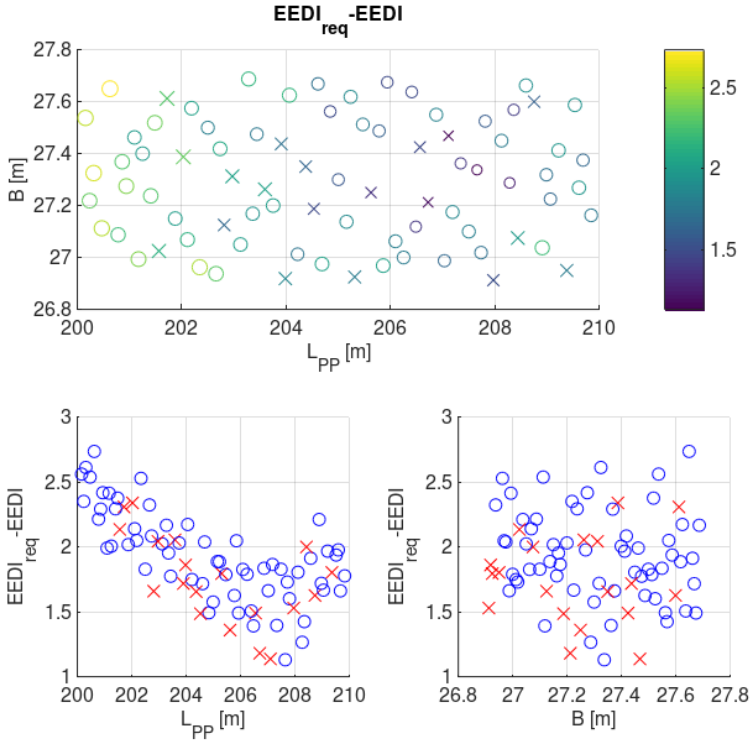

Figure 6-13. EEDI scatter diagrams.

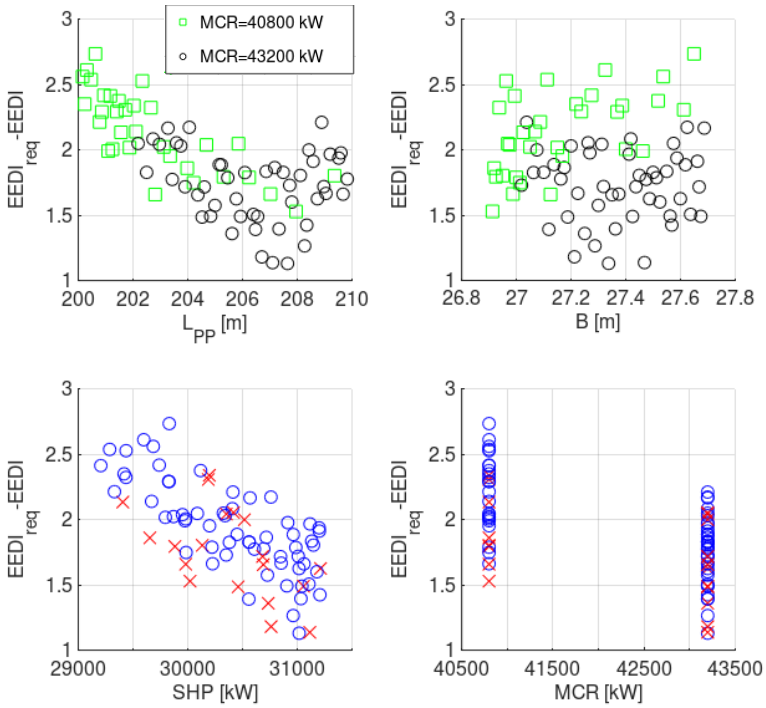

Figure 6-14. Further EEDI scatter diagrams.

The results of the DoE are summarized in Table 6-2, which presents the effect of each design variable on various characteristics of the ship. Pearson's correlation coefficient is used as a measure of correlation intensity, as defined in Table 6-3. It is noted that Pearson's coefficient is a measure of *linear* correlation, and thus the presented correlation intensities cannot necessarily substitute the visual observation of the figures presented above.

Table 6-2. Summary of design of experiment: influence of design variables on technical and financial characteristics.

	L_{PP}	**B**	**b_{LH}/B**	**h_1-$h_{DB,E/R}$**
NPV	Moderate positive	Negligible	Negligible	Negligible
Building cost	High positive	Low positive	Negligible	Negligible
Passenger number	High positive	Moderate positive	Negligible	Negligible
Lane meters	Very high positive	Negligible	Negligible	Negligible
Lightship	High positive	Low positive	Negligible	Negligible
DWT	Moderate positive	Negligible	Negligible	High positive
Propulsion power	High positive	Moderate positive	Negligible	Negligible
Installed power	Moderate positive	Low positive	Negligible	Negligible
Gross tonnage	High positive	Low positive	Negligible	Moderate positive
ΔKG_{intact}	Negligible	Moderate positive	Negligible	High negative
ΔA	Negligible	Moderate positive	Low positive	Negligible
ΔA_c	Negligible	Low positive	Negligible	Low positive
$\Delta KG_{R8.1}$	Negligible	Moderate positive	Negligible	Negligible
$\Delta KG_{R8.2\text{-}3}$	Negligible	Moderate positive	Negligible	Negligible
ΔKG_{WOD}	Negligible	Moderate positive	Negligible	Low negative
$\Delta EEDI$	Moderate negative	Negligible	Negligible	Low negative

Table 6-3. Correlation intensity according to Pearson's correlation coefficient.

Absolute value of correlation coefficient	Correlation
0 – 0.3	Negligible
0.3 – 0.5	Low
0.5 – 0.7	Moderate
0.7 – 0.9	High
0.9 – 1.0	Very high

6.3. Optimization results

Next, the genetic algorithm NSGA-II is used in order to conduct the formal optimization. Based on the DoE results, the longitudinal bulkhead position is kept fixed at 20% B and the relevant design variable is eliminated. Ten generations of 80 members each are generated, for a total population of 800 ships. Crossover and mutation probabilities are chosen as 0.9 and 0.01 respectively.

Overall, 93.6% of the generated designs are feasible. Once again, the most critical constraint is SOLAS Chapter II-1 Regulation 8.2-3, with 94.8% of the designs passing. One design is also rejected due to errors occurring in the NAPA project while running in batch mode. The percentage of feasible designs generally increases as the population evolves, starting from 82.5% in the first generation and reaching 93.8% in the tenth.

A historic plot of the generated designs and their fitness is displayed in Figure 6-15, with the stepped line denoting the mean fitness of each generation. Then, each design variable is plotted against the objective function in Figure 6-16. The characteristics of the ten fittest individuals are listed in Table 6-4.

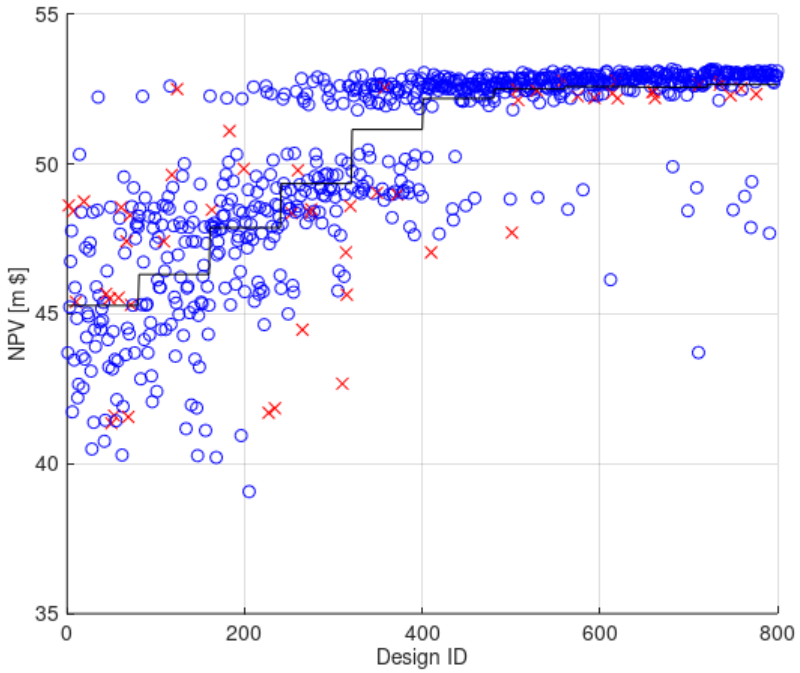

Figure 6-15. Evolution of the population.

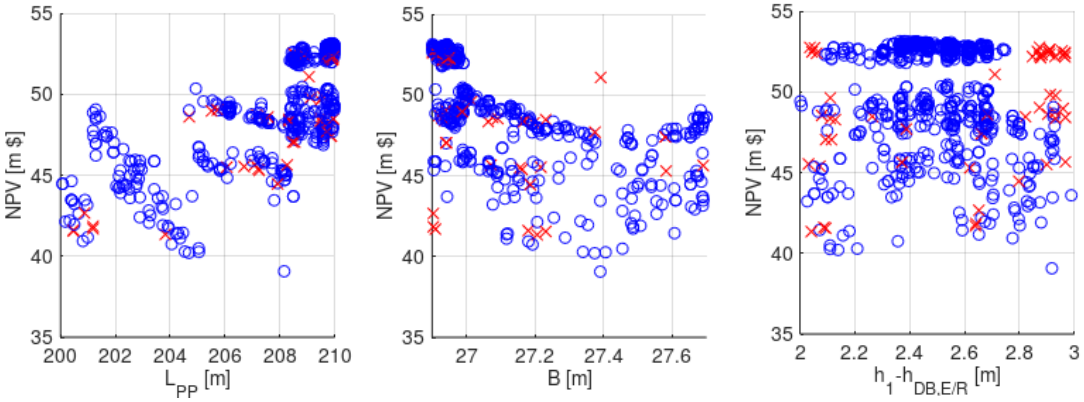

Figure 6-16. Design variables versus objective function scatter diagrams of the population.

Table 6-4. The ten fittest individuals generated by the algorithm.

Rank	L_{PP} [m]	B [m]	h_1-$h_{DB,E/R}$ [m]	NPV [m $]
1	209.856	26.943	2.382	53.16
2	209.944	26.901	2.364	53.16
3	209.907	26.944	2.380	53.15
4	209.868	26.944	2.398	53.14
5	209.869	26.943	2.413	53.12
6	209.867	26.943	2.418	53.12
7	209.867	26.943	2.418	53.12
8	209.856	26.944	2.436	53.10
9	209.883	26.944	2.428	53.10
10	209.942	26.944	2.428	53.09

It is clear that the optimum lies towards the maximum and minimum limits of length and beam respectively. Regarding the position of deck 1, the upper and lower limits are rejected due to stability constraints, while the objective function is maximized at a height around 2.40 m.

Using the above results as a starting point, an exhaustive search is conducted within a narrow subset of the design space so as to accurately locate the optimal point. A total of 64 designs are assessed within the following region:

$$L_{PP} \in [209.85m, 210.00m], B \in [26.90m, 26.96m], h_1 - h_{DB,E/R} \in [2.30m, 2.45m]$$

Some information regarding the resulting optimal ship is presented in Table 6-5.

Table 6-5. Characteristics of the optimal ship.

L_{PP}	209.85 m	MCR	40,800 kW
B	26.90 m	ΔKG_{intact}	0.769 m
b_{LH}/B	0.2	$\Delta KG_{R8.1}$	1.590 m
h_1-$h_{DB,E/R}$	2.35 m	$\Delta KG_{R8.2\text{-}3}$	0.617 m
Passengers	1,894	ΔKG_{WOD}	0.812 m
Lane meters	2,434	ΔA	0.034
Lightship	15,619 t	ΔA_c	0.056
DWT	6,755 t	$\Delta EEDI$	2.118 g/tm
GT	44,456	Building cost	143.78 m $
SHP	29,939 kW	NPV	53.35 m $

6.4. Further analysis on the objective function

The influence of the main dimensions on the profitability of the ship is an interesting matter which is chosen to be examined further. Constraints are temporarily ignored and the two design variables which are mainly linked to the satisfaction of constraints and do not significantly affect the objective function are removed. An exhaustive search is conducted in order to plot the net present value as a function of the length and beam. The resulting 25 points and a smooth fitted surface[*] are displayed in Figure 6-17 below, followed by relevant comments.

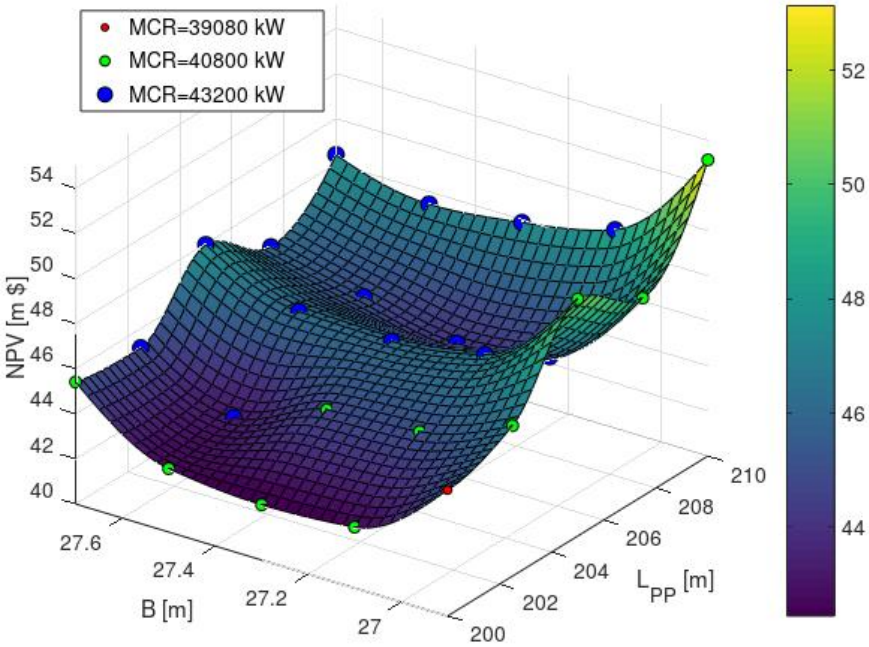

Figure 6-17. NPV as function of L_{PP} and B - calculated points and fitted smooth surface.

[*] This is an approximation, as the actual surface (which could have been obtained by examining a much larger number of designs) would be stepped. The reasons have been explained in Chapter 3 and Chapter 4 and will be noted again in this section. Of course, in reality the surface would be even more complex due to other factors which are not included in this model (eg. discontinuous variations of the lightship weight).

Iso-L_{PP} lines:

Comparing ships with the same main engines, an increase of the beam generally brings about a slight decrease of profitability; in other words, the extra profit from the increased passenger capacity is outweighed by the increased building and operational cost. This trend is reversed towards the upper B limit, where the calm water resistance surface flattens and the net result is an increase of the NPV as the beam increases.

Large gradients can be noticed in regions where the installed power changes. For example, moving from B=26.9 m to B=27.1 m at a constant length of 200 m, the NPV is considerably reduced because the corresponding small increase in propulsion power brings about a much larger increase in installed power, which is also accompanied by an increased specific fuel oil consumption.

Iso-B lines:

As a general trend, the NPV increases along with the length between perpendiculars, meaning that the profit from the increased passenger and lane capacity outweighs the increase in building and operational cost. The above remarks regarding the steps in the objective function in regions where the installed power changes are valid in this case as well.

Another factor affecting the form of iso-B curves is the presence of discontinuities in the general arrangement as a function of the length of the ship. For example, ships with L_{PP}=205 m and L_{PP}=207.5 m have exactly the same bulkhead positions and main vertical zones. For constant beam, this means that passenger capacity and lane capacities are practically the same. Thus, the two ships generate the same income, but the increased lightship weight and propulsion power of the latter translate into increased building and operational costs. Such local optima could not have been located by assuming that the internal arrangement of the ship is scaled along with the main dimensions, showing that the realistic parametrization of the general arrangement with a framing system independent of the main dimensions is important.

Finally, a small region near the edge of the design space (L_{PP}=200 m, B=26.9 m) which had not been explored by the genetic algorithm is discovered, where the power demand can be covered by smaller main engines than the two other examined models. This creates a local maximum in the region of short and narrow ships.

6.5. Influence of fuel price

Within the presented model, design evaluation is carried out based on a number of uncertain parameters, especially with regard to the financial assessment. Arguably, the most uncertain parameter of the problem is the cost of the consumed fuel. Therefore, a sensitivity study is useful in order to examine whether its effect can be critical for the results.

The influence of the fuel price is investigated by repeating the exhaustive search conducted in Chapter 6.4, which assumes an HFO price of 450 $/ton, for two different fuel prices: a low price of 250 $/ton and an increased one of 650 $/ton. The results are presented in Figure 6-18 and Figure 6-19 respectively.

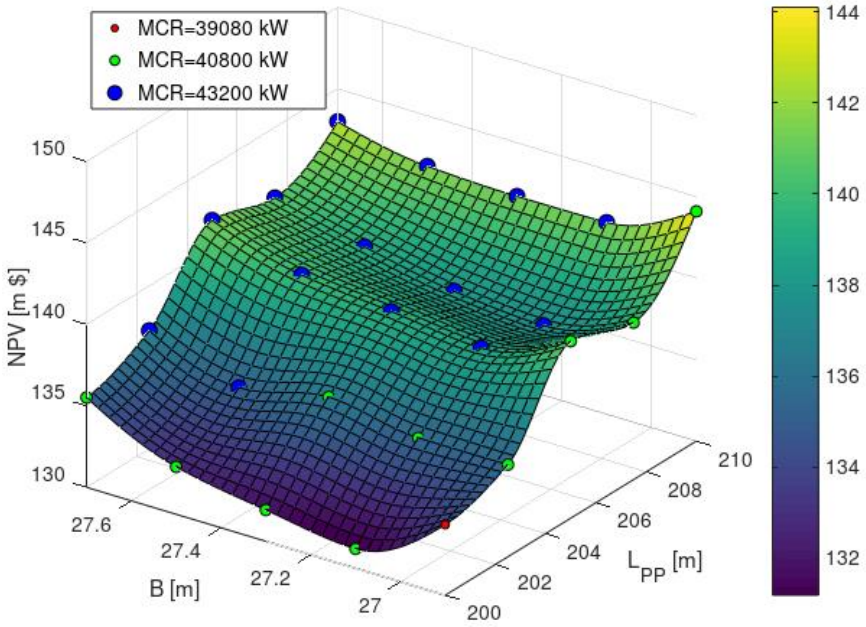

Figure 6-18. NPV as a function of L_{PP} and B for reduced fuel price (HFO: 250 $/ton).

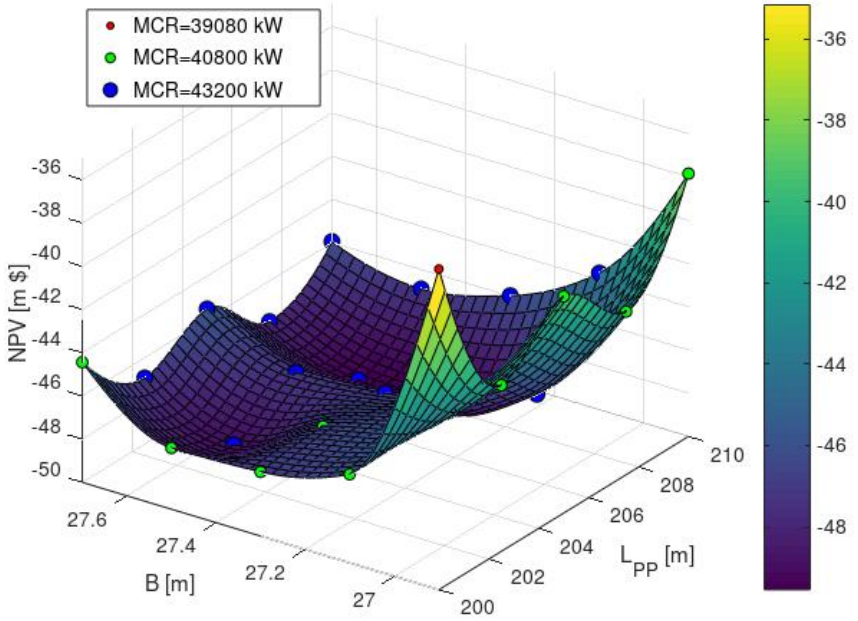

Figure 6-19. NPV as a function of L_{PP} and B for increased fuel price (HFO: 650 $/ton).

Naturally, values of NPV are significantly affected by the fuel cost. The noteworthy result however is that the form of the surface also changes. As fuel price rises, the importance of operational cost is amplified and the optimum is shifted to the smallest ship examined, in order to minimize fuel consumption. For the lower fuel price, the

optimal point remains the same. However, the form of iso-L_{PP} curves changes, with an increase of the beam for constant MCR slightly improving the NPV.

In the particular problem, the initially found solution (maximum length – minimum beam) would probably be selected, as it is attractive in all three cases, despite not remaining optimal for increased fuel price. In general however, the strong effect of uncertain parameters on the objective function highlights the need for inclusion of probabilistic models within the design procedure.

Discussion, Conclusions and Future Work

This diploma thesis presented the development of a parametric model for the preliminary design of large ro-pax ships, as well as its application to a realistic ship design optimization problem.

To sum up the main steps of the parametric design procedure, initially the hull form is generated by imposing transformations on a parent hull. This is followed by the powering calculations and the selection of main engines. Then, the internal subdivision of the ship takes place. Particular attention is paid to the parametrization of the internal layout, in order to ensure that a relatively wide design space is effectively covered. This is achieved by developing an algorithm for placing transverse bulkheads as a function of the length between perpendiculars, by internally evaluating a number of geometric and regulatory constraints and modifying the general arrangement if needed, and by introducing parameters which enable the examination of alternative layouts for given main dimensions. A series of calculations follows, with regard to passenger and lane capacity, lightship weight, loading conditions, intact and damage stability, energy efficiency and economic performance.

Whenever statistical methods or results of systematic series have been used, comparisons with existing similar ships have been made, in order to ensure that the results are realistic. Thus, a secondary outcome of this work has been the evaluation of well-known approximate methods for conventional large ro-pax ships. Lightship estimation methods have been found to be very accurate, predicting the lightship weight with an accuracy of ±2.5% for four ships for which data was available. Regarding propulsion power, it has been found that the combination of Holtrop's method for calm water resistance and hull – propeller interaction and Wageningen – B series data for propeller open water efficiency overestimate propulsion power by about 10%.

Subsequently, the developed model was used to solve a specific ship design optimization problem. The length, beam and depth of a ship were optimized for maximum profitability (NPV), while adhering to a set of ten constraints arising from owner's requirements, stability and energy efficiency regulations. The resulting optimal length was very close to the upper limit, the beam at the lower limit, while the optimal depth was found to lie at an intermediate value.

An approximate graph of the NPV surface as a function of the ship's length and beam was then generated, revealing the complexity of the objective function. Of particular interest are the local optima induced by changes in the installed power and by the discontinuities in the transverse bulkhead positions as a function of the length between perpendiculars. Finally, this procedure was repeated for increased and decreased fuel prices, showing how changes in the fuel cost deform the objective function surface and even change the optimal point. Thus, the strong effect of

uncertain parameters on the objective function should be addressed, for example by introducing probabilistic models.

Overall, the presented work demonstrated the capabilities of parametric optimization methods in preliminary ro-pax ship design. The overwhelming number of design variables and constraints, the multiple objectives and the complex impact of the design variables on the objective functions highlight the need for formal optimization procedures to solve such problems. Of course, the results must always be treated with caution, taking into account the capabilities of the model and the simplifications which have been made.

There is always room for improvement in the extent and accuracy of the geometric modeling as well as of the various calculation methods. Particular possibilities for future work are listed below. Some of them will be applied to the developed model in the future, as part of the EU project HOLISHIP.

- The use of a fully parametric hull model would increase flexibility and allow for the introduction of more detailed hull form parameters.
- The prediction of calm water resistance would be improved by performing further RANS simulations and generating more accurate response surfaces. Alternatively, potential flow software in combination with empirical methods could be used in order to directly compute the resistance within the design loop. First principles could also be used for optimal propeller design (eg. lifting line / lifting surface methods), as well as for calculating the added resistance.
- With regard to the general arrangement, flexibility of the transverse bulkhead positioning algorithm can be increased, enabling the designer to optimize the number and positions of transverse bulkheads, for example for minimum lightship weight while adhering to damage stability constraints.
- Further flexibility between lane meters and passenger capacity could also be provided in order to increase generality of application.
- The steel weight could be directly calculated based on a structural model, while more detailed models for outfitting, accommodation and machinery weights could be used. This would also allow for a much more accurate estimation of the building cost.
- An internal optimization of the loading conditions with regard to ballasting and distribution of bunkers between the various tanks would be possible.
- Uncertain economic parameters could be modeled as random variables. This would give a stochastic nature to the objective function and allow for the minimization of its standard deviation as an additional objective.

References

[1] G. Zaraphonitis, Introduction to Naval Architecture and Marine Technology, NTUA Lecture Notes (in Greek), 2015.

[2] The World Merchant Fleet in 2015, Equasis, 2015.

[3] A. Papanikolaou and E. Eliopoulou, The European Passenger Car Ferry Fleet - Review of Design Features and Stability Characteristics of Pre- and Post- SOLAS 90 Ro-Ro Passenger Ships, in *Euroconference on Passenger Ship Design, Construction, Safety and Operation*, 2001.

[4] M. Brambilla and A. Martino, Research for TRAN Committee - The EU Maritime Support System: Focus on Ferries, European Union, 2016.

[5] A. Papanikolaou, Ship Design - Methodologies of Preliminary Design, Springer, 2014.

[6] G. Politis, Ship Resistance and Propulsion, NTUA Lecture Notes (in Greek), 2018.

[7] Deltamarin Introduces Ro-pax of the Future, Deltamarin, 2015. www.deltamarin.com

[8] IMO and Ro-Ro Safety, 1997. http://www.imo.org/en/OurWork/Safety/Regulations/Documents/RORO.pdf

[9] K. Spyrou, Ship Dynamic Stability, HEALLINK.

[10] Final Report on the MV Estonia Disaster of 28 September 1994, The Joint Accident Investigation Commission of Estonia, Finland and Sweden, December 1997.

[11] SOLAS Consolidated Edition, International Maritime Organisation, 2014.

[12] MARPOL 73/78, International Maritime Organisation.

[13] Directive 2003/25/EC of the European Parliament and of the Council (Stockholm Agreement), 2003.

[14] Ship Energy Efficiency Regulations and Related Guidelines, in *IMO Train the Trainer (TTT) Course on Energy Efficient Ship Operation*, International Maritime Organisation, 2016.

[15] J. H. Evans, Basic Design Concepts, *American Society of Naval Engineers Journal*, pp. 671-678, 1959.

[16] A. Papanikolaou, H. Nowacki, G. Zaraphonitis, A. Kraus and M. Androulakakis, Concept design and optimisation of a SWATH passenger/car ferry, in *Applications of New Technology in Shipping*, 1989.

[17] G. Zaraphonitis, T. Plessas, A. Kraus, H. Gudenschwager and G. Schellenberger, Parametric Optimisation in Concept and Pre-Contract Ship Design Stage, in *A Holistic Approach to Ship Design*, Springer, 2018.

[18] H. Nowacki, Five Decades of Computer-Aided Ship Design, *Computer-Aided Design,* pp. 956-969, 2010.

[19] J. Maisonneuve, S. Harries, J. Marzi, H. Raven, U. Viviani and H. Piippo, Towards Optimal Design of Ship Hull Shapes.

[20] S. Skoupas, Development of Methodology for the Design and Optimization of New Technology Ro-pax Ships, PhD Thesis, NTUA (in Greek), 2011.

[21] J. Holland, Adaption in Natural and Artificial Systems, University of Michigan Press, 1975.

[22] S. Raptis, Computational Intelligence - Fuzzy Logic, Neural Networks, Genetic Algorithms, NTUA Lecture Notes (in Greek).

[23] S. Harries, C. Cau, J. Marzi, A. Kraus, A. Papanikolaou and G. Zaraphonitis, Software Platform for the Holistic Design and Optimisation of Ships, in *STG Jahrbuch,* 2017.

[24] J. Holtrop, A Statistical Re-analysis of Resistance and Propulsion Data, *International Shipbuilding Progress,* vol. 31, no. 363, pp. 272-276, 1984.

[25] D. Watson, Practical Ship Design, Elsevier, 1998.

[26] H. Schneekluth and V. Bertram, Ship Design for Efficiency and Economy, Butterworth-Heinemann, 1998.

[27] Resolution MSC.421(98), International Maritime Organisation, 2017.

[28] IMO MEPC 72 Brief, American Bureau of Shipping, 2018. www.eagle.org

[29] A. Papanikolaou, Holistic Ship Design Optimization, *Computer-Aided Design,* 2010.